Preview-based techniques for vehicle suspension control: a state-of-the-art review

Annual Reviews in Control 51 (2021) 206–235

Contents lists available at ScienceDirect

Annual Reviews in Control

journal homepage: www.elsevier.com/locate/arcontrol

Preview-based techniques for vehicle suspension control: a state-of-the-art review

Johan Theunissen [a], Antonio Tota [b], Patrick Gruber [a], Miguel Dhaens [c], Aldo Sorniotti [a,*]

[a] University of Surrey, Guildford GU2 7XH, U.K.
[b] Politecnico di Torino, Torino 10129, Italy
[c] Tenneco Automotive Europe bvba, Sint-Truiden 3800, Belgium

ARTICLE INFO

Keywords:
Active and semi-active suspension systems
Road preview
Ride comfort
Handling
Preview time
Feedforward compensator
Optimal control

ABSTRACT

Automotive suspension systems are key to ride comfort and handling performance enhancement. In the last decades semi-active and active suspension configurations have been the focus of intensive automotive engineering research, and have been implemented by the industry. The recent advances in road profile measurement and estimation systems make road-preview-based suspension control a viable solution for production vehicles. Despite the availability of a significant body of papers on the topic, the literature lacks a comprehensive and up-to-date survey on the variety of proposed techniques for suspension control with road preview, and the comparison of their effectiveness. To cover the gap, this literature review deals with the research conducted over the past decades on the topic of semi-active and active suspension controllers with road preview. The main formulations are reported for each control category, and the respective features are critically analysed, together with the most relevant performance indicators. The paper also discusses the effect of the road preview time on the resulting system performance, and identifies control development trends.

1. Introduction

In road vehicles, controlled suspension systems use actuators that generate controllable forces between the sprung and unsprung masses (Cao et al., 2011; Genta & Morello, 2019; Savaresi et al., 2010), to improve ride comfort and handling. Today's industrial and academic research in the field of controlled suspension systems must consider the following trends in the automotive sector:

- The increasing ride comfort demand in all vehicle segments (Savaresi et al., 2010; Ueno et al., 2018; Vella et al., 2020), even if this expectation is not reflected in recent experimental assessments of the ride comfort level of different generations of passenger cars (Mastinu et al., 2017).
- The increasing level of vehicle automation, according to the scale in the SAE standard J3016 (2016), with progressive shift towards automated driving (Elbanhawi et al., 2015; Nguyen et al., 2019; Wu et al., 2020).

Ride comfort is associated with the vehicle system capability of attenuating the level of mechanical vibrations transmitted to the vehicle users, caused by irregular road elevation profiles (Heißing & Ersoy, 2011). While in human driven vehicles the transmission of moderate vibration levels can be useful to inform the driver on the current road condition, in the long term vehicles with high levels of driving automation are expected to allow the users to carry out various activities, e.g., working on a laptop or watching a video, while the vehicle is moving (Burkhard et al., 2018; Diels et al., 2017). This requires a train-like ride comfort level (Förstberg, 2000; Ueno et al., 2018), capable – together with appropriate path planning and tracking controllers, e.g., see Gallep & Müller, 2018, Saruchi et al., 2020, Tota et al., 2018, Wang et al., 2018, and innovative interior design and motion cue solutions, see Diels & Bos, 2015a,b – of preventing motion sickness effects, and minimising mechanical vibrations across the relevant frequency range.

Controlled suspension systems include actuators that vary the forces exchanged between the sprung and unsprung masses of the vehicle, and are key to the expected ride comfort increase in the next generation of road vehicles. They have been the subject of extensive research over the years, and have penetrated the automotive market to some extent (Schindler, 2009; Streiter, 2008). In this context, recent technologies,

Important note: the main changes have been highlighted in yellow.

* Corresponding author.
E-mail address: a.sorniotti@surrey.ac.uk (A. Sorniotti).

https://doi.org/10.1016/j.arcontrol.2021.03.010
Received 21 January 2021; Received in revised form 28 March 2021; Accepted 28 March 2021
Available online 8 June 2021

such as dynamic navigational maps (Kiran et al., 2019; Milz et al., 2018), interconnectivity (Campolo et al., 2017; Siegel et al., 2018) and road pre-scan sensors (Ma et al., 2018), can play an important role in enhancing controlled suspension system performance through road-preview-based algorithms, i.e., suspension controllers benefitting from the information on the expected road profile ahead. In particular, while in the past only high-end road pre-scan sensor solutions existed for laboratory use and prototype vehicles, nowadays low-cost and high-performance pre-scan sensors have become available (Dhiman, Chien, & Klette, 2017; Schindler, 2009; Streiter, 2008; Sugasawa, Kobayashi, Kakimoto, Shiraishi, & Tateishi, 1985), and have already been introduced on top-segment production passenger cars. The increasing consumer demand for enhanced ride comfort and the availability of the required technological enablers lead to a large exploitation potential for preview-augmented suspension systems, which can achieve significantly enhanced performance also in presence of the inevitable actuation dynamics.

Several literature surveys deal with suspension control topics. Poussot-Vassal et al., and Dugard (2012) only discusses controllers without preview, in which the road profile is considered an unknown disturbance. Other reviews or comparison papers include consideration of road-preview-based formulations (Brown et al., 2011; Hrovat, 1993; Sharp & Peng, 2011; Tseng & Hrovat, 2015); however, given the breadth of their scope and the fact that they date back to years ago, before the publication of the last generation of control formulations and results, to the best of our knowledge none of the available surveys comprehensively covers preview-based suspension control research.

This literature review targets the identified gap, and provides categorisation, description and critical analysis of preview-based suspension control strategies, including consideration of relevant dynamic models for control design, system constraints, computational power demand, performance indicators, and achieved results. The review is based on the following criteria:

- Only formulations in which the preview information is represented by the profile of the road irregularities are considered, i.e., the review does not provide details on pre-emptive body control formulations that compensate the effect of the longitudinal and lateral accelerations caused by traction, braking and cornering forces.
- Suspension controllers without road preview are not covered, except when they are used as benchmarks for evaluating their preview-based version.
- The sensing and state estimation aspects are not included.
- Only journal and conference papers, books, PhD theses and standards are considered.

The manuscript is organised as follows: Section 2 provides a preliminary overview of suspension system functions and relevant ride comfort indicators; Section 3 introduces the concept of preview-augmented suspension control; Section 4 presents the non-optimal control solutions, while Section 5 covers the optimal control implementations; Section 6 discusses the main control trends, and analyses the effect of preview time on control system performance; finally, conclusions are drawn in Section 7.

2. Suspension systems and relevant performance metrics

2.1. Suspension system functions

Automotive suspension systems have the following main functions (Cao et al., 2011; Ulsoy et al., 2012):

- To maintain the correct vehicle body orientation, i.e., roll and pitch behaviour, when the vehicle is subject to braking, traction and cornering forces.
- To provide good ride comfort by insulating the occupants from road irregularities.
- To guarantee desirable road holding and vehicle safety by reducing the vertical tyre load variations induced by road irregularities and driving dynamics, as well as by providing the required elasto-kinematic characteristics.
- To avoid excessive wheel travel thus preventing bump stop impacts.

Suspension systems mainly consist of: i) rigid links, such as wishbones and tie rods, which define the suspension typology (MacPherson, multi-link, etc.), and in passenger cars connect the suspension upright to the chassis through joints with bushings (Genta & Morello, 2009); ii) springs (including anti-roll bars), bump stops and shock absorbers, which provide desirable stiffness and damping properties (Genta & Morello, 2009); and optionally iii) controllable actuators between the unsprung masses and the sprung mass, in case of active or semi-active implementations. The actuators are installed in parallel or series with respect to the passive springs/dampers (Göhrle et al., 2012), and can replace some of the passive components, i.e., typically the shock absorbers. Most automotive suspensions only include the components in i) and ii), i.e., they have a conventional passive spring/damper architecture. However, many production vehicles are equipped with semi-active and active suspension solutions, which are the focus of this survey.

2.2. Semi-active and active suspension actuators

In semi-active suspension systems the generated force always opposes the actuator motion, i.e., the actuators operate as dampers with variable force-speed characteristics. On the one hand, this property poses a major limitation to the achievable performance; for example, semi-active suspensions cannot control the ride height, or the roll angle in steady-state cornering conditions, or the pitch angle induced by the longitudinal acceleration. On the other hand, semi-active suspension systems can be implemented through low power consumption hardware, i.e., they require a power input only for the actuation of their modulating devices, but not directly for the generation of the actuator force, and thus they do not have any substantial impact on the overall vehicle energy consumption. Typical semi-active actuators are:

- Hydraulic shock absorbers with controllable orifice areas, implemented through solenoid valves or servo-valves (Faraj et al., 2019; Savaresi et al., 2010).
- Magnetorheological (MR) and electrorheological (ER) dampers (Gavin et al., 1996; Savaresi et al., 2010; Spencer et al., 1997), consisting of a piston with valves and a hydraulic cylinder containing an MR or ER fluid, usually with non-Newtonian characteristics, which changes its properties as a function of a magnetic or electric field, because of the presence of micron-sized polarizable particles. These implementations do not contain any moving parts, and therefore are mechanically very reliable.
- Electromagnetic dampers (Soliman & Kaldas, 2019), which use the interaction between the movement of a coil and the magnetic field of a permanent magnet or an electromagnet to provide a damping effect. The damping level can be varied by changing the external resistance or the strength of the magnetic field.

In active suspension systems, the direction of the actuator force is independent of the sign of the actuator speed, which is highly beneficial in terms of performance. In fact, this feature permits to compensate the roll, pitch and heave motions of the vehicle body caused by the lateral and longitudinal accelerations, as well as to control the ride height, e.g., to reduce it during high speed operation to decrease aerodynamic drag and energy consumption. However, the generation of positive mechanical work requires a significant power input, and the implementation of power conversion devices, such as hydraulic pumps and electric motors, which have an impact on the energy consumption of the vehicle.

Typical active suspension actuators are:

- Hydraulic actuators, connected to a system including pump, valves and – depending on the arrangement – an accumulator, to generate the required level of fluid pressure and/or flow rate (Sam & Hudha, 2006).
- Electro-magnetic actuators, with similar operating principle to the electro-magnetic dampers (Martins et al., 2006).
- Electro-mechanical actuators (Kawamoto et al., 2008), e.g., including an electric motor and a mechanical system to convert the angular displacement of the rotor into a linear actuator displacement.

Air springs can also be used as controllable suspension actuators, e.g., for varying the ride height and compensating the effect of the vehicle payload, however their low bandwidth makes them unsuitable – on their own – for the pre-emptive implementations of this survey.

The semi-active and active suspension actuators, managed by electronic controllers, are typically located at each vehicle corner, and operate as linear actuators, which is the common configuration considered in this review, or can be implemented in the form of controllable anti-roll bars or torsion springs.

Active and semi-active suspension controllers are usually designed to enhance ride comfort and road holding on irregular roads, which can represent conflicting objectives, as well as to reduce the vehicle body motions caused by traction/braking and cornering. Secondary objectives, not covered in this review, include the control of yaw rate and sideslip angle dynamics, e.g., achieved through front-to-total anti-roll moment distribution. To motivate the requirement for a compromise between the different aspects, Fig. 1 is a typical conflict diagram between comfort and road holding, obtained through passive quarter car model simulations (see the following Section 5 and Fig. 9 for further details on the model) on an irregular road profile for different values of the damping coefficient, c_S, of the linear suspension damper. Lower value of the indices, i.e., the handling index (root mean square of the dynamic vertical wheel load) and comfort index (root mean square of the filtered body acceleration), correspond to improved performance for the respective target. The results indicate that the damping coefficient value optimising comfort, $c_{S,C}$, is lower than the value optimising handling, $c_{S,H}$, with a trade-off region between the two values. The selection of the optimal damping level requires a compromise between harder "safer dampers" and softer "more comfortable" dampers. This is also complicated by the fact that the optimal damper settings are dependent on the road profile as well as the manoeuvre imposed by the human driver or automated driving controller. Controlled suspension systems are developed to resolve this conflict. In particular, the trade-off between conflicting targets, shown for the simple passive quarter car model, is a common feature of optimal suspension control formulations

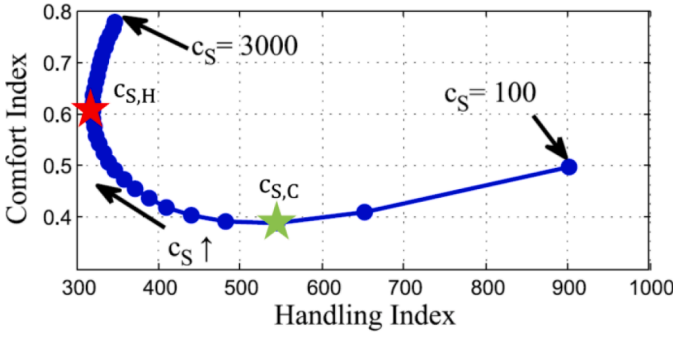

Fig. 1. Conflict diagram reporting a comfort index as a function of a handling index for a range of damping coefficients of the shock absorber, evaluated through a quarter car passive suspension model. The red and green stars indicate the optimal damping coefficients for handling and comfort performance. Adapted from De Bruyne et al. (2012).

(see Section 5), where the different objectives are typically combined into a single cost function to be minimised.

2.3. Performance indicators

The preview-augmented suspension systems from the literature are objectively assessed through typical ride comfort indicators. Many researchers use indices derived from the standards BS 6841 (1987) and ISO 2631-1 (1997), for the evaluation of the level of human exposure to whole-body vibrations. Although most studies consider the vertical acceleration of the sprung mass as the main relevant variable, often also other variables, such as the jerk (the time derivative of the acceleration, see Hoberock (1977)), or the sprung mass displacement, are analysed. One of the most immediate methods to assess suspension performance, especially over an isolated road event, is through the computation of the peak or peak-to-peak values of the considered variables, over a prescribed measurement period (Canale et al., 2006; Zhu et al., 2012). The peak-to-peak evaluation is often combined with the frequency weighted root mean square acceleration (*WRMS*) over a time period T (BS 6841, 1987; Canale et al., 2006; Gangadharan et al., 2004; Hoberock, 1977; ISO 2631-1, 1997; Leatherwood & Barker, 1984; Little et al., 1999; Maciejewski et al., 2011; Nastac & Picu, 2010; Paddan & Griffin, 2002; Pazooki et al., 2011; X. Zhao et al., 2013; Zhu et al., 2012), which is defined by Maciejewski et al. (2011) and Nastac and Picu (2010) as:

$$WRMS = \sqrt{\frac{1}{T}\int_0^T [a_w(t)]^2 \mathrm{d}t} \tag{1}$$

where t is time, and $a_w(t)$ is the frequency weighted acceleration, which is computed by applying filtering functions, W_i (defined in BS 6841 (1987), and ISO 2631-1 (1997)) to the unweighted acceleration profile. These functions express the human sensitivity to certain frequency ranges. In fact, humans are most sensitive to vertical vibrations: a) below 0.5 Hz due to motion sickness (BS 6841, 1987; Gysen et al., 2010); b) in the 4-8 Hz range due to body resonance; and c) in the 18-20 Hz range due to the resonance of neck and head. Above 20 Hz the human sensitivity to vertical vibrations decreases. Compared to averaging, the *WRMS* assigns more weight to the acceleration peaks, and is applicable to the evaluation of both primary ride in the 0-5 Hz frequency range (Badiru & Cwycyshyn, 2013) and secondary ride between 5 Hz and 25 Hz (Badiru & Cwycyshyn, 2013); however, additional high-pass or low-pass filters are sometimes applied to distinguish the frequency ranges of interest (Maciejewski et al., 2011). Alternatively, to evaluate the acceleration levels in different frequency ranges, many authors use the root mean square (*RMS*) acceleration computed for 1/3 octave frequency bands (BS 6841, 1987; Gangadharan et al., 2004; ISO 2631-1, 1997; Sezgin & Yagiz, 2012).

According to Little et al. (1999), the *WRMS* of the acceleration insufficiently matches with the subjective human experience along shocks, transients and non-stationary vibrations. The boundary between stationary and non-stationary conditions can be determined through the crest factor (*CF*), i.e., the ratio of the peak value to the average value of the relevant signals (BS 6841, 1987; ISO 2631-1, 1997; Mastinu et al., 2017), where the condition $CF > 9$ is typical of non-stationary conditions (BS 6841, 1987; ISO 2631-1, 1997; Nastac & Picu, 2010; X. Zhao et al., 2013). In case of non-stationary vibrations, other ride comfort metrics apply, such as: a) the running weighted *RMS* acceleration (*RWRMS*); b) the maximum transient vibration value (*MTVV*) (BS 6841, 1987; ISO 2631-1, 1997; Nastac & Picu, 2010; X. Zhao et al., 2013), i.e., the maximum value of *RWRMS* for the considered measurement period; c) the fourth power vibration dose value (*VDV*) (BS 6841, 1987; ISO 2631-1, 1997; Little et al., 1999; Nastac & Picu, 2010; Paddan & Griffin, 2002; X. Zhao et al., 2013); and d) the frequency weighted root mean quad (*WRMQ*, see BS 6841 (1987), and Little et al. (1999)). Their mathematical definitions are:

$$RWRMS(t_0) = \sqrt[2]{\frac{1}{\tau_I}\int_{t_0-\tau_I}^{t_0} [a_w(t)]^2 \mathrm{d}t} \tag{2}$$

$$MTVV = \max(RWRMS(t_0)) \tag{3}$$

$$VDV = \sqrt[4]{\int_0^T [a_w(t)]^4 \mathrm{d}t} \tag{4}$$

$$WRMQ = \sqrt[4]{\frac{1}{T}\int_0^T [a_w(t)]^4 \mathrm{d}t} \tag{5}$$

where t_0 is the observation or instantaneous time; and τ_I is the integration time, e.g., 1 s according to ISO 2631-1 (1997). The *WRMQ* differs from the *WRMS* in its higher sensitivity to impulsive events, as it uses the fourth power of the acceleration magnitude. In comparison with the *WRMQ*, the *VDV* specifies the relation between vibration levels and exposure duration, i.e., the same value of *VDV* can be obtained through different combinations of acceleration magnitudes and durations.

In case of multiple measurement directions and locations, the overall vibration level is evaluated by the weighted sum of accelerations in different directions and measurement points, e.g., seat rail, seat surface, feet support and steering wheel (BS 6841, 1987; ISO 2631-1, 1997; Nastac & Picu, 2010; Paddan & Griffin, 2002; Pazooki et al., 2011; X. Zhao et al., 2013; Zhu et al., 2012). For example, the preview-augmented suspension control study in Theunissen et al. (2020) uses the vibration total value, *VTV*:

$$VTV = \sqrt[2]{\sum_q \left(k_q\ WRMS_q\right)^2} \tag{6}$$

where the index q indicates the considered weighted *RMS* acceleration, e.g., heave, pitch or roll acceleration; and k_q is a weighting coefficient. To the same purpose, the British Standard (BS 6841, 1987) proposes the total vibration dose value (*TVDV*), defined as the fourth root of the sum of the fourth powers of the *VDV* values along each axis (BS 6841, 1987; ISO 2631-1, 1997; Paddan & Griffin, 2002; Vella et al., 2020).

The vehicle handling performance on irregular road profiles depends on the maximum available tangential tyre force at the axle and vehicle levels, which is directly related to the individual vertical tyre force variations (Hrovat, 1993; Lozia, 1992; Mashadi & Crolla, 2005), i.e., the reduction of normal tyre force variations improves road holding. To this purpose, an index frequently used in the literature is the normalised tyre force variation, or dynamic tyre load, $\sigma_{F_{z,t}}$ (Reybrouck et al., 2012):

$$\sigma_{F_{z,t}} = \sqrt[2]{\frac{1}{T}\int_0^T \frac{\left[F_{z,t}(t) - F_{z,t0}\right]^2}{F_{z,t0}^2}\mathrm{d}t} \tag{7}$$

where $F_{z,t}(t)$ is the instantaneous vertical tyre force at time t, and $F_{z,to}$ is the steady-state vertical tyre force.

3. The road preview control concept

Suspension controllers have been traditionally designed to be reactive, i.e., based on the current vehicle response to the road input, measured or estimated through on-board sensors, e.g., accelerometers located on the sprung and unsprung masses, and actuator displacement sensors. The performance of reactive formulations is penalised by: i) the typically rather fast dynamics of the road inputs; ii) the limited bandwidth of suspension actuators (Prokop & Sharp, 1995); and iii) the pure time delays of the vehicle communication buses that are responsible for the flow of the control inputs and outputs (Rahman & Rideout, 2012).

The effect of i)-iii) can be significantly attenuated through road preview control, in which the road profile is not an unknown disturbance anymore, but is a measured external input. Preview control formulations can be either based on: a) the information of the road elevation at a single point, i.e., typically at the longitudinal position of the considered vehicle corner at the time corresponding to the next control action application; or b) the information of the road elevation for a set of discretized points, ranging from the current longitudinal coordinate of the vehicle corner until a predicted future position of the wheel, to cover the so-called preview time.

Preview-based controllers were initially designed and investigated in Bender (1968); Iwata and Nakano (1976), and Sakami et al., and Shimogo (1976), by using the Wiener filter theory. These preliminary studies show that longer preview times lead to more gradual vehicle response to a road step input, and result in smaller relative displacements. In fact, with road preview the suspension actuator can proactively respond to a step in roadway elevation before actually reaching it, see Fig. 2 where the road step input is applied at $t = 0$. The preview information can reduce both sprung mass acceleration (curvature of the response) and suspension excursion (difference between the step input and the response curves). Following these pioneering implementations, the idea of preview-based suspension control has been extensively researched over the years, initially through simulations, and then through experiments, until the relatively recent production-vehicle-oriented implementations (Schindler, 2009; Streiter, 2008).

To highlight the potential of the technology, Fig. 3 compares experimental results of active suspension controllers without and with preview, internally developed and implemented by Tenneco Automotive Europe on a test vehicle with hydraulic actuators, and assessed on a quarter car poster rig (Theunissen, 2019), i.e., without road profile measurement or estimation errors. At each vehicle corner, a pump pressurises the hydraulic circuit of the respective actuator and inputs energy into the system. The pressure level in the hydraulic chambers is modulated through the currents of the base and piston valves of the actuator, which is installed in parallel to an air spring. Depending on the operating conditions, the time constant of the hydraulic actuators ranges from 25 ms to 60 ms, with a pure time delay of approximately 15 ms. The preview strategy is a feedforward compensator without state feedback, see Section 4. The performance is evaluated on smooth and rough road profiles, with reference to their characteristics according to ISO 8608 (1995), at two pressure levels in the hydraulic circuit feeding the actuators, i.e., 30 bar and 70 bar represent the maximum possible hydraulic actuator pressure achievable during the respective test. At 70 bar on the smooth road profile, the introduction of preview brings ~30% relative improvement in ride comfort and road holding performance, respectively evaluated in terms of vehicle body acceleration and vertical tyre force variation; on the rough road profile, for the case study implementation the ride comfort and road holding improvements amount to ~29% and ~60%.

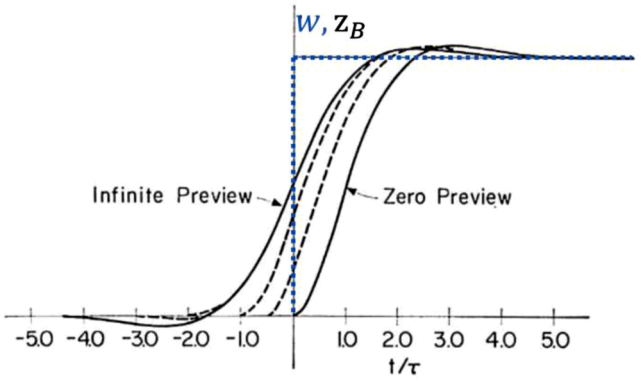

Fig. 2. Active suspension responses to road input steps for several values of preview time. w and z_B are the road profile and vehicle sprung mass displacements, while τ is a non-dimensionalising scale factor. Reproduced with permission from Bender (1968).

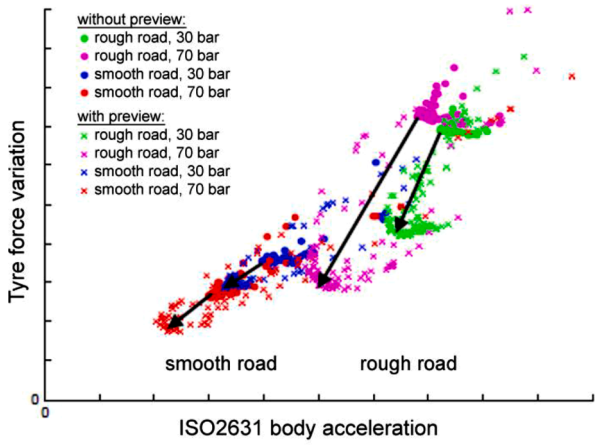

Fig. 3. Example of performance improvement achieved by the addition of preview on a hydraulic active suspension system, evaluated on a quarter car poster rig. Reproduced with permission from Theunissen (2019).

Several methods are available to obtain the road preview information. The typical solution, currently implemented in production vehicles with road preview, is to install a 'look-ahead' sensor on the front end of the car, by using reflected light (e.g., Lidar), ultrasonic or radar beam technologies (Ahmed & Svaricek, 2014; M. Ahmed & Svaricek, 2013; Akbari & Lohmann, 2008, 2010; Elmadany et al., 2011; Hać, 1992, 1994; Hać & Youn, 1992; Martinus et al., 1996; Marzbanrad et al., 2004; Prokop & Sharp, 1995; Schindler, 2009; Streiter, 2008; Theunissen et al., 2020; Thompson & Pearce, 1998; Tomizuka, 1976). A drawback of look-ahead sensors is that they can provide incorrect road information, e.g., a heap of leaves can be misinterpreted as a road irregularity, while a pothole filled in with water is not detected at all. Another solution, here referred to as wheelbase preview, is to estimate the road profile for the rear axle from the response of the front suspension, by assuming that the rear wheel road inputs are the same as the front ones, with appropriate time delay (Feng et al., 2009; Fukuda et al., 2004; P. Li, Lam & Cheung, 2014, 2014b; Marzbanrad et al., 2004; Oraby et al., 2007; Prabakar et al., 2009; Roh & Park, 1998; Soliman & Crolla, 2001; Thompson & Pearce, 1998; Van Der Aa et al., 1997), even if the real trajectory of the rear wheels can differ from that of the front ones, especially during cornering.

Wheelbase preview is relatively reliable and inexpensive (Elmadany et al., 2011; Kwon et al., 2020) in comparison with look-ahead sensors; however, differently from the other techniques, the road profile information is only available for rear suspension control. Ryu et al., and Suh (2011) is one of the very rare studies including a comparison between the performance of look-ahead preview and wheelbase preview (see Fig. 4) for the specific application of a tank with six road wheels per track. In case of wheelbase preview, the first wheel is used for terrain profile estimation, which is appropriately given as preview information to the suspension controllers of the following wheels. In connected vehicles, lead-vehicle preview can be implemented, which uses the lead vehicles as look-ahead sensors for pre-emptively estimating the road elevation profile for the suspension controller of the following vehicles (Asl & Rideout, 2010; Rahman & Rideout, 2012; Song & Wang, 2020). Lead-vehicle preview may be influenced by communication lag or lead delays (Rahman & Rideout, 2012), and is yet to be practically demonstrated in realistic automotive scenarios. Finally, a few studies (Z. Li et al., 2015) consider to download the road profile information from a cloud database, but also in this case disturbances and time delays may affect accuracy. All mentioned technologies neglect terrain profile alterations caused by the effect of the front wheels in the calculation of the preview contribution of the rear wheels, which is acceptable for most applications.

The key item in the implementation of preview-augmented suspensions is the preview-based control structure, which must meet the following requirements:

- High performance in terms of ride comfort and road holding.
- High level of robustness with respect to model uncertainties and process variations.
- Limited computational power, i.e., the controller must be implementable on low-cost automotive control hardware.

A wide range of control structures has been proposed for suspension systems with road preview, most of them using model-based control, i.e., controllers designed through a model of the system. The industrial controllers (Schindler, 2009; Streiter, 2008) tend to adopt state or output feedback set-ups with the addition of preview-based feedforward disturbance compensators, which are easy to implement and require low computational power. This review classifies as optimal the controllers whose design is based on an optimality criterion or an optimisation process. Accordingly, optimal controllers are Wiener-filter-based controllers, linear quadratic regulators (LQR), linear quadratic Gaussian controllers (LQG), H_2/H_∞ controllers, and model predictive controllers (MPC). Approximately 84% of the considered preview-augmented

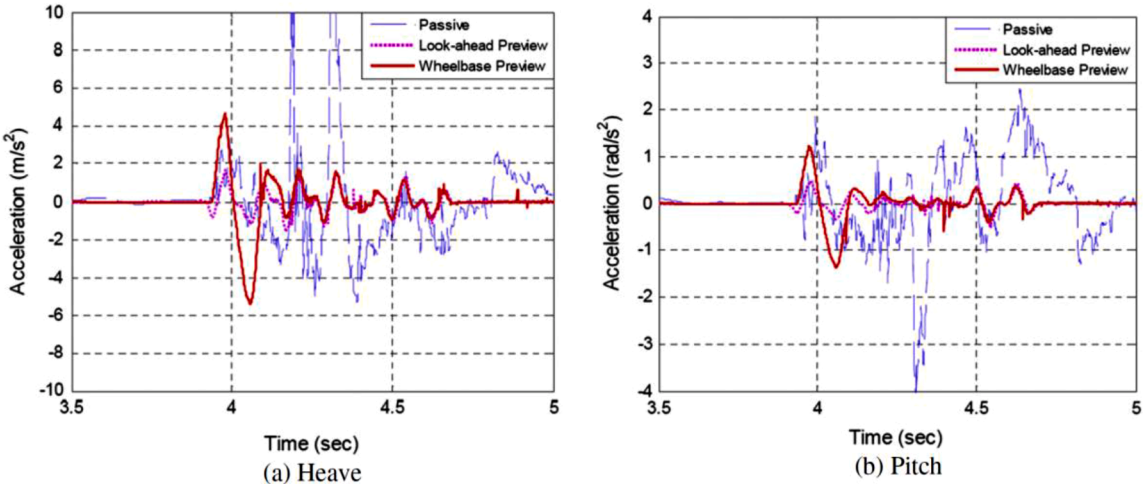

Fig. 4. Heave (a) and pitch (b) accelerations of the sprung mass along a road bump, for: i) the passive vehicle ('Passive'); ii) the vehicle with active suspension control based on look-ahead preview ('Look-ahead Preview'); and iii) the vehicle with active suspension control based on wheelbase preview ('Wheelbase Preview'). Reproduced with permission from Ryu et al. (2011).

suspension controllers are categorized as optimal strategies. H_2 /H_∞ controllers include formal consideration of robustness with respect to model uncertainties and/or parameter variations, and therefore are often referred to as robust controllers, i.e., they could constitute a category on their own, separate from the optimal controllers. However, in this survey, in accordance with classical control theory textbooks such as Skogestad and Postlethwaite (2007), H_2/H_∞ controllers are treated as a specific category of optimal controllers, as their design implies some form of optimisation. LQR/LQG have been heavily researched for preview suspension control in the past, as they are reasonably easy to implement, and require limited computational power; however, they are less performing than MPC. Being based on the prediction of the future behaviour of the system along a prediction horizon, MPC is the natural control structure to implement the road preview concept. Moreover, MPC formally deals with system constraints, e.g., in terms of actuator force and suspension displacement. On the downside, the relatively high computational power demand for the real-time operation of typical implicit MPC (iMPC) formulations, in which the optimisation problem is solved online at each time step, can pose implementation limitations on automotive microcontrollers, even if their continuously increasing computational capability does not represent a major obstacle anymore. An alternative and computationally efficient approach is represented by explicit MPC (eMPC), in which the MPC optimisation is solved offline, and then stored in the online controller, at the price of significantly increased memory requirements (Theunissen et al., 2020). The non-optimal and optimal suspension control implementations with road preview from the literature are detailed in the following Sections 4 and 5.

4. Non-optimal controllers

Mercedes-Benz has been particularly active in the development of this category of controllers within the programme "Vision of Accident-free Driving" (1999), which resulted into a prototype system, i.e., the Pre-scan suspension, demonstrated on the F700 concept car in 2007. This was followed by the implementation and industrialisation of the Magic Body Control system, i.e., an upgrade of the active body control suspension system of the same car maker to incorporate the Pre-scan function, which was introduced on the market with the production 2013 Mercedes-Benz S-Class (W222). The preview-based controller of the F700, equipped with low-bandwidth active suspensions and Lidar sensors, is described in Streiter (2008) and Schindler (2009), which propose a feedback and feedforward road disturbance compensator with an integrated approach that accounts for the closed-loop dynamics in the feedforward term.

The detailed formulation of the algorithm is reported in this section, given the industrial significance of the implementation. The design is based on the half car model in Fig. 5, i.e., including front and rear suspension systems, but not considering roll dynamics. The heave and pitch dynamics are described by:

$$\begin{aligned} m_B\ddot{z}_B &= F_{SD,F} + F_{SD,R} + F_z \\ J_B\ddot{\theta}_B &= F_{SD,F}l_F - F_{SD,R}l_R + M_N \end{aligned} \tag{8}$$

where m_B and J_B are the sprung mass (vehicle body) and its pitch mass moment of inertia about the centre of gravity (note that their values consider only half of the vehicle if the front and rear suspension stiffness and damping characteristics are those of a single corner); $\ddot{z}_B$ and $\ddot{\theta}_B$ are the vertical and pitch accelerations of the sprung mass; $F_{SD,F}$ and $F_{SD,R}$ are the forces of the front and rear spring and damper assemblies; l_F and l_R are the front and rear semi-wheelbases; and F_z and M_N are the resultant vertical force and pitch moment caused by the traction and braking forces, which depend on the anti-dive, anti-lift and anti-squat properties of the front and rear suspensions, see Milliken W. F. and Milliken D.L. (1995). (8) can be re-written in matrix form as:

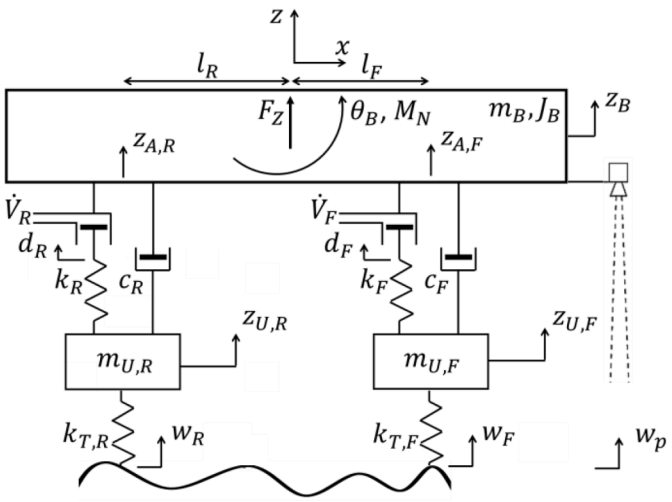

Fig. 5. Schematic of the half car model for preview-augmented suspension control system design, with controllable spring seat displacement.

$$\boldsymbol{I_B}\begin{bmatrix}\ddot{z}_B\\ \ddot{\theta}_B\end{bmatrix} = \boldsymbol{T_{BA}}\left\{-\boldsymbol{K_S}\left(\boldsymbol{T_{BA}^T}\begin{bmatrix}z_B\\ \theta_B\end{bmatrix} - \boldsymbol{z_U}\right) + \boldsymbol{K_S u} - \boldsymbol{C_S}\left(\boldsymbol{T_{BA}^T}\begin{bmatrix}\dot{z}_B\\ \dot{\theta}_B\end{bmatrix} - \dot{\boldsymbol{z}}_U\right)\right\} + \begin{bmatrix}F_z\\ M_N\end{bmatrix} \tag{9}$$

with:

$$\begin{aligned} &\boldsymbol{I_B} = \begin{bmatrix}m_B & 0\\ 0 & J_B\end{bmatrix},\ \boldsymbol{K_S} = \begin{bmatrix}k_F & 0\\ 0 & k_R\end{bmatrix},\ \boldsymbol{C_S} = \begin{bmatrix}c_F & 0\\ 0 & c_R\end{bmatrix}, \\ &\boldsymbol{z_A} = \begin{bmatrix}z_{A,F}\\ z_{A,R}\end{bmatrix} = \boldsymbol{T_{BA}^T}\begin{bmatrix}z_B\\ \theta_B\end{bmatrix},\ \boldsymbol{z_U} = \begin{bmatrix}z_{U,F}\\ z_{U,R}\end{bmatrix},\ \boldsymbol{u} = \begin{bmatrix}d_F\\ d_R\end{bmatrix} \end{aligned} \tag{10}$$

where $\boldsymbol{I_B}$ is the vehicle body inertia matrix; $\boldsymbol{K_S}$ is the suspension stiffness matrix, including the front and rear suspension stiffness values; $\boldsymbol{C_S}$ is the suspension damping matrix; $\boldsymbol{z_A}$ is the vector of the vertical displacement of the front and rear suspension attachments, $z_{A,F}$ and $z_{A,R}$, to the sprung mass; $\boldsymbol{z_U}$ is the vector of the vertical displacements of the front and rear unsprung masses, $z_{U,F}$ and $z_{U,R}$; $\boldsymbol{T_{BA}}$ converts the vertical displacement and pitch angle of the sprung mass into the vertical displacements at the spring/damper attachment points; and $\boldsymbol{u}$ is the control action vector, i.e., the vector of the front and rear spring seat displacements, respectively d_F and d_R. The active suspension actuator is a hydraulic piston installed in series to the passive spring on each strut, which enables ride height adjustment.

In the model for control design, the actuator dynamics are described by:

$$\boldsymbol{u} = \boldsymbol{K_{PL}}\int \boldsymbol{i}\mathrm{d}t \tag{11}$$

where $\boldsymbol{i}$ the vector with the currents sent to the hydraulic system servo-valves, which generate the flow rates $\dot{V}_F$ and $\dot{V}_R$; and $\boldsymbol{K_{PL}}$ includes the amplifier factors of each piston. The vertical unsprung mass dynamics are described by:

$$\boldsymbol{M}_U \begin{bmatrix} \ddot{z}_{U,F} \\ \ddot{z}_{U,R} \end{bmatrix} = -\left\{ -\boldsymbol{K}_S \left(\boldsymbol{T}_{BA}^T \begin{bmatrix} z_B \\ \theta_B \end{bmatrix} - \boldsymbol{z}_U \right) + \boldsymbol{K}_S \boldsymbol{u} - \boldsymbol{C}_S \left(\boldsymbol{T}_{BA}^T \begin{bmatrix} \dot{z}_B \\ \dot{\theta}_B \end{bmatrix} - \dot{\boldsymbol{z}}_U \right) \right\} - \boldsymbol{K}_T (\boldsymbol{z}_U - \boldsymbol{w}) \tag{12}$$

with:

$$\boldsymbol{M}_U = \begin{bmatrix} m_{U,F} & 0 \\ 0 & m_{U,R} \end{bmatrix}, \boldsymbol{K}_T = \begin{bmatrix} k_{T,F} & 0 \\ 0 & k_{T,R} \end{bmatrix}, \boldsymbol{w} = \begin{bmatrix} w_F \\ w_R \end{bmatrix} \tag{13}$$

where $\boldsymbol{M}_U$ is the matrix of the front and rear unsprung masses, $m_{U,F}$ and $m_{U,R}$; $\boldsymbol{K}_T$ is the matrix of the vertical stiffness of the front and rear tyres, $k_{T,F}$ and $k_{T,R}$; and $\boldsymbol{w}$ is the vector with the vertical road elevations at the front and rear tyres, w_F and w_R.

By imposing in (9) $\boldsymbol{z}_U = \boldsymbol{z}_{rel,RW} + \boldsymbol{w}$, where $\boldsymbol{z}_{rel,RW}$ is the vector of the front and rear vertical tyre deflections, and transforming the equation into the Laplace domain, the sprung mass dynamics become:

$$\left(\boldsymbol{I}_B s^2 + \boldsymbol{T}_{BA} \boldsymbol{C}_S \boldsymbol{T}_{BA}^T s + \boldsymbol{T}_{BA} \boldsymbol{K}_S \boldsymbol{T}_{BA}^T\right) \begin{bmatrix} z_B \\ \theta_B \end{bmatrix} = (\boldsymbol{T}_{BA} \boldsymbol{C}_S s + \boldsymbol{T}_{BA} \boldsymbol{K}_S) \boldsymbol{z}_{rel,RW} + (\boldsymbol{T}_{BA} \boldsymbol{C}_S s + \boldsymbol{T}_{BA} \boldsymbol{K}_S) \boldsymbol{w} + \boldsymbol{T}_{BA} \boldsymbol{K}_S \boldsymbol{u} + \begin{bmatrix} F_z \\ M_N \end{bmatrix} \tag{14}$$

where s is the Laplace operator, and for simplicity the same notation is used for the variables in the Laplace and time domains. Similarly, the unsprung mass dynamics become:

$$\left\{\boldsymbol{M}_U s^2 + \boldsymbol{C}_S s + (\boldsymbol{K}_S + \boldsymbol{K}_T)\right\} \boldsymbol{z}_{rel,RW} = \left(\boldsymbol{C}_S \boldsymbol{T}_{BA}^T s + \boldsymbol{K}_S \boldsymbol{T}_{BA}^T\right) \begin{bmatrix} z_B \\ \theta_B \end{bmatrix} - \boldsymbol{K}_S \boldsymbol{u} - \left(\boldsymbol{M}_U s^2 + \boldsymbol{C}_S s + \boldsymbol{K}_S\right) \boldsymbol{w} \tag{15}$$

Based on (14), the preview term can be used to compensate the effect of the road excitation on the sprung mass dynamics, according to:

$$(\boldsymbol{T}_{BA} \boldsymbol{C}_S s + \boldsymbol{T}_{BA} \boldsymbol{K}_S) \boldsymbol{w} + \boldsymbol{T}_{BA} \boldsymbol{K}_S \boldsymbol{u}_{pre,1} = \boldsymbol{0} \rightarrow \boldsymbol{u}_{pre,1} = -\left(\boldsymbol{K}_S^{(-1)} \boldsymbol{C}_S s + \boldsymbol{I}\right) \boldsymbol{w} \tag{16}$$

Through (16), the road excitation terms in (14) are equal and opposite to the preview control action $\boldsymbol{u}_{pre,1}$. Similarly, based on (15), the preview term $\boldsymbol{u}_{pre,2}$ that compensates the unsprung mass dynamics is given by:

$$-\boldsymbol{K}_S \boldsymbol{u}_{pre,2} - (\boldsymbol{T}_{BA} \boldsymbol{C}_S s + \boldsymbol{T}_{BA} \boldsymbol{K}_S) \boldsymbol{w} = \boldsymbol{0} \rightarrow \boldsymbol{u}_{pre,2} - \left(\boldsymbol{K}_S^{(-1)} \boldsymbol{M}_U s^2 + \boldsymbol{K}_S^{(-1)} \boldsymbol{C}_S s + \boldsymbol{I}\right) \boldsymbol{w} \tag{17}$$

If the unsprung mass is neglected, i.e., $\boldsymbol{M}_U = \boldsymbol{0}$, (16) and (17) are the same ($\boldsymbol{u}_{pre,1} = \boldsymbol{u}_{pre,2}$).

The road preview implementations proposed in Streiter (2008) and Schindler (2009) are more complex than those in (16)-(17), although they are based on the same principle. In fact, the control action vector, $\boldsymbol{i}$, consists of the sum of three contributions:

$$\boldsymbol{i} = \boldsymbol{i}_{reg} + \boldsymbol{i}_{comp} + \boldsymbol{i}_{pre} \tag{18}$$

where $\boldsymbol{i}_{reg}$ is the feedback control action of the system dynamics resulting from unknown road irregularities; $\boldsymbol{i}_{comp}$ compensates the pitch and heave motions caused by the traction and braking forces; and $\boldsymbol{i}_{pre}$ is the preview term. On top of the assumption $\boldsymbol{M}_U = 0$, the implementation in Schindler (2009) considers the tyre force equal to the suspension spring force, i.e., the formulation neglects the effect of the shock absorbers on tyre deflection, which is thus given by:

$$\boldsymbol{z}_{rel,RW} \approx (\boldsymbol{K}_S + \boldsymbol{K}_T)^{-1} \boldsymbol{K}_S \left(\boldsymbol{T}_{BA}^T \begin{bmatrix} z_B \\ \theta_B \end{bmatrix} - \boldsymbol{u} - \boldsymbol{w} \right) \tag{19}$$

Hence, by substituting (19) into (14), the system dynamics are described by:

$$\begin{aligned} &\left(\boldsymbol{I}_B s^2 + \boldsymbol{T}_{BA} \boldsymbol{C}_S \boldsymbol{T}_{BA}^T s + \boldsymbol{T}_{BA} \boldsymbol{K}_S \boldsymbol{T}_{BA}^T\right) \begin{bmatrix} z_B \\ \theta_B \end{bmatrix} \\ &= (\boldsymbol{T}_{BA} \boldsymbol{C}_S s + \boldsymbol{T}_{BA} K_S) \left\{ (\boldsymbol{K}_S + \boldsymbol{K}_T)^{-1} \boldsymbol{K}_S \left(\boldsymbol{T}_{BA}^T \boldsymbol{K}_S \begin{bmatrix} z_B \\ \theta_B \end{bmatrix} - \boldsymbol{u} - \boldsymbol{w} \right) \right\} + (\boldsymbol{T}_{BA} \boldsymbol{C}_S s + \boldsymbol{T}_{BA} K_S) \boldsymbol{w} + \boldsymbol{T}_{BA} \boldsymbol{K}_S \boldsymbol{u} + \begin{bmatrix} F_Z \\ M_N \end{bmatrix} \end{aligned} \tag{20}$$

By substituting $\boldsymbol{u} = \boldsymbol{K}_{PL}\, \boldsymbol{i}/s$ into (20), the equation structure becomes:

$$\left(\boldsymbol{A}_3 s^3 + \boldsymbol{A}_2 s^2 + \boldsymbol{A}_1 s\right) \begin{bmatrix} z_B \\ \theta_B \end{bmatrix} = \boldsymbol{B}_0 \left(\boldsymbol{i}_{reg} + \boldsymbol{i}_{comp} + \boldsymbol{i}_{pre}\right) + \left(\boldsymbol{C}_2 s^2 + \boldsymbol{C}_1 s\right) \boldsymbol{w} + s \begin{bmatrix} F_Z \\ M_N \end{bmatrix} \tag{21}$$

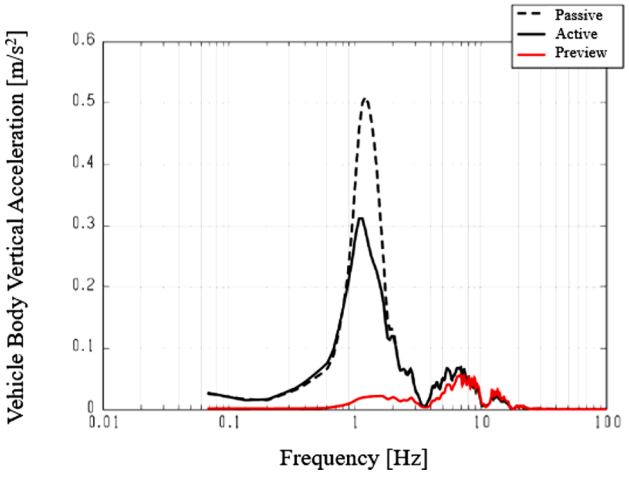

Fig. 6. Simulation results of vehicle body vertical acceleration frequency content on a ride comfort assessment road for: i) the passive set-up ('Passive'); ii) the vehicle with the active suspension controller with feedback contribution only ('Active'); and iii) the vehicle with the integrated preview strategy ('Preview'). Reproduced from Schindler (2009).

where A_1, A_2, A_3, B_0, C_1 and C_2 and are the resulting coefficients in matrix form. The regulator is formulated as:

$$i_{reg} = \frac{(K_{BS2}s^2 + K_{BS1}s)s^2\begin{bmatrix} z_B \\ \theta_B \end{bmatrix} + K_I\left(T_{BA}^T\begin{bmatrix} z_B \\ \theta_B \end{bmatrix} - w\right)}{\{T_{BA}(K_S + K_T)^{-1}K_SK_TK_{PL}\}(T_{K4}s^4 + T_{K3}s^3 + T_{K2}s^2 + T_{K1}s + I)} \tag{22}$$

where the matrices K_{BS1}, K_{BS2}, K_I, T_{K1},…, T_{K4}, represent its tuning parameters. The regulator is based on the heave and pitch accelerations of the sprung mass, see the first term of the numerator of (22), and the front and rear suspension displacements, see the second term of the numerator of (22), and is designed to achieve a desired free response of the system, i.e., through pole placement. By substituting the regulator equation into (21), defining $N_{reg} = T_{K4}s^4 + T_{K3}s^3 + T_{K2}s^2 + T_{K1}s + I$, and expanding the resulting terms, the system dynamics are given by:

$$\{N_{reg}[I_Bs^3 + T_{BA}C_ST_{BA}^Ts^2 + T_{BA}(K_S + K_T)^{-1}K_SK_TT_{BA}^Ts] - K_{BS2}s^4 - K_{BS1}s^3 - K_IT_{BA}^T\}\begin{bmatrix} z_B \\ \theta_B \end{bmatrix} = \{N_{reg}T_{BA}[C_Ss^2 + (K_S + K_T)^{-1}K_SK_Ts] - K_I\}w$$
$$+N_{reg}T_{BA}(K_S + K_T)^{-1}K_SK_TK_{PL}(i_{comp} + i_{pre}) + N_{reg}s\begin{bmatrix} F_Z \\ M_N \end{bmatrix} \tag{23}$$

The term i_{comp} is designed to compensate the heave force and pitch moment caused by the traction and braking forces:

$$N_{reg}T_{BA}(K_S + K_T)^{-1}K_SK_TK_{PL}i_{comp} + N_{reg}s\begin{bmatrix} F_Z \\ M_N \end{bmatrix} = 0 \rightarrow i_{comp}$$
$$= -\left(T_{BA}(K_S + K_T)^{(-1)}K_SK_TK_{PL}\right)^{(-1)}s\begin{bmatrix} F_Z \\ M_N \end{bmatrix} \tag{24}$$

With the inclusion of i_{comp} given by (24), the structure of the dynamic equation of the system becomes

$$N_{GRK}\begin{bmatrix} z_B \\ \theta_B \end{bmatrix} = Z_{GRK}w + N_{reg}T_{BA}(K_S + K_T)^{-1}K_SK_TK_{PL}i_{pre} \tag{25}$$

where N_{GRK} and Z_{GRK} condense the relevant terms of (23). Similarly to what discussed for (16) and (17), the scope of the preview term, $i_{pre,int}$, in the integrated controller is to compensate the effect of the road elevation term w in (25), which results in:

$$i_{pre,int} = -\{N_{reg}T_{BA}(K_S + K_T)^{-1}K_SK_TK_{PL}\}^{-1}Z_{GRK}\ w = -\{N_{reg}T_{BA}(K_S + K_T)^{-1}K_SK_TK_{PL}\}^{-1}\{N_{reg}T_{BA}[C_Ss^2 + (K_S + K_T)^{-1}K_SK_Ts] - K_I\}w \tag{26}$$

(26) is the preview-based feedforward control law. Its integration with the closed-loop control system occurs through its dependency on N_{reg} and Z_{GRK} . Animportant observation is that this feedforward preview algorithm only considers the compensation of the expected road elevation at the next control action application time; the controller does not directly use multiple points along the road profile ahead, i.e., the benefit of preview is not achieved at its full extent. Nevertheless, in the higher level of the control structure, the algorithm generating the road elevation profile for (26) could consider some form of filtering based on multiple measurement points.

Fig. 6 reports simulation results for a typical road profile for ride comfort assessment. The vertical acceleration response of the vehicle body with the proposed strategy is compared with that of the active controller without preview contribution, and the one of the same vehicle with passive suspension system. The preview strategy allows a significant ride comfort improvement, especially around the first resonance frequency of the vehicle body, while slight improvements occur in the secondary ride frequency range. Streiter and Schindler also validated the algorithm through experiments on the Mercedes-Benz F700 demonstrator vehicle. The results of a test run on a ride comfort assessment road, see Fig. 7, show a ~100% reduction in the *RMS* value of the vertical acceleration of the vehicle body for frequencies <3 Hz.

Many other road preview strategies based on non-optimal control are available in the literature, in the form of feedback (FB) controllers, in many cases supported by a feedforward (FF) contribution, according to FF+FB arrangements. An exception is represented by Yamamoto et al., and Buma (2014), which considers only the feedforward contribution. The adopted algorithms include conventional proportional integral derivative (PID) controllers, fuzzy logic implementations, neural networks, and rule-based algorithms, often combined in hybrid arrangements.

Yamamoto et al. (2014) proposes a feedforward force compensator for an active system with an electric rotary actuator on the front anti-roll bar, and linear electromechanical actuators in parallel to the spring and damper on each rear corner. Even though a feedback contribution is not considered, the results of 4-poster rig experiments show significant improvements in roll behaviour, with a 10 dB reduction of the response magnitude near the vehicle body resonance frequency in comparison with the passive case.

Examples of PID-based strategies for preview-augmented suspension control are presented in Fukuda et al. (2004), Oraby et al. (2007), Soliman and Crolla (2001), and Feng et al. (2009). Soliman and Crolla (2001) proposes an adaptive control scheme for active suspensions with limited bandwidth. A wheelbase preview controller adjusts the gains as functions of the front vehicle body acceleration. Vehicle simulations show that preview augmentation brings an average reduction of the vertical body acceleration ranging from 4.5% to 14.5%, depending on the preview time. Fukuda et al. (2004) studies the control of the inclination angle, i.e., of roll and pitch angles, applied to a rough terrain vehicle with interconnected active suspensions. The algorithm uses a proportional derivative (PD) controller based on the angle error, i.e., the difference between the reference angles and the actual angles, where the actual angles are corrected through the output of a preview contribution, based on the measured ground profile in front of the vehicle. Oraby et al. (2007) deals with a hydro-pneumatic active suspension system with a 6 Hz bandwidth. The road holding performance benefit brought by the combination of a PD controller and an FF compensator based on a

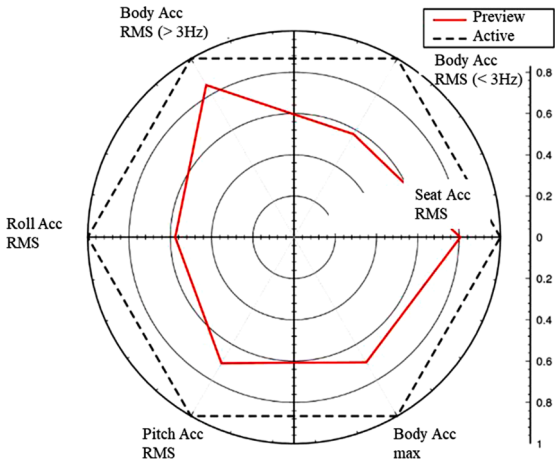

Fig. 7. Experimental results on a Mercedes-Benz demonstrator vehicle on a ride comfort assessment road for: i) the integrated preview strategy ('Preview'); and ii) the active suspension controller with the feedback contribution only ('Active'). Reproduced from Schindler (2009).

half car model is assessed in terms of vehicle handling. Feng et al. (2009) proposes a so-called single neuron PID controller for a semi-active suspension system with wheelbase preview, in which the PID gains are adjusted online, and do not rely on accurate vehicle modelling. Simulation results on a half vehicle model show up to 10% ride comfort performance improvements, in comparison with the case without preview.

Fuzzy logic algorithms are well-known for their simple and flexible design, which is suitable to control non-linear systems, such as semi-active suspensions. Kaldas et al., and Küçükay (2014) discusses a rule-based fuzzy feedforward controller for semi-active suspensions, which calculates the reference actuator force starting from the current and previewed road displacements. The FF contribution is summed to a feedback contribution that depends on vertical body acceleration and velocity. Fig. 8 shows the simulation results on a rough road, including the comparison with the conventional semi-active (without preview) suspension controller, and the passive set-up. With respect to the case without preview, the results highlight a 30% improvement in ride comfort around the vehicle body resonance peak, at the price of a response deterioration in proximity of the wheel hop resonance frequency. Desikan and Kalaichelvi (2015) proposes a fuzzy logic controller to select the damping coefficient of a semi-active suspension system with preview input elaborated from an image processing sensor. Fuzzy logic and PID control schemes are integrated in in the implementation in J. Zhao et al. (2019), based on wheelbase preview and the wavelet noise filter theory. The dominating control method is determined through switching, depending on the dynamic states of the system. When the sprung mass acceleration of the rear suspension exceeds a predefined threshold, the fuzzy logic algorithm takes effect; otherwise, the PID contribution dominates the control process.

Langlois and Anderson (1995), Langlois et al., and Anderson (1992), and Yeh and Tsao (1994) propose zero-force or force cancellation schemes, which aim to isolate the vehicle body from the dynamic loads resulting from relatively small terrain irregularities, i.e., to produce a zero net vertical force at each corner of the vehicle for small road disturbances. An off-road vehicle application is considered in Langlois et al. (1992), and Langlois and Anderson (1995). In the words of the authors, "the preview information is used to increase the transmitted force and the damping proportionally with the average height of the disturbance." Simulation results confirm that the controller provides better acceleration and pitch performance than a linear quadratic controller based on a quarter car model, but only over specific road shapes (small discrete bumps). Yeh and Tsao (1994) describes a similar control concept for active suspensions, defined as force cancellation scheme. According to the study, if the sprung mass is completely isolated by the force cancellation control scheme, the unsprung mass tends to show unstable behaviour, due to the low dissipative characteristics of the tyres. Thus, a virtual damper concept is proposed for attenuating tyre deflection, which is enhanced by a fuzzy preview contribution to limit actuator stroke.

In conclusion, non-optimal controllers have been constantly investigated by academia and industry, and they still attract significant attention, thanks to their relative ease of design and calibration. Furthermore, the FF+FB configurations are characterised by a high level of modularity, as the reference values obtained with different control modules can be simply summed to evaluate the resulting actuator command. However, the level of their design and calibration complexity

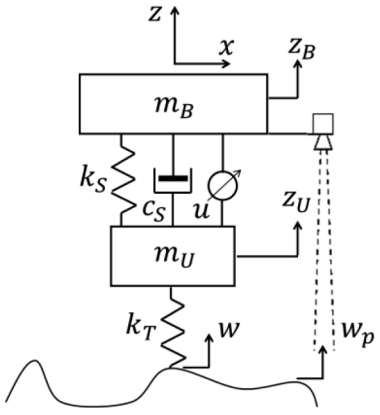

Fig. 9. Schematic of the quarter car model with active suspension actuator in parallel with the passive components.

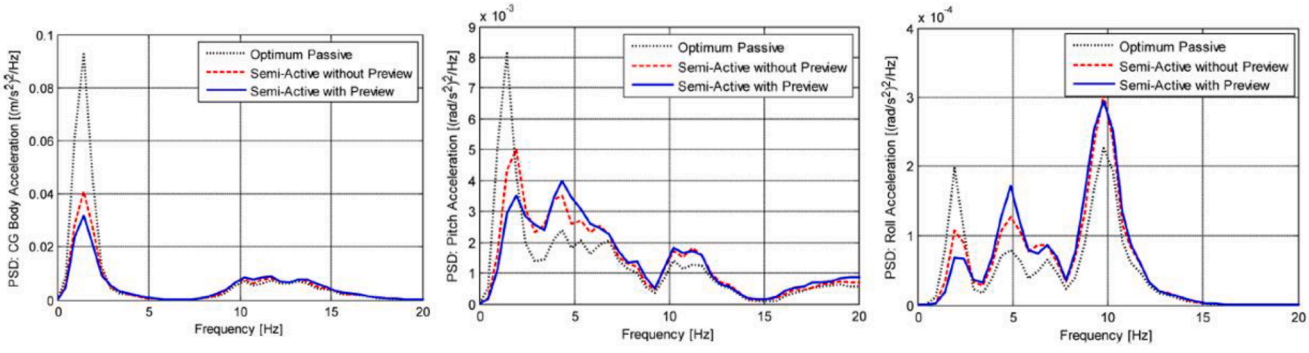

Fig. 8. Simulation results of the power spectral density (PSD) of the vehicle body heave, pitch and roll accelerations on a rough road profile for the passive set-up ('Optimum Passive'), and the semi-active suspension set-up without ('Semi-Active without Preview') and with ('Semi-Active with Preview') road preview. Reproduced with permission from Kaldas et al. (2014).

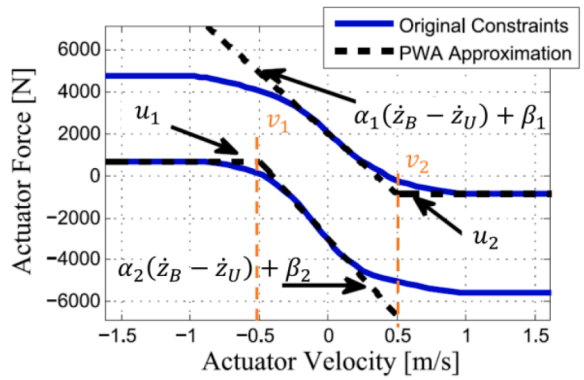

Fig. 10. Nonlinear constraints on semi-active actuator operating range and piecewise affine (PWA) approximation. Inspired by De Bruyne et al. (2012).

can drastically increase when increasing the number of degrees of freedom of the respective model for control system design.

5. Optimal controllers

5.1. Models for control design and cost functions

Optimal road-preview-based suspension controllers aim to find a control law that minimises a cost function, which typically addresses multiple objectives. In H_∞ formulations, the optimality refers to the criteria related to the specific H_∞ optimisation method, which deals with the robustness of the resulting controller (see details in Skogestad & Postlethwaite, 2007), but is not directly related to the vehicle performance aspects. On the contrary, the cost functions of LQR/LQG and MPC formulations directly target ride comfort and vehicle dynamics performance improvements.

Optimal controllers use simplified model formulations to derive the control law that minimises the selected cost function. To this purpose, a frequently adopted model is the two-degree-of-freedom quarter car model with controllable suspension, see Fig. 9. The linear system dynamics are described by:

$$\begin{aligned} &m_B\ddot{z}_B + k_S(z_B - z_U) + c_S\left(\dot{z}_B - \dot{z}_U\right) - u = 0 \\ &m_U\ddot{z}_U + k_S(z_U - z_B) + k_T(z_U - w) + c_T\left(\dot{z}_U - \dot{z}_B\right) + u = 0 \end{aligned} \tag{27}$$

where m_B is the sprung mass of the quarter car model; m_U is the unsprung mass; k_S, k_T and c_S are the passive suspension spring stiffness, vertical tyre stiffness, and passive suspension damping coefficient; z_U is the vertical displacement of the unsprung mass; w is the road elevation; and u is the force generated by the suspension actuator, located in parallel with the passive spring and damper, in a more frequent and alternative layout with respect to the one in Fig. 5. Several variants are possible; for example, in many implementations, the passive damper is absent, as the damping effect is obtained through the actuator. (27) is the linear form of the quarter car model; however, the real experimental characteristics of passive automotive shock absorbers are highly nonlinear with speed, i.e., the gradient of the force decreases with the absolute value of damper speed, and the magnitude of the force is larger during the damper extension motion than during the compression motion for the same absolute value of damper speed (Reimpell et al., 2001). Also, specific formulations and restrictions are imposed on u in case of semi-active actuators, which must satisfy the condition $u(\dot{z}_U - \dot{z}_B) \geq 0$. In these implementations, the maximum and minimum achievable force levels are nonlinear functions of actuator speed. For instance, De Bruyne et al., and Swevers (2012) includes the following approximated state dependent actuator constraints to consider the semi-active actuator limitations within the optimal control problem formulation (see Fig. 10):

$$\begin{aligned} &u_1 \leq u \leq \alpha_1(\dot{z}_B - \dot{z}_U) + \beta_1 && \text{if } (\dot{z}_B - \dot{z}_U) < v_1 \\ &\alpha_2(\dot{z}_B - \dot{z}_U) + \beta_2 \leq u \leq \alpha_1(\dot{z}_B - \dot{z}_U) + \beta_1 && \text{if } v_1 \leq (\dot{z}_B - \dot{z}_U) < v_2 \\ &\alpha_2(\dot{z}_B - \dot{z}_U) + \beta_2 \leq u \leq u_2 && \text{if } (\dot{z}_B - \dot{z}_U) \geq v_2 \end{aligned} \tag{28}$$

where u_1, u_2, α_1, α_2, β_1, β_2, v_1, and v_2 are tuning parameters.

For example, the quarter car model set-up is adopted by Akbari and Lohmann (2008, 2010), Akbari et al., and Lohmann (2010), Asl and Rideout (2010), De Bruyne et al. (2012), Gordon and Sharp (1998), Hać (1992, 1994), Hać and Youn (1992), Karlsson et al., and Hrovat (2001), Pearce and Thompson (2004), Prokop and Sharp (1995), Rahman and Rideout (2012), Roh and Park, (1998), Savaresi and Silani (2004), Savaresi et al. (2010), Theunissen et al. (2020), Thompson and Pearce, 2001b, 2003), Ursu et al., and Vladimirescu (1997), and Van Der Aa et al. (1997). Multiple quarter car models can be obviously used within the same control structure, e.g., the wheelbase preview controller of Roh and Park (1998) is based on two dynamically decoupled quarter car models, representing the front and rear suspension system dynamics.

Optimal preview suspension controllers can also be based on more advanced vehicle models with higher number of degrees of freedom than the quarter car model, i.e.: i) half car models, including consideration of the heave and pitch dynamics of the sprung mass, and the vertical dynamics of the front and rear unsprung masses (four degrees of freedom), see the schematics in Figs. 5 and 11, and the control implementation examples in Gopala Rao and Narayanan (2008), Kaldas and Soliman (2014), Martinus et al. (1996), Marzbanrad et al. (2004), Mehra et al., and Gopalasamy (1997), Prabakar et al. (2009), Thompson and Pearce (1998, 2001a), and Thompson and Davis (2003, 2005); and ii) full car models, which also include the roll dynamics, and therefore can account for the effect of the anti-roll bars as well. Examples of full-car-model-based controllers are in Donahue and Hedrick (2001), Göhrle et al. (2012), 2013, 2014, 2015), Kim et al., and Park (2002), Ulsoy et al. (2012), Youn et al. (2014), and Yoshimura et al., and Ananthanarayana (1993).

In LQR/LQG and MPC implementations, optimisation criteria may include ride comfort, road holding, suspension travel, and actuator energy consumption, which can be weighted within the cost function, to achieve appropriate trade-offs.

A typical cost function J for optimal suspension control based on the quarter car model is (Rahman & Rideout, 2012):

$$J = \lim_{T\to\infty}\frac{1}{2T}\int_0^T E\left[\rho_1\ddot{z}_B^2 + \rho_2(z_U - w)^2 + \rho_3(z_B - z_U)^2 + \rho_4 u^2\right]\mathrm{d}t \tag{29}$$

where the notation E denotes the expected value within a stochastic framework; the coefficients ρ_i, $i = 1{:}4$, are the weighting factors,

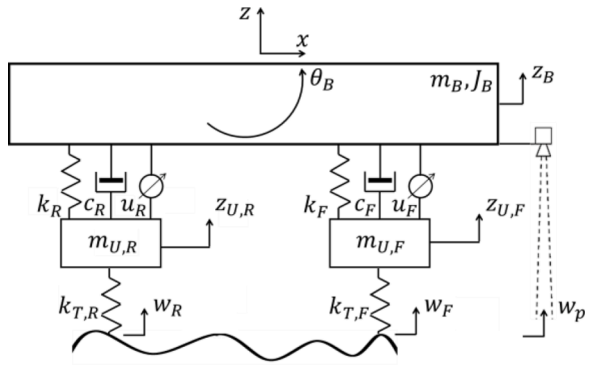

Fig. 11. Schematic of the half car model with active suspension actuators in parallel with the passive components.

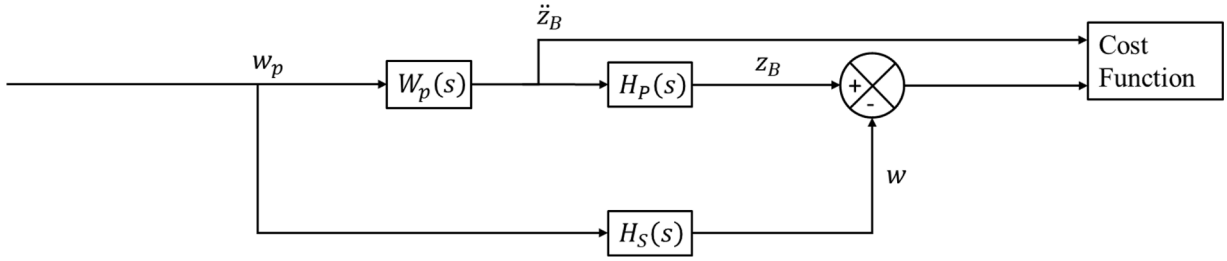

Fig. 12. Block diagram of the Wiener filter design routine for preview-augmented suspension systems. Inspired by Bender (1968).

respectively for ride comfort, handling, suspension stroke, and actuator effort; and T is the time horizon for the computation of J. Most of the LQR/LQG and MPC suspension controllers based on quarter car models use cost functions similar to the quadratic form described in (29), or subsets of this general form, which is also typical of controllers without road preview, e.g., see the examples of conventional optimal suspension controllers in Chen et al., and Yao (2012); Elmadany and Abduljabbar (1999); Sharkawy (2005), and Thompson and Davis (2000). Alternative cost function formulations have been used in the literature; for example, Ahmed and Svaricek (2014) penalises the vehicle body heave position, while, instead of tyre deflection, Hać (1994) adopts the vertical speed of the unsprung mass as cost function term related to the handling target.

Among the studies considering half and full car models, a typical example of cost function is given by Youn et al. (2014):

$$J=\lim_{T\to\infty}\frac{1}{2T}\int_0^T E\left[\rho_{1,z}\ddot{z}_B^2+\rho_{1,\theta}\ddot{\theta}_B^2+\rho_{1,\phi}\ddot{\phi}_B^2+\sum_{m=1}^{4}\rho_{2,m}\left(z_{U,m}-w\right)^2+\sum_{m=1}^{4}\rho_{4,m}u_m^2\right]\mathrm{d}t \tag{30}$$

where the coefficients $\rho_{1,z}$, $\rho_{1,\theta}$, $\rho_{1,\phi}$, $\rho_{2,m}$ and $\rho_{3,m}$ are the weighting factors, respectively for heave acceleration $\ddot{z}_B$, pitch acceleration $\ddot{\theta}_B$, roll acceleration $\ddot{\phi}_B$, vehicle handling, and actuator effort; and the index m indicates the vehicle corner. Alternative cost functions are included in Yoshimura et al. (1993), which proposes a cost function including heave, roll and pitch displacement as well as suspension travel, for a rail vehicle application; and in the linear quadratic implementation of Donahue and Hedrick (2001), which penalises chassis acceleration, pitch rate, roll rate, unsprung mass velocity, and control effort. The formulations in (29) and (30) refer to a time interval that tends to infinity; however, although this is typical of LQR/LQG controllers, MPC implementations consider finite time intervals.

The following subsections discuss the details of the main optimal controller formulations for suspension control with road preview.

5.2. Wiener-filter-based controllers

Although they are not use anymore in the recent studies on road preview suspension control, Wiener-filter-based controllers have been rather extensively evaluated for the pioneering suspension control implementations with road preview, and therefore are included in this literature review. In particular, Bender (1968) was the first to propose a preview-based suspension controller using the Wiener filter theory. The control design routine aims to find the optimal closed-loop transfer function, $W_p(s)$, that guarantees the minimum value of a cost function based on a quarter car model, see Fig. 12. The solution for the optimal preview-based synthesized suspension controller and vehicle dynamics transfer function, $W_p(s)$, is obtained through variational calculus:

$$W_p(s)=\frac{[\Gamma(s)/\Delta^-(s)]_+}{\Delta^+(s)} \tag{31}$$

in which $\Gamma(s)$ and $\Delta(s)$ are defined as:

$$\begin{aligned}\Gamma(s)&=2\pi H_P(s)H_S(-s)\Phi(s)\\ \Delta(s)&=2\pi[H_P(s)H_P(-s)+\rho]\Phi(s)\end{aligned} \tag{32}$$

where $H_P(s)$ is the body acceleration to vertical displacement transfer function (i.e., a double integrator); $H_S(s)$ is the sensor delay transfer function; $\Phi(s)$ is the power spectral density of the road profile; and ρ is a weighting factor to emphasise ride comfort or handling. The plus and minus superscripts of the factors $\Delta^+(s)$ and $\Delta^-(s)$ in (31) indicate that only the poles and zeros of $\Delta(s)$ respectively in the left half side and right half side of the complex plane are to be retained. The notation '$[]_+$' in (31) designates the terms of the transfer function corresponding to poles in the left half complex plane.

Since the synthesised transfer function from (31)-(32) is very difficult to be experimentally implemented via an appropriate mechatronic system, Bender (1968) also proposes a parameter search technique to optimise a fixed-structure controller, which is more easily implementable in practice. Bender's simulation results on a single-degree-of-freedom quarter car model, i.e., excluding the unsprung mass dynamics, reveal a sixteen-fold potential reduction in the *RMS* values of the heave acceleration. The follow-up studies in Iwata and Nakano (1976) and Sakami et al. (1976) extended Bender's technique to the half car model.

5.3. Linear quadratic controllers

Linear quadratic regulators (LQR) and linear quadratic Gaussian (LQG) controllers (also referred to as LQ controllers in the remainder) are based on the assumption of linear time-invariant systems and quadratic cost functions, which ensures the convexity of the optimisation problem.

Hać (1992) provides an introduction to the deterministic linear quadratic problem (LQR) formulation and solution for suspension control with road preview, which is based on the following generic state space formulation of the model of the system:

$$\dot{\boldsymbol{x}}=\boldsymbol{A}\boldsymbol{x}+\boldsymbol{B}\boldsymbol{u}+\boldsymbol{D}\boldsymbol{w} \tag{33}$$

where $\boldsymbol{x}$ is the state vector; $\boldsymbol{u}$ is the control input; $\boldsymbol{w}$ is the road disturbance vector, including either a single value for each considered axle if the tyre is modelled as a spring, or road elevation and elevation rate for each axle when the vertical tyre damping is not neglected; and $\boldsymbol{A}$, $\boldsymbol{B}$, and $\boldsymbol{D}$ are the state space matrices containing the system parameters. In typical LQ systems, the cost function J is expressed with the following matrix formulation for infinite time horizon:

$$J=\lim_{T\to\infty}\frac{1}{2T}\int_0^T\left(\boldsymbol{x}^T\boldsymbol{Q}_1\boldsymbol{x}+2\boldsymbol{x}^T\boldsymbol{N}\boldsymbol{u}+\boldsymbol{u}^T\boldsymbol{R}_1\boldsymbol{u}+2\boldsymbol{x}^T\boldsymbol{Q}_{12}\boldsymbol{w}+\boldsymbol{w}^T\boldsymbol{Q}_2\boldsymbol{w}\right)\mathrm{d}t \tag{34}$$

where $\boldsymbol{Q}_1$, $\boldsymbol{N}$, $\boldsymbol{R}_1$, $\boldsymbol{Q}_{12}$ and $\boldsymbol{Q}_2$ are symmetric, time-invariant matrices containing system parameters and weighting factors. The last term in (34) can be neglected, since road irregularities are independent from the control input $\boldsymbol{u}$. The finite time cost function formulation, of which (34) is the limit case for $T\to\infty$, can be expressed as:

$$J = \frac{1}{2}\boldsymbol{x}^T(T)\boldsymbol{P}_T\boldsymbol{x}(T) + \frac{1}{2}\int_{t_0}^{T}\left(\boldsymbol{x}^T\boldsymbol{Q}_1\boldsymbol{x} + 2\boldsymbol{x}^T\boldsymbol{N}\boldsymbol{u} + \boldsymbol{u}^T\boldsymbol{R}_1\boldsymbol{u} + 2\boldsymbol{x}^T\boldsymbol{Q}_{12}\boldsymbol{w} + \boldsymbol{w}^T\boldsymbol{Q}_2\boldsymbol{w}\right)\mathrm{d}t \tag{35}$$

where t_0 is the initial time; T is the final finite time of the optimal control problem; and $\boldsymbol{P}_T$ contains weighting factors. The structure of the cost functions in (34) and (35) permits to include all the terms of the vehicle-oriented formulations in (29) and (30).

The solution $\boldsymbol{u}^*(t)$ of the deterministic optimal linear preview control problem consists of a state feedback term, i.e., function of $\boldsymbol{x}(t)$, and a feedforward contribution, $\boldsymbol{r}(t)$, which depends on the measured road disturbance, $\boldsymbol{w}(t)$:

$$\boldsymbol{u}^*(t) = -\boldsymbol{R}_1^{-1}\left[\left(\boldsymbol{N}^T + \boldsymbol{B}^T\boldsymbol{P}(t)\right)\boldsymbol{x}(t) + \boldsymbol{B}^T\boldsymbol{r}(t)\right] \tag{36}$$

where $\boldsymbol{P}(t)$ is found recursively by solving the Riccati differential equation:

$$-\dot{\boldsymbol{P}} = \boldsymbol{P}\boldsymbol{A}_n + \boldsymbol{A}_n^T\boldsymbol{P} - \boldsymbol{P}\boldsymbol{B}\boldsymbol{R}_1^{-1}\boldsymbol{B}^T\boldsymbol{P} + \boldsymbol{Q}_1 - \boldsymbol{N}\boldsymbol{R}_1^{-1}\boldsymbol{N}^T,\ \boldsymbol{P}_T = \boldsymbol{P}(T) \tag{37}$$

in which $\boldsymbol{A}_n = \boldsymbol{A} - \boldsymbol{B}\boldsymbol{R}_1^{-1}\boldsymbol{N}^T$. $\boldsymbol{r}(t)$ is also calculated recursively by solving the following Hamilton-Jacobi differential equation:

$$-\dot{\boldsymbol{r}}(t) = \left[-\boldsymbol{A}_n^T + \boldsymbol{P}(t)\boldsymbol{B}\boldsymbol{R}_1^{-1}\boldsymbol{B}^T\right]\boldsymbol{r}(t) - \left[\boldsymbol{P}(t)\boldsymbol{D} + \boldsymbol{Q}_{12}\right]\boldsymbol{w}(t),\ \boldsymbol{r}(t_r) = \boldsymbol{0} \tag{38}$$

where:

$$t_r = \min(t + t_h, T) \tag{39}$$

in which t_h is the preview time of the road profile measurements ahead.

(37) requires recursive calculations at each time step. However, when assuming infinite horizon, i.e., $T\to\infty$, $\dot{\boldsymbol{P}} = \boldsymbol{0}$ holds, and the value of $\boldsymbol{P}$, indicated as $\overline{\boldsymbol{P}}$ in this specific case, is only computed once by solving the algebraic Riccati equation resulting from (37). Under the assumption $T\to\infty$, for a preview-based suspension controller where the road unevenness $\boldsymbol{w}(t)$ is available up to a time t_h ahead of the current time t, the feedforward term can be explicitly expressed as:

$$\boldsymbol{r}(t) = \int_0^{t_h} e^{\boldsymbol{A}_c^T\sigma}\left(\overline{\boldsymbol{P}}\boldsymbol{D} + \boldsymbol{Q}_{12}\right)\boldsymbol{w}(t+\sigma)\mathrm{d}\sigma \tag{40}$$

where $\boldsymbol{A}_c = \boldsymbol{A}_n - \boldsymbol{B}\boldsymbol{R}_1^{-1}\boldsymbol{B}^T\overline{\boldsymbol{P}}$ represents the closed-loop system matrix; and σ is the integration time. The important result in (40), which is the widely used solution in the literature, means that even if the model formulation in (33) considers a single road elevation point, the feedforward term in (40) includes the road elevation profile along the preview time, which, in the opinion of the authors, is a major benefit with respect to the feedforward formulations in Section 4 (see also the analysis of the effect of the preview time in Section 6).

The result of the stochastic linear optimal preview control problem (LQG) can be found in a similar way, with the main difference being the estimation of $\boldsymbol{x}(t)$ and $\boldsymbol{r}(t)$ through an appropriate Kalman filter. Hać (1992) and Hać and Youn (1992) use a stochastic optimal linear problem approach for preview-based high-bandwidth active and semi-active suspensions, and consider a two-degree-of-freedom vehicle model, which is excited by different road profiles. The results show that the cost function J value of the semi-active suspension controller with preview on a random road profile is reduced by ~50% in comparison with the passive system, and by ~35% in comparison with the semi-active case without preview. Furthermore, the investigation of the preview time effect reveals a saturation point of the performance index for $t_h \approx 0.3$ s, beyond which the performance does not significantly improve anymore (see Section 6 for more details on this topic). Hać (1994) also proposes a decentralised controller based on the quarter car model, where the decoupling of the vehicle body dynamics and unsprung mass dynamics reduces the computational effort for calculating the optimal actuator force, without compromising performance (discrepancies of less than 2%) with respect to the coupled system. Louam et al., and Sharp (1992) applies the ideas of the overtaking optimality to the LQ problem, to achieve a closed-form solution for suspension control with preview based on linear quarter car and half car models, where the road profile only needs to be bounded and continuous.

The LQ framework for preview suspension control according to (33)-(40) is used in many other studies, each of them with some distinctive features, see Asl and Rideout (2010); Cvok et al., and Hrovat (2020); Elmadany et al. (2011); Gopala Rao and Narayanan (2008); Kaldas and Soliman (2014); Kim et al. (2002); Kwon et al. (2020); Martinus et al. (1996); Marzbanrad et al. (2004); Pearce and Thompson (2004); Rahman and Rideout (2012); Roh and Park (1998); Thompson and Davis (2003, 2005); Thompson and Pearce (1998, 2001a, 2001b, 2003); Thompson et al., and Pearce (1980); Van Der Aa et al. (1997); and Youn et al. (2014). For example, Martinus et al. (1996) applies the preview-based semi-active suspension LQ control concept to the half vehicle model setup. Hać and Youn (1992) and Martinus et al. (1996) include constraints into the semi-active suspension control strategy by clipping the control command according to the operating condition of the considered vehicle corner, which leads to a sub-optimal solution. The force generated by the damper follows the one of the optimal active system, according to (36), when the request meets the damper energy dissipation criteria; otherwise, the damping coefficient is set to one of its limit values, i.e., c_{min} or c_{max}. In particular, by referring to the quarter car model, the clipped damping coefficient is obtained in Hać and Youn (1992) as:

$$c_S = \begin{cases} c_{min} & if\ -u^*\left(\dot{z}_B - \dot{z}_U\right) \le c_{min}\left(\dot{z}_B - \dot{z}_U\right)^2 \\ c_{max} & if\ -u^*\left(\dot{z}_B - \dot{z}_U\right) \ge c_{max}\left(\dot{z}_B - \dot{z}_U\right)^2 \\ -u^*\Big/\left(\dot{z}_B - \dot{z}_U\right) & otherwise \end{cases} \tag{41}$$

where u^* is the optimal solution for an active force generator. Van Der Aa et al. (1997) proposes a clipped LQ solution for a semi-active suspension implementation, and compares it with another controller using a predictive nonlinear model-based approach with hard constraints, which is implemented through sequential quadratic programming, see also Section 6. Roh and Park (1998) adopts the infinite horizon discrete LQR framework based on the half vehicle model with active suspensions, and uses the front axle road input information, estimated by means of a

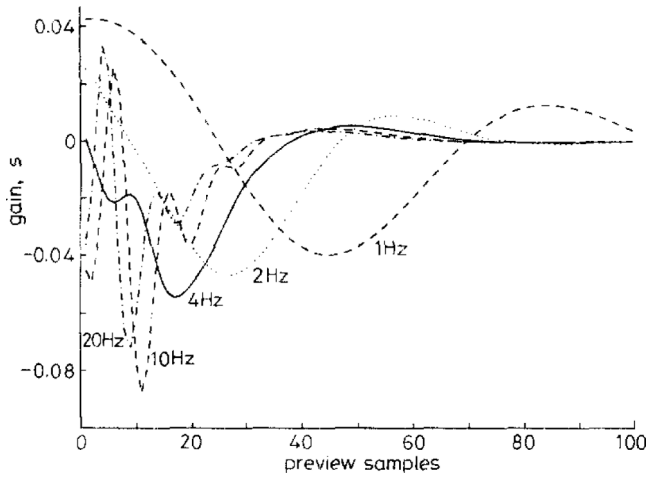

Fig. 13. Gains of the preview control matrix $\boldsymbol{K}_2$, for different preview times (sampling time $T_s = 0.01$ s) and actuator bandwidths. Reproduced with permission from Prokop and Sharp (1995).

disturbance observer, as preview source for the rear axle controller. The method improves system robustness with respect to preview sensor measurement noise. The implementations in Asl and Rideout (2010) and Rahman and Rideout (2012) use an observer for road input estimation based on the lead vehicle response. Marzbanrad et al. (2004) extends the optimal stochastic problem solution proposed by Hać (1992) to the half car model, by also considering the wheelbase preview for the rear axle. Thompson and Pearce (1998) re-define the feedforward preview contribution, $\boldsymbol{r}(t)$, for the two-axle case. Additionally, the studies by Thompson provide the analytical derivations for the direct computation of the cost function and relevant *RMS* values for the quarter car model (Thompson & Davis, 2003; Thompson & Pearce, 2001b) and half car model (Thompson & Davis, 2003, 2005; Thompson & Pearce, 2001a) with optimal active suspension control with preview.

The important studies in Tomizuka (1975, 1976) and Prokop and Sharp (1995) propose a discrete optimal control approach for suspension control with preview. Instead of being considered as an exogenous input like in Hać (1992), in this case the road profile is part of an augmented state vector. By assuming the preview time to be an integer multiple of the sampling time T_s, i.e., $t_h = N_{tp}T_s$, where N_{tp} is the number of preview points, an additional state vector $\boldsymbol{w}_a$, containing all the preview inputs, is introduced and defined through the following discrete equation, where k is the current discretisation step:

$$\boldsymbol{w}_a(k+1) = \boldsymbol{A}_w\boldsymbol{w}_a(k) + \boldsymbol{D}_w\boldsymbol{w}_p(k) \tag{42}$$

with:

$$\boldsymbol{A}_w = \begin{bmatrix} 0 & 1 & 0 & \cdots & 0 \\ 0 & 0 & 1 & \cdots & 0 \\ \vdots & \vdots & \vdots & \ddots & \vdots \\ 0 & 0 & 0 & \cdots & 1 \\ 0 & 0 & 0 & \cdots & 0 \end{bmatrix}, \boldsymbol{D}_w = \begin{bmatrix} 0 \\ \vdots \\ 0 \\ 1 \end{bmatrix} \tag{43}$$

where $\boldsymbol{w}_a(k) = [w_{a1}(k),\ w_{a2}(k),\ \cdots,\ w_{aN_{tp}}(k)]^T = [w(k),\ w(k+1),\ \cdots,\ w(k+N_{tp})]^T$ is the vector of the system inputs that are known in advance, and $w_p(k) = w(k+N_{tp})$ is the new road elevation value measured by the preview sensor or estimation system at each time step $t = kT_s$. $w_p(k)$ is a scalar for a quarter car model without tyre damping, which is the simplified case in Prokop and Sharp (1995) that is reported in (42), while it is a vector if either tyre damping or multiple vehicle corners are considered. The system in (42)-(43) operates as a shift register that delays the information from the preview sensor according to the time it takes to become an actual disturbance input to the suspension system. The augmented system model is expressed by incorporating (42) into the discretised version of (33):

$$\boldsymbol{x}_a(k+1) = \boldsymbol{A}_a\boldsymbol{x}_a(k) + \boldsymbol{B}_a\boldsymbol{u}(k) + \boldsymbol{D}_a w_p(k) \tag{44}$$

where $\boldsymbol{x}_a(k) = [\boldsymbol{x}(k) \quad \boldsymbol{w}_a(k)]^T$ represents the augmented state vector, and $\boldsymbol{A}_a$, $\boldsymbol{B}_a$ and $\boldsymbol{D}_a$ are the augmented matrices of the considered vehicle model formulation.

Based on (44), Prokop and Sharp (1995) express the solution of the optimal control problem as:

$$u(k) = -[\boldsymbol{K}_1 \quad \boldsymbol{K}_2]\begin{bmatrix} \boldsymbol{x}(k) \\ \boldsymbol{w}_a(k) \end{bmatrix} \tag{45}$$

where $\boldsymbol{K}_1$ and $\boldsymbol{K}_2$ are obtained by solving the algebraic Riccati equation. This solution is equivalent to (36), since the gain matrices $\boldsymbol{K}_1$ and $\boldsymbol{K}_2$ correspond to the controller feedback and feedforward contributions. Fig. 13 shows how the optimal feedforward gains are influenced by the suspension actuator bandwidth (in the specific study the actuator dynamics are modelled through two second-order low-pass filters in series with the quarter car model) and number of preview samples (sampling time $T_s = 0.01$ s), while Fig. 14 compares the simulation results of optimal controllers with and without preview, for three settings of the cost function weights. As expected, the performance index curves are monotonically decreasing functions of the actuator bandwidth. Interestingly, a low-bandwidth actuator can provide substantial benefits only if the controller mainly targets ride comfort rather than vehicle handling (indicated as 'ride safety' in the figure) improvement.

In conclusion, LQ control has been one of the most frequently adopted control structures for preview-augmented suspension control, because of its design simplicity and relatively low on-line computational requirements. In fact, the LQ control problem definition relies on the state space formulation of the vehicle model, which can be easily set by vehicle dynamics specialists, and the on-line implementation of the typically adopted LQ controllers only requires a relatively straightforward function evaluation. However, LQ controllers are not able to handle hard constraints, e.g., related to the physical limitations in terms of actuator force and stroke, and their considered implementations for preview-augmented suspension control do not guarantee robustness with respect to model uncertainties and/or external disturbances.

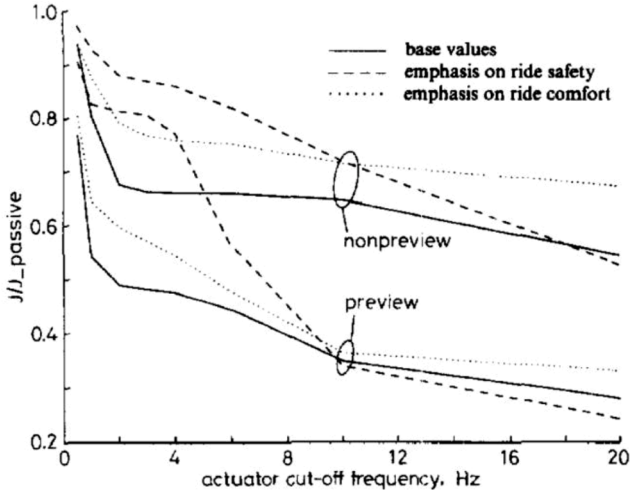

Fig. 14. Normalized cost function values as functions of the actuator cut-off frequency, for optimal controllers with and without preview, and three settings of the weighting factors of the cost function. Reproduced with permission from Prokop and Sharp (1995).

5.4. H_2 and H_∞ controllers

Sensor noise as well as model mismatches and uncertainties are inevitable in the experimental implementation of controlled suspension systems. For example, this effect might be particularly significant for the preview-augmented suspension systems of off-road vehicles, which typically operate on soft surfaces, or rigid surfaces with false profile heights, e.g., caused by soft objects. Also, model mismatches are intrinsic in the very simplified representation of the tyre behaviour in the models for control system design, in which the tyre is usually modelled as a linear spring and – optionally – a linear damper in parallel. An effective solution is represented by robust controllers that guarantee desirable performance even in presence of model uncertainties and parameter variations. In this respect, H_∞ control (Skogestad & Postlethwaite, 2007) became popular in the 1980s and 1990s to overcome the following drawbacks of LQR/LQG approaches:

- Performance deterioration for non-white-noise inputs;
- Performance reduction and potential stability issues in case of model mismatches and state estimation inaccuracies;
- Lack of formal and explicit treatment of hard state constraints, e.g., on suspension travel space in the specific problem of suspension control.

Typical robust suspension control implementations with preview use

a multi-objective output feedback approach, based on the minimization of the H_2 and/or H_∞ norm of the transfer functions from exogenous inputs to relevant outputs. In particular, in the specific application, the H_∞ norm is used to optimise the ride quality, while the generalized H_2 norm is used to deal with the hard constraints on the peak amplitude of specific variables. Before discussing the examples from the literature, a brief introduction to the problem formulation is reported from P. Li et al. (2014a), considering the discrete augmented system in (44), where $\boldsymbol{w}_p(k)$ represents the exogenous input (not necessarily a white noise one). The output variables are defined as:

$$\begin{aligned}\boldsymbol{y}_1(k+1) &= \boldsymbol{C}_{a1}\boldsymbol{x}_a(k) + \boldsymbol{E}_{a1}\boldsymbol{u}(k)\\ \boldsymbol{y}_2(k+1) &= \boldsymbol{C}_{a2}\boldsymbol{x}_a(k) + \boldsymbol{E}_{a2}\boldsymbol{u}(k)\end{aligned} \tag{46}$$

where $\boldsymbol{y}_1$ and $\boldsymbol{y}_2$ represent the output vectors on which to impose soft and hard constraints, respectively, which are expressed as linear functions of the augmented state vector, $\boldsymbol{x}_a(k)$, and actuator input, $\boldsymbol{u}(k)$, through the output matrices $\boldsymbol{C}_{a1}$, $\boldsymbol{C}_{a2}$, $\boldsymbol{E}_{a1}$ and $\boldsymbol{E}_{a2}$. Typically, $\boldsymbol{y}_1$ includes vertical and pitch accelerations for ride quality enhancement, while $\boldsymbol{y}_2$ may include suspension deflection, tyre deformation, and actuator forces.

If $\boldsymbol{T}_1$ and $\boldsymbol{T}_2$ are the transfer functions from the road disturbance $\boldsymbol{w}$ to the outputs $\boldsymbol{y}_1$ and $\boldsymbol{y}_2$, their H_∞ norm and generalized H_2 norm can be expressed as:

$$\begin{aligned}\|\boldsymbol{T}_1\|_\infty &= \sup\frac{\|\boldsymbol{y}_1\|_2}{\|\boldsymbol{w}_2\|}\\ \|\boldsymbol{T}_2\|_2 &= \sup\frac{\|\boldsymbol{y}_2\|_\infty}{\|\boldsymbol{w}_2\|}\end{aligned} \tag{47}$$

By assuming a static feedback controller $\boldsymbol{K}$ of the form:

$$\boldsymbol{u}(k) = \boldsymbol{K}\boldsymbol{C}_a\boldsymbol{x}_a(k) \tag{48}$$

where the matrix $\boldsymbol{C}_a$, given by the composition of $\boldsymbol{C}_{a1}$ and $\boldsymbol{C}_{a2}$, depends on the available measurements and the number of preview points, the closed-loop system is asymptotically stable and satisfies $\|\boldsymbol{T}_1\|_\infty < \gamma_1$ and $\|\boldsymbol{T}_2\|_2 < \gamma_2$, if there exist matrices $\boldsymbol{P}_a > 0$ and $\boldsymbol{K}$ such that:

$$\begin{bmatrix} \boldsymbol{P}_a & \boldsymbol{0} & (\boldsymbol{A}_a + \boldsymbol{B}_a\boldsymbol{K}\boldsymbol{C})\boldsymbol{P}_a & \boldsymbol{D}_a \\ * & \gamma_1\boldsymbol{I} & (\boldsymbol{C}_{a1} + \boldsymbol{E}_{a1}\boldsymbol{K}\boldsymbol{C})\boldsymbol{P}_a & \boldsymbol{0} \\ * & * & \boldsymbol{P}_a & \boldsymbol{0} \\ * & * & * & \gamma_1\boldsymbol{I} \end{bmatrix} > \boldsymbol{0} \tag{49}$$

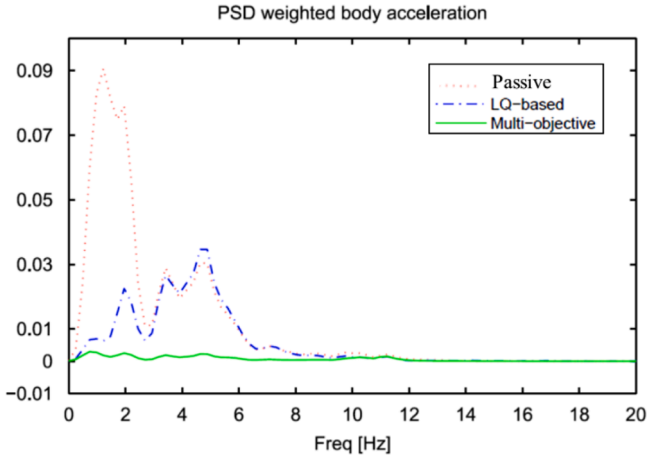

Fig. 15. Power spectral density (PSD) of vertical body acceleration with the multi-objective and LQ-based controllers, for a realistic road input profile. Reproduced with permission from Akbari and Lohmann (2010).

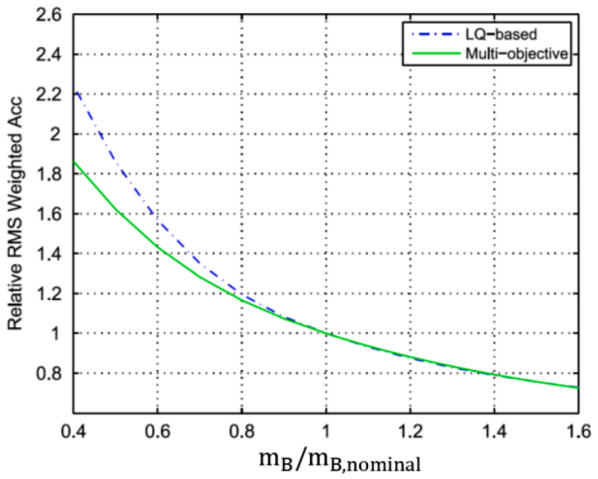

Fig. 16. Relative *WRMS* values of vertical body acceleration for the multi-objective and LQ-based controllers, as functions of the non-dimensional sprung mass value, for a realistic road input profile. Reproduced with permission from Akbari and Lohmann (2010).

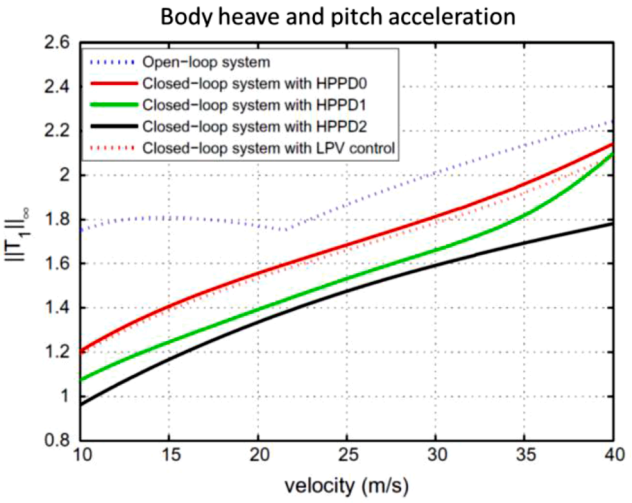

Fig. 17. H_∞ norm of the transfer function $\boldsymbol{T}_1$ from the road input profile to the body vertical and pitch accelerations for the considered configurations, as a function of vehicle speed. Reproduced with permission from P. Li et al. (2014b).

$$\begin{bmatrix} \boldsymbol{P}_a & (\boldsymbol{A}_a + \boldsymbol{B}_a\boldsymbol{K}\boldsymbol{C})\boldsymbol{P}_a & \boldsymbol{D}_a \\ * & \boldsymbol{P}_a & \boldsymbol{0} \\ * & * & \boldsymbol{I} \end{bmatrix} > \boldsymbol{0} \tag{50}$$

$$\begin{bmatrix} \gamma_2\boldsymbol{I} & (\boldsymbol{C}_{a2} + \boldsymbol{E}_{a2}\boldsymbol{K}\boldsymbol{C})\boldsymbol{P}_a \\ * & \boldsymbol{P}_a \end{bmatrix} > \boldsymbol{0} \tag{51}$$

where $\boldsymbol{C}$ is the output matrix for the original model without road preview augmentation. The solution of the matrix inequalities in (49)-(51) requires an iterative procedure. The idea of the control scheme is to characterise model uncertainties as norm-bounded perturbations, and to verify that the stability and performance requirements are achieved for the worst-case uncertainty and road disturbances.

Studies using H_∞ technology for controlled suspensions with road preview were conducted by Akbari and Lohmann (2008, 2010), Akbari

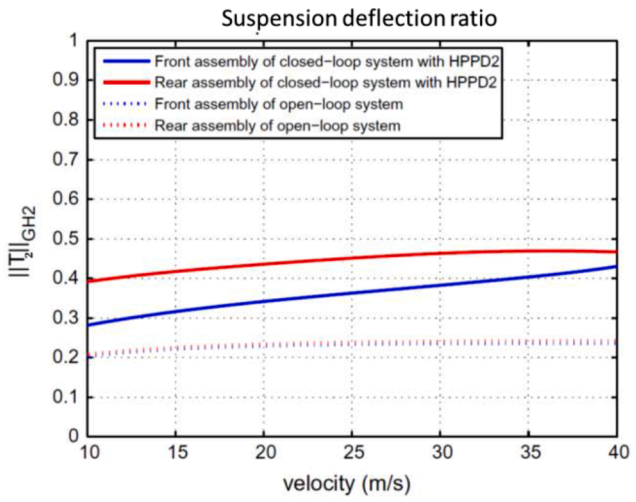

Fig. 18. H_2 norm of the transfer function $\boldsymbol{T}_2$ from the road input profile to the normalised front and rear suspension deflections for the considered configurations, as a function of vehicle speed. Reproduced with permission from P. Li et al. (2014b).

et al. (2010), Z. Li et al. (2015), P. Li et al. (2014a), 2014b, Pang et al., and Xu (2019), Prabakar et al. (2009), Ryu et al. (2011), Ryu et al., and Park (2008)), and Vahidi and Eskandarian (2002). In particular, in the key studies in Akbari et al. (2010) and Akbari and Lohmann (2008, 2010), the idea is to find a controller, referred to as multi-objective controller, minimising the H_∞ norm of the closed-loop transfer function related to the vertical body acceleration, while limiting the H_2 norm of the closed-loop transfer functions related to tyre deflection, suspension excursion, and actuator force. The H_2/H_∞ controller is compared with an LQ implementation through quarter car model simulations. Results on a white noise road profile show similar performance for the two controllers; on the contrary, on a realistic road profile, the H_2 /H_∞ implementation brings a ~30% reduction of the *WRMS* value of the vertical body acceleration, which is confirmed by Fig. 15, reporting the power spectral density (PSD) of the weighted acceleration. Moreover, the H_2/H_∞ controller provides increased robustness with respect to parameter changes, see the sensitivity analysis to vehicle mass variations in Fig. 16, where the multi-objective implementation provides better results than the LQ controller for lower than nominal values of the sprung mass.

P. Li et al. (2014a) extends a similar H_2/H_∞ control design to the case of a half car model, and derives the solution through the iteration of linear matrix inequalities and cone complementarity linearisation algorithms. The results show the performance improvements brought by the increase in the number of preview points. In P. Li et al., and Cheung (2014b), the same authors propose a velocity-dependent multi-objective controller, where the feedback gain matrix depends on the current vehicle speed, which is treated either as time-invariant parameter, in the context of homogeneous polynomial parameter-dependent controllers (HPPDx, where x indicates the order of the adopted polynomial), or as a time-varying parameter, in the framework of a linear parameter varying controller (LPV). In Fig. 17 the three considered HDDP controllers, i.e., HDDP0, HDDP1, and HDDP2, with different orders of the polynomial, and the LPV implementation achieve a lower H_∞ norm of the transfer function $\boldsymbol{T}_1$ from the road input profile to the body vertical and pitch accelerations, with respect to the passive vehicle (open-loop system) for all vehicle speeds. On the contrary, Fig. 18 shows that the H_2 norm of the transfer function $\boldsymbol{T}_2$ from the road input profile to the normalised front and rear suspension deflections is larger for the controlled configurations, i.e., the improvement of ride quality is at the cost of larger suspension deflections, which, however, remain within the physical limits defined by the authors.

The road preview-augmented input in (44) gives the system a much larger dimension than for the original vehicle model without preview, and an increased computational time is required to generate the feedback control input in (48). Ryu et al. (2008) addresses this problem by transforming the feedback controller into a combination of feedback and feedforward contributions, where the FB part has the same order as the original system. To identify the resulting computational performance, the computation time for obtaining the control input is investigated with Strassen's matrix multiplication algorithm (Cormen et al., 2010), where $M(n) = M_1 n^{2.81} - M_2 n^2$ represents the computation time for a multiplication between two n x n matrices, with M_1 and M_2 being appropriate constants. Based on this principle, Ryu et al. (2008) estimates the computational demand for the proposed decomposed-type preview H_∞ controller, in comparison with the classic feedback-type approach in (48), as a function of the number of preview samples, N_{tp}. The computational time for the FB H_∞ controller applied to a two-degree-of-freedom quarter car model ($n = 4$) is estimated as $T_{c,FB} = 33M(n_a)$, where $n_a = n + (N_{tp} + 1)$ is the dimension of the augmented state vector, while the decomposed-type H_∞ controller described by Ryu et al. (2008) only requires a computational time $T_{c,dc} = (41 + 12N_{tp})M(n)$, which is equal to $T_{c,FB}/350$ for $N_{tp} = 100$.

In conclusion, H_2/H_∞ control structures are very appropriate when robust stability is a fundamental requirement for the preview-augmented suspension controller. Furthermore, differently from LQ strategies, H_2/H_∞ designs can include forms of consideration of both hard and soft constraints. On the downside, these controllers require multi-variable design routines in the frequency domain, and imply the formulation and solution of complex optimisation problems, which are rather disjointed from the physics of the vehicle system, and are complex to manage for non-specialists in advanced control.

5.5. Model predictive approaches

5.5.1. Optimal control problem

Model predictive controllers (MPC) incorporate a prediction of the future behaviour of the system and allow to formally account for system constraints directly within the optimisation process that computes the

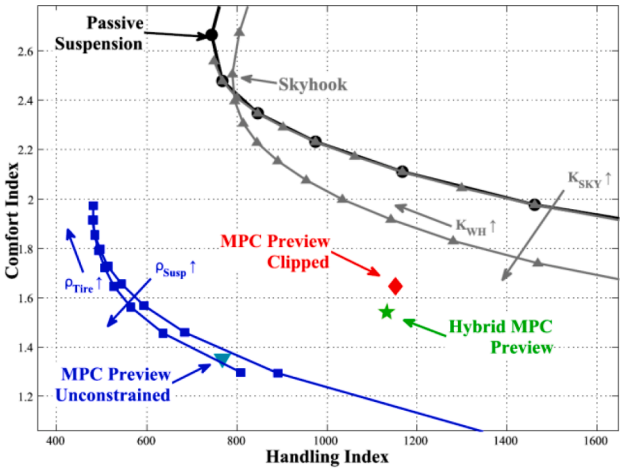

Fig. 19. Conflict diagram for the vehicle with the passive set-up (circles), with a skyhook controller (triangles), and with a preview-augmented unconstrained MPC (squares), driven over a sinusoidal bump. For one setting of the cost function weights, the plot also includes the comparison among the following iMPCs: i) an unconstrained MPC with preview ('MPC Preview Unconstrained'); ii) a clipped MPC with preview ('MPC Preview Clipped'); and iii) the proposed hybrid MPC approach with preview ('Hybrid MPC Preview'). $\rho_{Tire} = \rho_2$ and $\rho_{Susp} = \rho_3$ are the tyre deflection and suspension stroke weights in (29); k_{SKY} is the skyhook gain; and k_{WH} is the wheel hop gain (see the original reference for more details). Reproduced with permission from De Bruyne et al. (2012).

control input, see Maciejowski et al., and Kerrigan (2007). For these reasons, MPC is the natural control technology for the implementation of suspension controllers with road preview. MPC formulations can be linear or nonlinear, depending on the nature of the internal model, also called prediction model, which is embedded in the controller formulation. For the specific problem of suspension control with preview, most of the formulations from the literature are linear, and are based, depending on the implementation, on quarter car, half car or full car models, considering the road preview information through augmented state vectors, $\boldsymbol{x}_a$, according to (44).

A typical linear optimal control problem formulation for MPC for active suspension with road preview can be expressed as (Mehra et al., 1997; Song & Wang, 2020):

$$\begin{aligned}
&\min_{u} J(\boldsymbol{x}(0),\boldsymbol{u}(\cdot))\cdot = \sum_{j=1}^{N}\boldsymbol{y}^{\boldsymbol{T}}(k+j)\boldsymbol{Q}\boldsymbol{y}(k+j) + \sum_{j=0}^{N_c}\boldsymbol{u}^{\boldsymbol{T}}(k+j)\boldsymbol{R}\boldsymbol{u}(k+j) = \widehat{\boldsymbol{y}}^{T}\widehat{\boldsymbol{Q}}\widehat{\boldsymbol{y}} + \widehat{\boldsymbol{u}}^{T}\widehat{\boldsymbol{R}}\widehat{\boldsymbol{u}}\\
&s.t.\\
&\boldsymbol{x}(0) = \boldsymbol{x}_{in}\\
&\boldsymbol{x}_a(k+j+1) = \boldsymbol{A}_a\boldsymbol{x}_a(k+j) + \boldsymbol{B}_a\boldsymbol{u}(k+j) + \boldsymbol{\Gamma}_a\boldsymbol{\gamma}(k+j)\\
&\boldsymbol{y}(k+j) = \boldsymbol{C}_a\boldsymbol{x}_a(k+j) + \boldsymbol{E}_a\boldsymbol{u}(k+j)\\
&\boldsymbol{u}_{\min} \le \boldsymbol{u}(k+j) \le \boldsymbol{u}_{\max}\\
&\boldsymbol{\Delta u}_{\min} \le \boldsymbol{\Delta u}(k+j) \le \boldsymbol{\Delta u}_{\max}\\
&\boldsymbol{y}_{\min} \le \boldsymbol{y}(k+j) \le \boldsymbol{y}_{\max}\\
&\boldsymbol{u}(\cdot):\ [k,\ k+N_c]\\
&\boldsymbol{u}(k+j+1) = \boldsymbol{u}(k+j),\ \text{for} j > N_c
\end{aligned} \tag{52}$$

where the index k indicates the current time; the index j indicates the step along the prediction horizon; $\boldsymbol{Q}$ and $\boldsymbol{R}$ are the weight matrices of the cost function J; N is the number of samples corresponding to the prediction horizon; N_c is the number of samples defining the control horizon; $\widehat{\boldsymbol{y}} = [\boldsymbol{y}(k+1)\quad \boldsymbol{y}(k+2)\cdots \boldsymbol{y}(k+N)]^T$ is the sequence of system outputs along the prediction horizon; $\widehat{\boldsymbol{u}} = [\boldsymbol{u}(k)\quad \boldsymbol{u}(k+1)\cdots \boldsymbol{u}(k+N_c)]^T$ is the sequence of control moves along the control horizon; $\boldsymbol{\gamma}$ is the vector of the road elevation displacement/s and (when relevant) displacement rate/s, measured by the preview sensor or output by the estimation system, which depends on the considered model formulation; $\boldsymbol{\Gamma}_a$ is a constant matrix; $\boldsymbol{u}_{min}$ and $\boldsymbol{u}_{max}$ are the lower and upper limits of the control action, i.e., the actuator forces or spring seat displacements; $\boldsymbol{\Delta u}$ is the control action rate, constrained between $\boldsymbol{\Delta u}_{min}$ and $\boldsymbol{\Delta u}_{max}$; $\boldsymbol{y}_{min}$ and $\boldsymbol{y}_{max}$ are the lower and upper limits of the system outputs; and $\boldsymbol{x}_{in}$ expresses the initial condition. In (52) soft constraints can be defined – even if they are not used in the considered suspension control literature – through the introduction of appropriate inequality constraints using slack variables, which become part of the system states and are minimised in the cost function. Under typical assumptions, (52) can be rearranged into a convex quadratic programming (QP) optimisation problem of the form:

$$\begin{aligned}
&\min_{\widehat{u}} \frac{1}{2}\widehat{\boldsymbol{u}}^{T}\boldsymbol{H}\widehat{\boldsymbol{u}} + \boldsymbol{g}^{T}\widehat{\boldsymbol{u}}\\
&\text{s.t.}\\
&\boldsymbol{G}\widehat{\boldsymbol{u}} \le \boldsymbol{S}
\end{aligned} \tag{53}$$

where $\boldsymbol{H}$ is the Hessian matrix; $\boldsymbol{g}$ is the gradient vector, containing system parameters and cost function weighting factors; and the matrices $\boldsymbol{G}$ and $\boldsymbol{S}$, which can be constant or dependent on $\boldsymbol{x}_a(k)$, define the inequality constraints. Several methods are available to solve the QP problem, e.g., interior point, active set, augmented Lagrangian method, conjugate gradient, gradient projection, and simplex algorithm. Once the optimal control input vector, $\widehat{\boldsymbol{u}}^*$, is found, only the first control move is applied to the suspension actuators, as in the meantime a new optimal solution is computed for the next time step. The process is repeated at each time step, according to the receding horizon approach (Maciejowski et al., 2007).

5.5.2. Implicit model predictive control

In the so-called implicit MPC (iMPC) implementations, the optimal solution of the problem in (52)-(53) is computed online on the vehicle micro-controller, which implies rather high online computational effort (issue which is becoming less critical with the new generations of automotive control hardware) but low flash memory requirements.

With respect to iMPC implementations for controllable suspensions with preview, one of the semi-active control approaches evaluated in Van Der Aa et al. (1997) uses sequential quadratic programming to calculate the control action that optimises the future behaviour of the modelled nonlinear system, subject to hard constraints; although the authors never define their controller as an MPC, the implementation includes the typical features of iMPC. Mehra et al. (1997) is one of the first studies to propose linear iMPC for preview-augmented active suspensions, with encouraging comfort improvement results, in comparison with the corresponding vehicle with the baseline passive suspension system.

Among the very rare experimental studies on iMPC for suspension control, Donahue and Hedrick (2001) tested non-preview and preview-based iMPC for active suspensions on a US army off-road vehicle, by using a 300 MHz Alpha processor, with a controller implementation time of 30 ms. The preview-based iMPC is compared with more conventional LQR and skyhook controllers without preview, along manoeuvres at constant speed on off-road test tracks, with results showing the significant benefits of the preview-augmented iMPC.

De Bruyne et al. (2012) and Savaresi et al. (2010) propose hybrid preview-augmented iMPCs for semi-active suspensions, with actuator limits determined through logic rules, which depend on damper velocity. By linearisation of the nonlinear constraints through piecewise affine approximations, the optimisation problem is solved through mixed integer quadratic programming (MIQP). De Bruyne et al. (2012) performs quarter car model simulations on a sinusoidal bump, and compares different MPC formulations, namely: i) an unconstrained MPC with preview; ii) a clipped MPC with preview; and iii) the proposed hybrid MPC approach with preview. The results in the conflict diagram in Fig. 19, also considering the passive vehicle and the vehicle with a skyhook controller, highlight the importance of considering actuator constraints in the simulation model and control formulation, as the performance of controller i) implemented on the simulation model

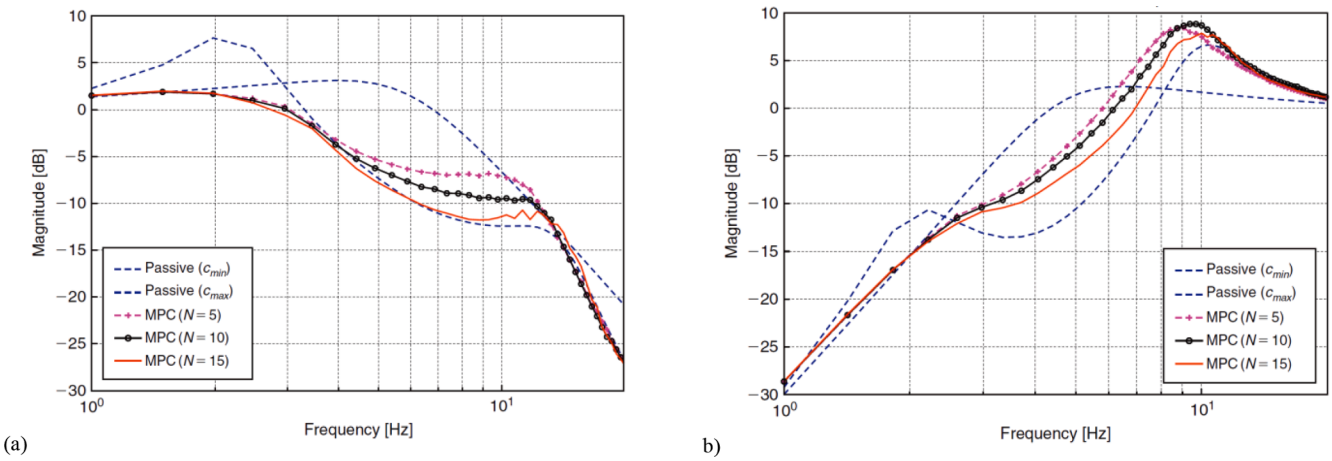

Fig. 20. Frequency response characteristics from the vertical road disturbance to the body displacement (a) and to the tyre deflection (b), obtained through a quarter car model, with the proposed comfort-oriented iMPC preview strategy with $N = 5, 10, 15$, and for the passive vehicle set-up with hard (c_{max}) and soft (c_{min}) suspension damping settings. Reproduced with permission from Savaresi et al. (2010).

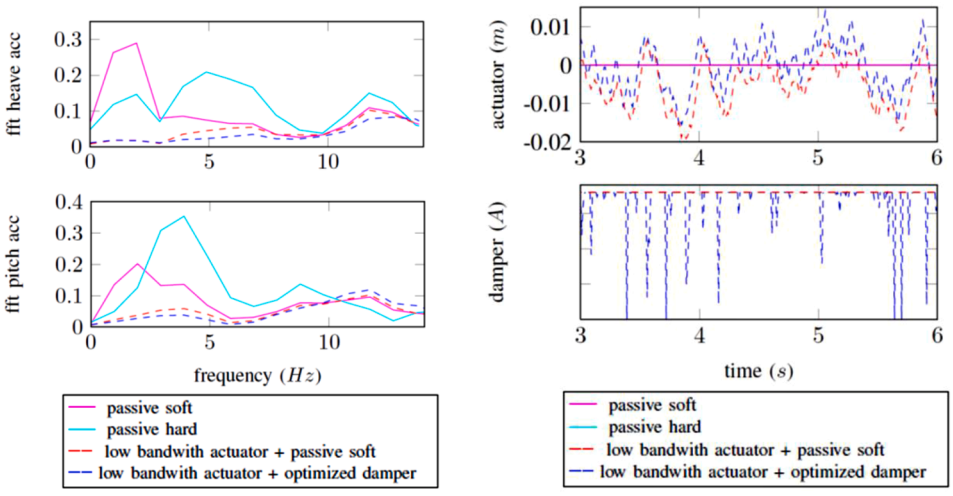

Fig. 21. Fast Fourier transforms (FFT) of the heave and pitch accelerations, actuator displacement, and absorbed damper current, computed through the full car model on a rough road for: i) the passive suspension set-ups with hard ('passive hard') and soft ('passive soft') damping; ii) a preview-based iMPC controlling the low-bandwidth actuators, working in parallel with passive dampers with a soft set-up ('low bandwidth actuator + passive soft'); and iii) a preview-based iMPC, controlling the combination of active low-bandwidth actuators and controllable dampers ('low bandwidth actuator + optimized damper'). Reproduced with permission from Göhrle et al. (2013).

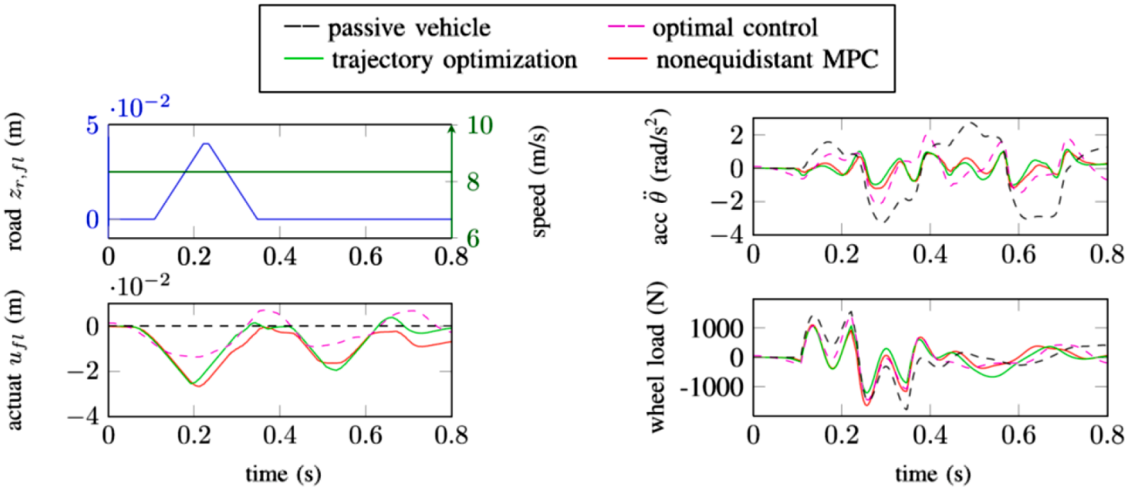

Fig. 22. Simulation results over a speed bump for: i) the passive set-up ('passive vehicle'); ii) an LQ strategy ('optimal control'); iii) the proposed model predictive trajectory optimisation controller ('trajectory optimization'); and iv) an iMPC implementation ('nonequidistant MPC'). Reproduced with permission from Göhrle et al. (2014).

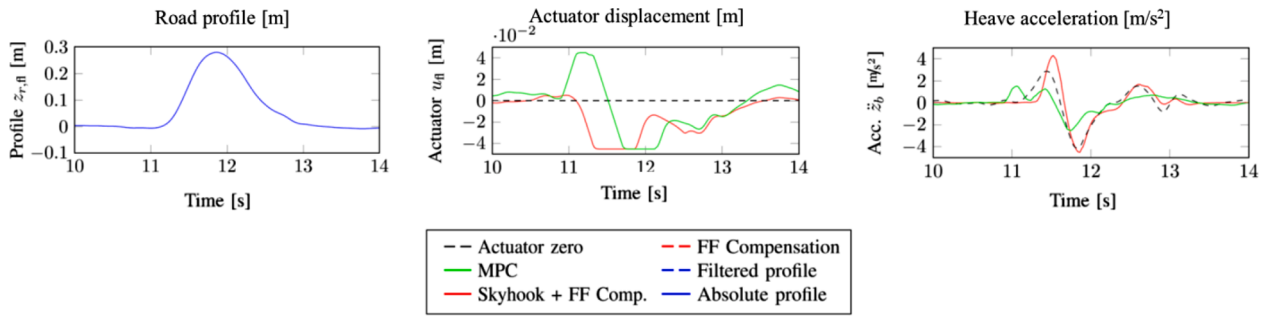

Fig. 23. Simulation results over a road bump for: i) a preview-based feedforward compensator ('FF Compensation'); ii) a skyhook strategy augmented with a preview-based feedforward compensator ('Skyhook + FF Comp.'); and iii) the preview-based iMPC ('MPC') from Göhrle et al. (2014). Reproduced with permission from Göhrle et al. (2015).

neglecting actuator limitations is unrealistically good, with respect to that of controllers ii) and iii). The values of the indices in the figure show that the road holding performance is more affected by the actuation constraints than the comfort performance. The hybrid MPC approach can reduce the handling performance index by 3% and the comfort index by almost 8%, with respect to the clipped MPC strategy. Fig. 20 reports simulation results from Savaresi et al. (2010) in terms of frequency response characteristics of the quarter car model for the proposed preview-augmented iMPC strategy, for different numbers of prediction steps, N. The MPC is compared with the passive vehicle set-up with high and low damping constants of the shock absorbers, c_{max} and c_{min}. The trade-off between soft and hard damping values is effectively handled by the MPC, whose performance improves with increasing preview and prediction times, which are coincident in the specific implementation.

Göhrle et al. (2012)) proposes a linear preview-based iMPC for active suspensions with ride height adjustment capability, with an actuator per corner installed in parallel with a first passive spring and in series with a second spring, by using a full car prediction model. Due to the low actuator bandwidth (5 Hz), the internal vehicle model complexity is reduced by neglecting the unsprung mass dynamics. The actuator dynamics are accounted for through a first order transfer function, and constraints are imposed on the actuator displacement and displacement rate. The MPC outputs the four reference actuator displacements. The controller performance is verified for several road inputs, i.e., bump, sinusoidal profile, and rough road. If the bump profile exceeds the possible actuator displacement range, the simulation results show that the controller uses the front actuators to lift the vehicle body before reaching the bump, to increase the available travel in the appropriate direction. Among multiple considered approaches, Göhrle et al., and Sawodny (2013) extends the strategy of Göhrle et al. (2012)) through the addition of controllable dampers, which replace the passive dampers, to the low-bandwidth active suspension actuators, within an integrated MPC, which outputs four reference actuator displacements and four reference damper forces. Fig. 21 reports the simulated fast Fourier transform (FFT) of the heave and pitch accelerations of the vehicle body on a rough road, for: i) the passive suspension set-ups with hard and soft damping; ii) the preview-based MPC controlling the low-bandwidth actuators, working in parallel with passive dampers with a soft set-up; and iii) the preview-based MPC, controlling the combination of active low-bandwidth actuators and controllable dampers. The inclusion of the variable damping in the optimisation problem, i.e., case iii), improves comfort in comparison with case ii). The current absorption profile of the variable damper in Fig. 21, with high currents corresponding to soft characteristics, highlights that the MPC-optimised damper force is usually close to the soft characteristic of the component, and only occasionally approaches high damping values.

Göhrle et al., and Sawodny (2014) controls low-bandwidth suspension actuators in series with springs, and in parallel to passive dampers. The study proposes a novel nonlinear suspension control formulation, namely model predictive trajectory optimisation, which, although it cannot be considered a model predictive controller, is rather close to MPC in its principle. In fact, a nonlinear predictive quadratic programming formulation with constraints optimises the heave, pitch and roll dynamics, expressed in the form of accelerations, and outputs the knots of spline basis functions for heave, pitch, and roll. Then the reference actuator displacements are computed through model inversion, using the known road profile. This formulation can produce reasonable results also in case of failure of the trajectory optimisation; in fact, in that circumstance, the reference trajectories can be set to zero, and the inverse model generates the corresponding actuator commands. The simulation results of the paper, see Fig. 22, over a speed bump, include the comparison among: i) the passive vehicle; ii) the preview-based LQ approach from Hać (1992); iii) the newly proposed formulation, indicated as 'trajectory optimization'; and iv) a more conventional preview-augmented iMPC, outputting the four actuator displacements, indicated as 'nonequidistant MPC' in the figure, as it considers a non-equidistant grid of points along the preview horizon. The two implicit predictive approaches clearly outperform the LQ controller as well as the passive case, and are implemented in real time on an experimental vehicle demonstrator, which is rare in preview-augmented suspension control. The authors highlight that the predictive trajectory optimisation is less computationally demanding than the iMPC, because of the reduced number of optimisation variables.

Göhrle et al., and Sawodny (2015) compares the iMPC from Göhrle et al. (2014), using a preview time of 0.5 s, with a skyhook algorithm augmented with a model-based feedforward compensator. The simulation results in Fig. 23 over a single road bump show the evident performance benefit of the iMPC. The comments reported in the paper highlight that the skyhook with feedforward contribution could be further improved by appropriate processing and filtering of the road preview profile through cumulated redundant measurements, thus producing similar vertical acceleration performance to the iMPC, which, however, requires less preview time. An important conclusion is that the skyhook controller with feedforward contribution is better suited for a modular control design, since its independent contributions can be easily summed together. On the contrary, the proposed MPC is less flexible; for example, while cornering on a flat road, the arising roll angle is further increased by the MPC to minimise the roll acceleration, instead of being reduced, which would be desirable for good handling characteristics.

A comfort optimisation strategy that combines vehicle speed planning and preview-augmented semi-active suspension control is designed by Wu et al. (2020). A horizon-varying iMPC is used for speed-dependent time-domain preview data. The hybrid iMPC approach allows formal consideration of actuator saturation. Interestingly, the study presents a coordinated structure for the synergic control of the longitudinal dynamics and suspension actuators, which is suitable for autonomous driving applications. Simulation results over multiple uneven roads confirm that the method can enhance multiple aspects, including vertical vibrations, driving times, and speed profiles.

Table 1
Selection of simulation and experimental results, in terms of heave, pitch and roll accelerations, as well as *VTV*, from Theunissen et al. (2020).

	Simulation results (ride comfort road, next generation actuators)				Experimental results (speed bump, current generation low-frequency actuators)					
	Mode	Pass.	e-MPC w/o preview	e-MPC w/ preview	Mode	Freq. range	Pass.	Skyhook	e-MPC w/o preview	e-MPC w/ preview
RMS	Heave (m/s^2)	1.00	0.53 (-47%)	0.34 (-35%)	Heave (m/s^2)	0-4 Hz	1.60	0.87 (-45%)	0.78 (-11%)	0.69 (-12%)
						0-15 Hz	1.61	0.93 (-42%)	0.84 (-9%)	0.74 (-12%)
	Pitch (rad/s^2)	0.63	0.34 (-47%)	0.27 (-19%)	Pitch (rad/s^2)	0-4 Hz	0.99	0.68 (-31%)	0.63 (-7%)	0.58 (-8%)
						0-15 Hz	1.00	0.70 (-30 %)	0.66 (-6%)	0.63 (-4%)
	Roll (rad/s^2)	0.63	0.32 (-48%)	0.26 (-21%)	a_v (m/s^2)	0-15 Hz	0.76	0.47 (-38%)	0.43 (-9%)	0.38 (-12%)
Freq. weighted	Heave (m/s^2)	0.73	0.39 (-46%)	0.28 (-29%)	Heave (m/s^2)	0-15 Hz	0.82	0.55 (-32%)	0.50 (-10%)	0.47 (-5%)
	Pitch (rad/s^2)	0.29	0.13 (-55%)	0.11 (-13%)	Pitch (rad/s^2)	0-15 Hz	0.70	0.39 (-43%)	0.41 (+4%)	0.37 (-8%)
	Roll (rad/s^2)	0.34	0.17 (-51%)	0.12 (-27%)	*VTV* (m/s^2)	0-15 Hz	0.43	0.27 (-37%)	0.26 (-4%)	0.24 (-8%)

Note: The % variations are with respect to the system in the column to the immediate left.

5.5.3. Explicit model predictive control

The main drawback of the real-time implementation of iMPC is its high computational power demand. The couple of studies including experimental validations of preview-augmented iMPC suspension controllers (Donahue & Hedrick, 2001; Göhrle et al., 2014) use high-end embedded platforms and relatively low sampling rates, where the latter could have a negative impact on performance. To reduce the on-line computational cost, in Ahmed and Svaricek (2013, 2014) several control laws – three for ride comfort control and three for road holding control – are extracted from the frequency response characteristics of the vehicle system with comfort-oriented and handling-oriented MPC formulations, according to the frequency range. The result is a computationally efficient rule-based strategy design.

Alternatively to the on-line optimisations typical of iMPC, the solution of the optimal control problem can be computed offline for all possible values of $\boldsymbol{x_a}$, thus generating an explicit solution to the control law $\boldsymbol{u}^* = \boldsymbol{u}^*(\boldsymbol{x_a})$, through the so-called explicit model predictive control (eMPC, for the theory see (Bemporad, Borrelli, & Morari, 2000a,b,c and Bemporad et al., and Pistikopoulos, 2000). The explicit solution is then stored on the flash memory of the automotive control hardware for online implementation.

In a typical eMPC formulation, the quadratic programming optimisation problem is reformulated as:

$$\begin{aligned} &\min_{\widehat{u}} \frac{1}{2}\widehat{\boldsymbol{u}}^T\boldsymbol{H}\widehat{\boldsymbol{u}} + \boldsymbol{x_a}(k)^T\boldsymbol{F}\widehat{\boldsymbol{u}} \\ &s.t. \\ &\boldsymbol{G}\widehat{\boldsymbol{u}} \le \boldsymbol{S_1} + \boldsymbol{S_2}\boldsymbol{x_a}(k) \end{aligned} \tag{54}$$

where $\boldsymbol{F}$ contains the system parameters and cost function weights, and $\boldsymbol{S}_1$ and $\boldsymbol{S}_2$ are constant matrices. The idea is to determine offline a global set of feasible parameters X^* of all $\boldsymbol{x_a} \in X$ for which a solution of the problem exists, together with the piecewise affine state feedback control law, defined by a partitioning of the state space into p polyhedral critical regions:

$$\boldsymbol{u}^*(\boldsymbol{x_a}) = \begin{cases} \boldsymbol{F_1}\boldsymbol{x_a} + \boldsymbol{h_1}, & \boldsymbol{Z_1}\boldsymbol{x_a} \le z_1 \\ \vdots & \vdots \\ \boldsymbol{F_p}\boldsymbol{x_a} + \boldsymbol{h_p}, & \boldsymbol{Z_p}\boldsymbol{x_a} \le z_p \end{cases} \tag{55}$$

where $\boldsymbol{F_i}$, $\boldsymbol{h_i}$, $\boldsymbol{Z_i}$ and z_i are constant matrices, which are stored in the control hardware. The benefits of eMPC are: a) a major reduction of the required online computational effort, as the online algorithm reduces to a function evaluation; and b) the possibility of assessing the solution a priori, which allows stability, robustness and functional safety analyses before the deployment of the algorithm. The drawbacks are: a) the higher design complexity; and b) the increased memory requirements, which tend to exponentially grow with the number of samples in the prediction and control horizons (e.g., see the analysis in Cseko et al., and Lantos (2010)), and the number of states, and pose significant limitations to algorithm implementation on real automotive control units. Region-based eMPC has already been implemented in several studies on semi-active and active suspension control without road preview, involving both simulations (Canale et al., 2006; Cseko et al., 2010, 2015; Dessort & Chucholowski, 2017; Giorgetti et al., 2006; Houzhong et al., 2019) and experimental tests (Mai et al., 2020; Montanez et al., 2015; Morato et al., 2019; Theunissen et al., 2019).

The recent study in Theunissen et al. (2020) applies eMPC to active suspension control with road preview, and uses a regionless approach for substantially reducing the memory requirements in comparison with the traditional region-based eMPC. The method, based on the theory by Drgoňa et al., and Kvasnica (2017), does not need to compute or store all regions on the control hardware, but in the offline process all the possible active sets, $\boldsymbol{A_1}, \cdots, \boldsymbol{A_{Nr}}$, that can be locally optimal are considered through an extensive enumeration method based on the Karush–Kuhn–Tucker conditions. For each locally optimal active set, the solution is:

$$\boldsymbol{u}(\boldsymbol{x_a}) = -\boldsymbol{H}^{-1}\left(\boldsymbol{F}^T\boldsymbol{x_a} + \boldsymbol{G}_{\boldsymbol{A_i}}^T\boldsymbol{\lambda}^*\right) \tag{56}$$

where $\boldsymbol{G}_{\boldsymbol{A_i}}$ includes only the rows of $\boldsymbol{G}$ indexed by the set of active constraints $\boldsymbol{A_i}$, and $\boldsymbol{\lambda}^*$ represents the dual variables expressed by:

$$\boldsymbol{\lambda}^* = \boldsymbol{Q}(A_i)\boldsymbol{x_a} + \boldsymbol{q}(A_i) \tag{57}$$

with:

$$\begin{aligned} \boldsymbol{Q}(A_i) &= -\left(\boldsymbol{G}_{\boldsymbol{A_i}}\boldsymbol{H}^{-1}\boldsymbol{G}_{\boldsymbol{A_i}}^T\right)^{-1}\left(\boldsymbol{S}_{2,\boldsymbol{A_i}} + \boldsymbol{G}_{\boldsymbol{A_i}}\boldsymbol{H}^{-1}\boldsymbol{F}^T\right) \\ \boldsymbol{q}(A_i) &= -\left(\boldsymbol{G}_{\boldsymbol{A_i}}\boldsymbol{H}^{-1}\boldsymbol{G}_{\boldsymbol{A_i}}^T\right)^{-1}\boldsymbol{S}_{1,\boldsymbol{A_i}} \end{aligned} \tag{58}$$

where $\boldsymbol{S}_{1,\boldsymbol{A_i}}$ and $\boldsymbol{S}_{2,\boldsymbol{A_i}}$ contain only the rows of $\boldsymbol{S}_1$ and $\boldsymbol{S}_2$ corresponding to the active set A_i. The maps of $\boldsymbol{Q}(A_i)$ and $\boldsymbol{q}(A_i)$ are generated offline and stored in the controller together with $\boldsymbol{H}^{-1}$, $\boldsymbol{F}$, $\boldsymbol{G}$, $\boldsymbol{S}_1$ and $\boldsymbol{S}_2$. For the online implementation of the regionless controller, (56) and (57) are used to calculate $\boldsymbol{u}(\boldsymbol{x_a})$, by finding the optimal active set for the current $\boldsymbol{x_a}$ from the list of locally optimal active sets.

The specific regionless eMPC implementation with preview in Theunissen et al. (2020) brings memory requirement and generation time reductions by ~30 and ~7 folds, respectively, in comparison with the corresponding region-based eMPC. The performance of the resulting eMPCs (with and without preview) is firstly assessed through simulations of a vehicle with next-generation active suspension actuators on a typical ride comfort road (left part of Table 1), and then is experimentally tested on a sport utility vehicle demonstrator with a low-bandwidth hydraulic active suspension system, including also a benchmarking skyhook suspension system, along two speed bumps (see a selection of

Table 2
Summary of main available comparisons of preview-augmented suspension controllers from the considered literature, and main conclusions drawn.

Non-optimal	LQ	H_∞, H_2/H_∞	MPC	Papers	Comments
X	X			Langlois and Anderson (1995)	For a simulated sinusoidal bump at 10 km/h, 20 km/h and 30 km/h, the non-optimal strategy brings: • 16%, 31% and 28% reductions of the *RMS* values of $\ddot{z}_B$ with respect to (w.r.t.) the considered LQR; • 56%, 69% and 73% reductions of the *RMS* values of θ_B w.r.t. the LQR.
	X	X		Akbari et al. (2010)	For simulated realistic road profiles, the H_2/H_∞ strategy brings: • 45% reduction of the *RMS* values of $\ddot{z}_B$ w.r.t. the considered LQG; • 15% reduction of the *RMS* values of $z_U - w$ w.r.t. the LQG; • 47% reduction of the *RMS* values of $z_B - z_U$ w.r.t. the LQG; • 12% reduction of the *RMS* values of u w.r.t. the LQG.
	X	X		Akbari and Lohmann (2010)	For simulated white noise, single bump and realistic road profiles at 72 km/h, the H_2/H_∞ strategy brings: • 1%, 36% and 32% reductions of the *WRMS* values of $\ddot{z}_B$ w.r.t. the considered LQG; • 2% and 1% reductions and 7% increment of the *RMS* values of $z_U - w$ w.r.t. the LQG; • 2% reduction and 32% and 8% increments of the *RMS* values of $z_B - z_U$ w.r.t. the LQG; • 3% and 1% reductions and 1% increment of the *RMS* values of u w.r.t. the LQG.
	X	X		Ryu et al. (2011)	The LQR and H_∞ strategies bring 85% and 90% reductions of the *WRMS* values of $\ddot{z}_B$ w.r.t. the passive case, for a realistic road profile simulated at 30 km/h.
		X		P. Li et al. (2014a)	For a simulated white noise road profile at 20 m/s, the proposed H_2/H_∞ strategy with full preview and the H_2/H_∞ strategy with partial preview (only one preview point) bring: • 81% and 79% reductions of the *RMS* values of $\ddot{z}_B$ w.r.t. the passive case; • 80% and 63% reductions of the *RMS* values of $\ddot{\theta}_B$ w.r.t. the passive case.
X			X	Göhrle et al. (2015)	The proposed iMPC and FF+FB strategies provide the same ride comfort performance in terms of $\ddot{z}_B$ when the vehicle travels over a simulated localised high road obstacle at 100 km/h; • The iMPC strategy provides slightly better ride comfort performance over a simulated sinusoidal-shaped road with a wavelength of 35 m and a peak-to-peak amplitude of 4 cm, at 120 km/h. In this scenario, the iMPC requires a preview distance $P_d = 8$ m, which is lower than the 15 m needed by the FF+FB.
	X		X	Göhrle et al. (2014)	The considered iMPC, model predictive trajectory optimisation and LQR strategies respectively bring: • 90%, 85% and 74% reductions of the *RMS* value of $\ddot{z}_B$ w.r.t. the passive case over a simulated sine wave road profile (amplitude of 2 cm) at increasing speed; • 40% and 40% reductions, and 10% increment of the *RMS* value of $\ddot{z}_B$ w.r.t. the passive case over a simulated high road elevation (road profile peak of 0.3 m) at constant speed; • 71%, 72% and 49% reductions of the *RMS* value of $\ddot{\phi}_B$ w.r.t. the passive case over a simulated speed bump input only on the left vehicle side at constant speed; • 30%, 29% and 26% reductions of the *RMS* value of $\ddot{z}_B$ w.r.t. the passive case over a simulated rough road profile at increasing speed.
	X		X	Song and Wang (2020)	For a square wave-shaped road profile (amplitude of 1 cm and rate limit of 0.2 m/s) experimentally applied on a suspension test rig, the considered incremental eMPC, eMPC and LQR strategies bring: • 65%, 59% and 33% reductions of the RMS value of $\ddot{z}_B$ w.r.t. the passive case, with measured road preview from the lead vehicle for the controlled configurations; • 56%, 52% and 35% reductions of the RMS value of $\ddot{z}_B$ w.r.t. the passive case, with estimated road preview from the lead vehicle for the controlled configurations.
		X	X	Ahmed and Svaricek (2013)	The MPC-based look-up table controller shows a slightly better $\ddot{z}_B$ time response over a random road profile (class F) than the considered H_∞, while the handling performance is worse for the MPC.
			X	De Bruyne et al. (2012)	For a simulated sinusoidal bump (0.05 m height), the considered clipped iMPC and hybrid iMPC strategies bring: • 22% and 14% increments of the *WRMS* values of $\ddot{z}_B$ w.r.t. the considered unconstrained iMPC, when applied to the unconstrained system; • 50% and 47% increments of the *WRMS* values of $z_U - w$ w.r.t. the unconstrained iMPC, when applied to the unconstrained system.

results in the right part of Table 1). The simulations and measurements highlight the general improvement brought by the eMPC without preview with respect to the passive vehicle and the vehicle with the skyhook algorithm, and then by the eMPC implementation with preview, even if, also because of the particularly low bandwidth of the adopted experimental actuators, such benefit is especially evident in the simulation results. eMPC is also studied in Song and Wang (2020), which proposes an incremental MPC strategy for active suspensions, to achieve improved robustness with respect to the road preview estimation errors deriving from lead vehicle preview. While in the prediction model formulation conventional MPC strategies only use the present system states, $\boldsymbol{x}_a(k)$, incremental MPC also uses the previous system states, $\boldsymbol{x}_a(k-1)$, which augment the model formulation. The incremental system dynamics of the quarter car model, with the tyre modelled as a single spring, are described by:

$$\boldsymbol{\Delta x}(k+1) = \boldsymbol{A}_d \boldsymbol{\Delta x}(k) + \boldsymbol{B}_d \Delta u(k) + \boldsymbol{D}_d \Delta w(k) \tag{59}$$

where the notation Δ indicates an incremental variable, i.e., $\Delta \boldsymbol{x}(k) = \boldsymbol{x}(k) - \boldsymbol{x}(k-1)$, $\Delta u(k) = u(k) - u(k-1)$, and $\Delta w(k) = w(k) - w(k-1)$. By combining the augmented model in (44) for a quarter car model including the shift register formulation of the road profile, with the incremental model in (59), a new augmented system is obtained:

$$\boldsymbol{x}_{ad}(k+1) = \boldsymbol{A}_{ad}\boldsymbol{x}_{ad}(k) + \boldsymbol{B}_{ad}u(k) + \boldsymbol{D}_{ad}w_p(k) \tag{60}$$

where:

$$\boldsymbol{x}_{ad}(k) = \begin{bmatrix} \boldsymbol{\Delta x}(k) \\ \Delta w(k) \\ u(k-1) \\ \boldsymbol{x}_a(k) \end{bmatrix}, \boldsymbol{A}_{ad} = \begin{bmatrix} \boldsymbol{A}_d & \boldsymbol{D}_d & -\boldsymbol{B}_d & \boldsymbol{0} \\ \boldsymbol{0} & 0 & 0 & \boldsymbol{E}_d \\ \boldsymbol{0} & 0 & 0 & \boldsymbol{0} \\ \boldsymbol{0} & 0 & 0 & \boldsymbol{A}_a \end{bmatrix}, \boldsymbol{B}_{ad} = \begin{bmatrix} \boldsymbol{B}_d \\ 0 \\ 1 \\ \boldsymbol{B}_a \end{bmatrix}, \boldsymbol{D}_{ad} = \begin{bmatrix} \boldsymbol{0} \\ 0 \\ 0 \\ \boldsymbol{D}_a \end{bmatrix}, \boldsymbol{E}_d = [\boldsymbol{0}\ 1\ -1\ \boldsymbol{0}] \tag{61}$$

(61) can be used within the conventional formulation of an optimal

control problem for a linear region-based MPC, and provide enhanced robustness; in particular, robust stability conditions are formally derived in Song and Wang (2020) through the Lyapunov criterion. The performance of the resulting explicit formulation, based on the augmented incremental model in (60)-(61) as prediction model, is compared with that of an LQR and an eMPC excluding incremental model augmentation, both of them including preview, which shows the enhanced performance of the proposed controller, at the expense of increased memory requirement (from 377 kB to 496 kB) and offline computation time (from 3.7 s to 10.7 s) with respect to the benchmarking region-based eMPC.

5.5.4. Conclusions on model predictive control

In conclusion, implicit MPC strategies are becoming widely used – at least at the research level – for preview-augmented suspension systems, thanks to the progressive introduction of powerful automotive microcontrollers and computationally efficient solvers, which allow the real-time implementation of the associated on-line optimisations. In parallel, examples of explicit MPC formulations are also available, which address the computational power issues of MPC at the root, by solving the optimal control problem offline, at the expense of increased memory requirements, which can become critical if a significant number of preview points is selected. Compared to the previously discussed control structures, MPC represents a very attractive solution, due to the consideration of the future behaviour of the system within a finite prediction horizon, and the capability of formally considering the physical constraints of the available hardware. Moreover, the MPC design process is rather intuitive also for non-specialists in control science, such as typical vehicle dynamics engineers.

5.6. Other optimal controllers

The literature also includes optimal control formulations that do not fall in any of the previous categories. For example, Gordon and Sharp (1998) and Savaresi and Silani (2004) solve the optimal control problem for a time-invariant quarter car model with semi-active suspension system with non-linear damper characteristic, by using Pontryagin's Hamiltonian formulation. Gordon's simulations on a quarter car model show similar results to those of an LQR framework without preview. The approach in Karlsson et al. (2001), based on a quadratic cost function that penalises tyre and suspension displacements to the fourth power, does not permit to use the typical LQ theory; therefore, the study proposes nonlinear optimisation with Lagrange multipliers. The simulation results highlight improved combined ride and handling performance with respect to an LQ controller without preview.

6. Critical analyses and future developments

6.1. Critical analysis of preview-augmented control structures

The rather extensive literature on preview-augmented suspension control only includes a limited number of comparisons, involving approximately ten papers in total, among control structures with road preview, see Table 2, which also reports the main conclusions of the available analyses. In general, the results penalise the LQ formulations, while MPC implementations marginally have an edge over the non-optimal controllers, based on the combination of feedforward and feedback contributions (indicated as FF+FB in the table), and H_∞ implementations. In a larger number of cases from the considered literature, neglected in the table, the comparisons are made between non-preview and preview-augmented controllers, and thus highlight the possible level of performance advantage provided by the road preview, depending on specific features, e.g., the actuation bandwidth.

As the performance of the rather complex preview-augmented control structures is usually influenced by a high number of specific formulation details, such as the adopted cost function terms, and calibration parameters, such as the values of the cost function weights, a systematic and reliable comparison should be based on controller designs and calibrations achieved through optimisation-based tuning routines, similarly to what has been recently done on the topic of anti-jerk control for vehicle powertrains in Scamarcio et al., and Sorniotti (2020). For the same reasons, an indirect performance comparison involving control structures implemented in different papers is very difficult. In summary, the authors of this review believe that there is significant scope for an extensive and objective performance comparison study of the main control structures discussed in Sections 4 and 5. Nevertheless, some general considerations can be made regarding specific control performance aspects:

- Hard constraints. The capability of dealing with hard constraints, e.g., the physical limitations in terms of actuator force and stroke, is a very important feature, which can be explicitly imposed in the design process of MPC and – even if more indirectly – H_2/H_∞ control. On the contrary, LQ strategies can only consider soft constraints through the definition of the cost function J (Van Der Aa et al., 1997).
- Robustness, in terms of capability of maintaining performance and stability in presence of uncertainties or/and external disturbances. The typical design routines of H_∞ controllers allow the quantification of the achieved robustness level, and to meet defined robust stability and performance objectives for the worst-case scenarios (Skogestad & Postlethwaite, 2007). Robust model predictive control formulations are also available from the literature, e.g., see an example of recent application to the path tracking control problem of an automated vehicle in Yu et al., and Zhu (2020), but, to the best of our knowledge, they have not been applied to the specific problem of preview-augmented suspension control yet, with the recent exception in Song and Wang (2020), where the incremental MPC strategy extracts more information from the internal model, at the cost of increased complexity in the optimization problem.
- Design simplicity, i.e., the level of involved complexity in the control design process. Most of the considered controllers are model-based. On the one hand, LQ and MPC formulations rely on state space formulations of the system dynamics, and the rather intuitive definition of cost functions and – where appropriate and possible – constraints, which can be set by vehicle specialists, in the context of available LQ and MPC development tools. On the other hand, in the opinion of the authors of this survey, the non-optimal controllers (including feedback and feedforward compensation) as well as the H_∞ controllers, especially when based on models that are more advanced than the baseline quarter car model, imply multi-variable control designs in the frequency domain, which can be rather unintuitive for a typical vehicle dynamics specialist, and require some form of insight into the relevant control theory.
- Required computational power, i.e., the level of involved computational complexity during the control design phase and, more importantly, the vehicle deployment stage. During the design phase, H_∞ controllers are rather computationally demanding as they can require the iterative solution of a system of matrix inequalities; similarly, eMPC formulations imply the offline generation of the explicit solution of the optimal control problem. In the vehicle deployment phase, iMPC formulations need the online real-time solution of the associated optimal control problem, which is typically significantly more demanding than the on-line implementation of the transfer functions of feedforward compensators, H_∞ controllers, or the feedforward and feedback terms of LQ formulations. The deployment of eMPC only requires a function evaluation rather than an on-line optimisation, and therefore is computationally very efficient, at the price of a major increase of the flash memory requirement, which can represent an issue for an implementation with rather high number of states and prediction steps.

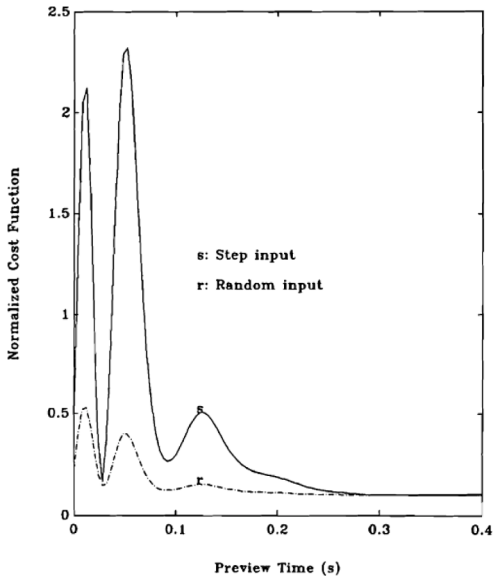

Fig. 24. Resulting cost function values as functions of preview time, for a quarter car mode1 with a preview-augmented active suspension system, subject to step and random road inputs at constant vehicle speed (10 m/s). Reproduced with permission from Louam et al. (1992).

6.2. *Effect of preview time and preview sensor noise on control system performance*

This section deals with aspects that are relevant to multiple preview-augmented suspension controllers discussed in Sections 4 and 5, in particular: i) the appropriate selection of the preview time, which is crucial for achieving the desired suspension performance, especially for the control strategies using the whole road profile information up to the preview time, e.g., LQ, H_∞ and MPC; and ii) the effect of preview information inaccuracies on control system performance.

The studies in Tomizuka (1975, 1976), based on LQ control, show that, as expected, the value of the cost function J, see (34)-(35), is reduced by the preview information, i.e., performance improves, and, importantly, there exists a preview length beyond which no significant further enhancement can be achieved. In the authors' words, "if the closed-loop system is asymptotically stable, roads input dynamics are not important for the determination of the control when the preview is long enough." This statement provides a useful indication for the appropriate design of the preview distance, and is confirmed by other authors applying optimal control to preview-augmented suspension systems, see Gordon and Sharp (1998); Hać (1994); Hać and Youn (1992); Louam et al. (1992); Prokop and Sharp (1995); Rahman and Rideout (2012); and Thompson and Pearce, 2001a, 2001b). In this respect, Fig. 24, from Louam et al. (1992), shows that for short preview times, the specific LQ controller can lead to significant oscillations of the resulting cost function value for step and random road inputs, while the performance of the same preview controller tends to stabilise for higher preview times. This means that the preview time should be larger than a minimum value, which depends on the manoeuvre; for example, at 10 m/s for step and random road input profiles, a preview time of 0.3 s is sufficient for optimising performance, which provides an indication of the correct order of magnitude. The time domain analysis in Gopala Rao and Narayanan (2008), for a random road input profile at different vehicle speeds, focuses on the handling performance, and considers (Fig. 25) the *RMS* values of the front wheel deflection as a function of vehicle speed, for different preview distances, P_d; interestingly, "beyond a particular distance the performance actually deteriorates indicating an optimum preview distance".

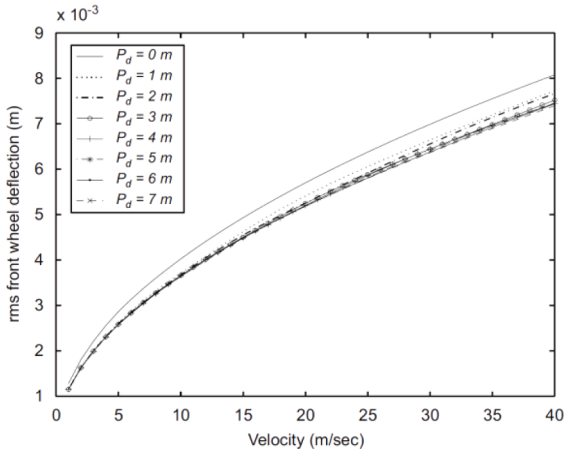

Fig. 25. *RMS* values of front tyre deflection as functions of vehicle speed, for different preview distances, P_d, along a random road input profile at different vehicle speeds. Reproduced with permission from Gopala Rao and Narayanan (2008).

According to Rahman and Rideout (2012), different vehicle speeds correspond to different optimal preview times, and thus the flexibility of lead vehicle preview – which, in the opinion of the authors of this survey, is much more difficult to implement in practice – is preferable to fixed look-ahead sensors, "for which a single preview time is associated with a given vehicle velocity." The same authors also state that their simulations show that the preview-related performance improvement with respect to the passive vehicle and the controlled vehicle without preview increases with increasing vehicle speed. In Thompson and Pearce (2001a), the recommended preview distance for an LQR implementation monotonically increases with vehicle speed, see the results in Fig. 26. In the speed-dependent hybrid horizon-varying iMPC in Wu et al. (2020), a constant preview distance is used at medium-to-high vehicle speeds, which implies a decrease of the number of preview points, N_{tp}, with increasing vehicle speed; however, to reduce the computational load, a fixed number of preview points, i.e., a fixed preview time, is used at low vehicle speed, see the curves in Fig. 27.

Most of the papers, including the previously cited Thompson and Pearce (2001a), analyse the preview time effect by considering ideal suspension actuators with infinite bandwidth. However, the minimum preview time to minimise the cost function is greatly influenced by the suspension actuation dynamics, see the LQR suspension controller analysis in Prokop and Sharp (1995), according to which the minimum recommended preview time reduces by increasing the actuator cut-off frequency. If the preview controller targets road holding improvements, i.e., by imposing a high weight on the tyre deflection term of J, significant cost function reductions with respect to the passive system can only be obtained through actuators with a cut-off frequency greater than 6 Hz, while actuators with cut-off frequencies up to 4 Hz hardly obtain any benefit, neither from introducing active control, nor from the

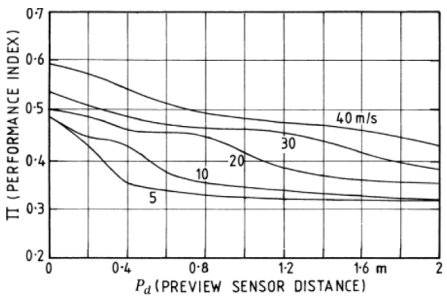

Fig. 26. Resulting cost function values (referred to as performance index) as functions of the preview sensor distance for a range of vehicle speeds, for a road step input. Reproduced with permission from Thompson and Pearce (2001a).

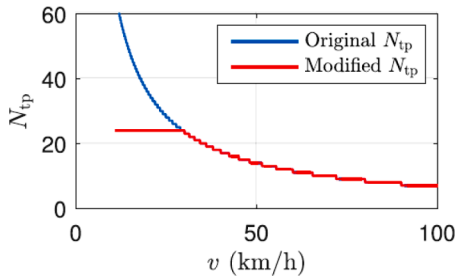

Fig. 27. Number of preview points, N_{tp}, as a function of vehicle speed. Reproduced with permission from Wu et al. (2020).

use of preview information, see Fig. 28(a). When ride comfort is the main target, i.e., the cost function has higher weight on the vertical acceleration of the sprung mass, also actuators with slow dynamics are sufficient to provide substantial improvements with respect to the passive vehicle, see Fig. 28(b).

For a constant preview time, the number of preview points is directly related to the performance of the preview-augmented controller. For example, for an H_2 /H_∞ controller, P. Li et al. (2014a) highlights that N_{tp} significantly influences the results of the system of matrix inequalities in (49)-(51). The dimension of the augmented output matrix, $\boldsymbol{C_a}$, depends on the number of available preview samples. For a given preview time t_h, which is kept constant, the study varies the sampling time, T_p, of the preview information, which is defined as a multiple of the controller sampling time T_s, i.e., $T_p = lT_s$ with $l = 1,2,\ldots,7$ for the case in Fig. 29. This means that for $l = 1$ the controller considers N_{tp} preview points, which are 7 in Fig. 29, while for the same example the condition $l = 7$ corresponds to the controller implementation without preview. For each l, Fig. 29 reports the resulting values of γ_1, i.e., the maximum value of $\| \boldsymbol{T}_1 \|_\infty$ in (47), for different initialisation values of $\boldsymbol{K}$ in (48). The important point is that there exists a correlation, shown in Fig. 29, between γ_1 and l, i.e., the larger the number of preview points for the same preview time, the smaller is the resulting γ_1, which improves control system performance.

The effect of uncertainties in the preview information is an important aspect to be considered in the experimental implementation of preview-augmented suspension controllers, since real scenarios are characterised by the inevitable presence of sensor noise, uncertainties and road profile measurement errors. Vahidi and Eskandarian (2002) evaluates the level of uncertainty that can be tolerated in the preview measurements, without significantly compromising the resulting suspension control performance. Fig. 30 plots the *RMS* values (normalised with the passive

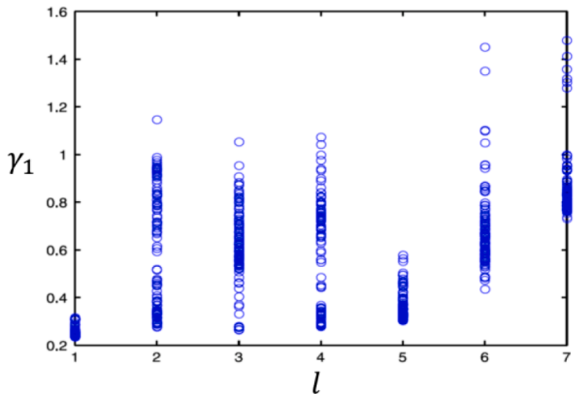

Fig. 29. Sensitivity of γ_1 (the maximum value of $\| \boldsymbol{T}_1 \|_\infty$) to the number of preview samples, for a fixed preview time, at constant vehicle speed (20 m/s). Reproduced with permission from P. Li et al. (2014a).

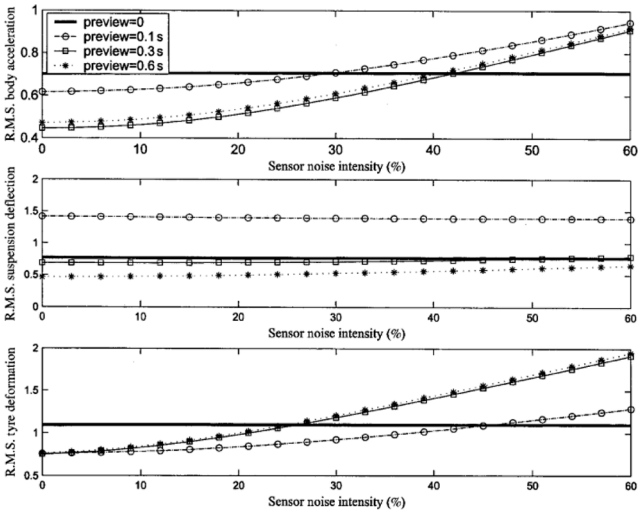

Fig. 30. Influence of preview sensor noise on the preview control response (the ratio of preview control response to passive one) when a random road profile is crossed at constant vehicle peed (20 m/s). Reproduced with permission from Vahidi and Eskandarian (2002).

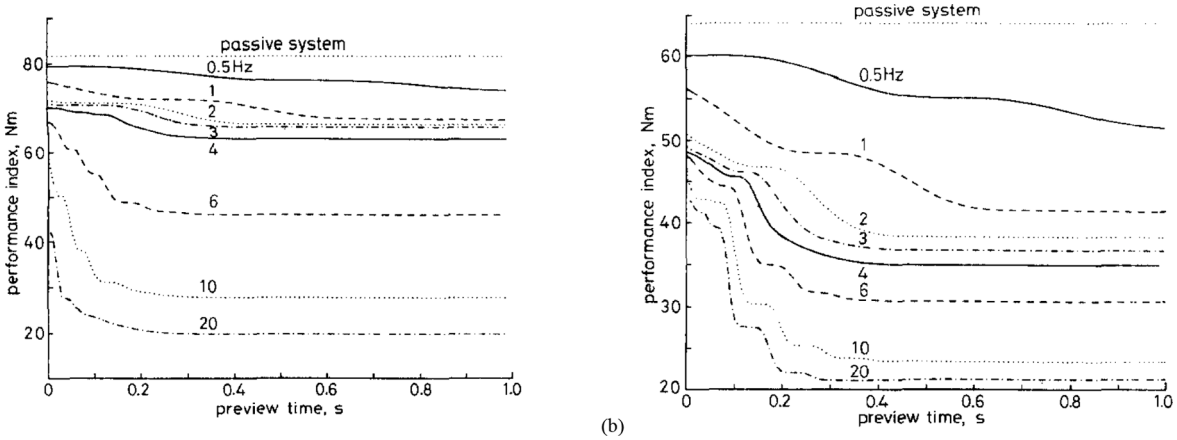

Fig. 28. Resulting cost function values (referred to as performance index) as functions of preview time for controller calibrations targeting: (a) handling improvement; and (b) ride comfort improvement, for different suspension actuator cut-off frequencies, on a random road profile at constant speed (10 m/s). Reproduced with permission from Prokop and Sharp (1995).

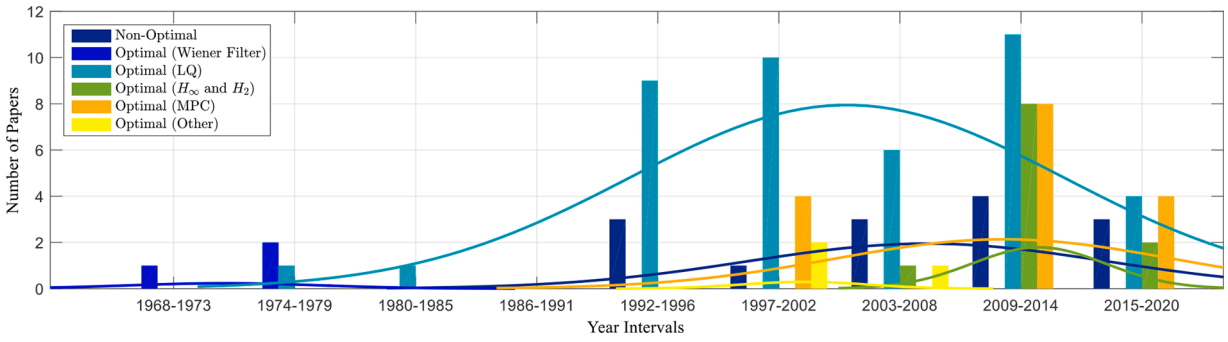

Fig. 31. Distribution of the considered preview-augmented suspension control structures over time.

vehicle results) of vehicle body acceleration, suspension travel, and tyre deflection, as functions of the intensity of the look-ahead sensor noise, which is assumed to be zero-mean Gaussian and white. The noise intensity is expressed as percentage of the mean value of the road elevation. The results, reported for different reasonable values of preview time, show that suspension deflection is the least sensitive variable to sensor noise, while tyre deformation is the most affected output. According to the authors, satisfactory performance can still be achieved for sensor noise intensities up to 20%.

6.3. Trends and potential future developments

Based on the references included in this literature survey, Fig. 31 shows the distribution of the different preview-augmented suspension control structures, according to the publication year of the respective studies, in the form of histograms and the corresponding fitting lines. The graph highlights an overall peak in the studies on the topic of preview-augmented suspension control in the period 2009-2014. Non-optimal controllers have been constantly studied and developed since the beginning of the 1990s, and still attract significant attention within the automotive industry, thanks to their relative ease of design and calibration. LQ implementations, after reaching a peak in the early 2000s, have been subject to decreasing research interest (currently they are mainly used as term of comparison for other controllers), as the attention has shifted towards H_∞ and especially MPC strategies. In fact, iMPC for suspension control has become practically feasible through the introduction of powerful automotive microcontrollers and computationally efficient solvers, which allow the real-time implementation of the required online optimisations. Moreover, MPC is getting widely used, at least at the research level, in the context of path tracking control for automated vehicles (see the pioneering implementation in Falcone et al., and Hrovat (2007)), and vehicle stability control (see the recent analysis in Metzler et al., and Sorniotti (2020)), which facilitates its adoption also for other control functions, such as suspension control.

For the main categories discussed in Sections 4 and 5, Table 3 shows the control structure distribution among the papers considered in this review, and indicates the respective number of implementations in terms of: a) typology of model for control system design, i.e., quarter car, half car and full car models, which shows a trend towards full car models in case of MPC implementations (7 out of the analysed 16 MPC examples use full car models as prediction models), even if, when considering all control structures, 36 implementations out of 83 are based on simple quarter car models; b) suspension actuation technology, i.e., semi-active or active, with a clear prevalence (62 out of 83 implementations) of active systems; and c) control system validation methodology, i.e., simulation-based or experimental, which highlights the low number of experimental implementations, i.e., 16 out of 83. As some of the experimental studies involve vehicle corner testing on poster and damper rigs, the important conclusion is that the number of experimental vehicle validations on roads or proving grounds is very limited.

In the opinion of the authors of this survey, potential future developments and analyses in the area of preview-augmented suspension control could involve:

- The enhancement of sensing technologies and sensor fusion algorithms for more accurate real-time generation of the road profile information. The performance of preview-augmented controllers is strongly influenced by the accuracy level provided by the available sensing technologies. In look-ahead preview configurations, three-dimensional (3D) sensors are installed in the frontal part of the vehicle to acquire the road information in advance. Many of the studies analysed in the previous sections do not provide the details of the methodology to extract the road profile elevation in real-time, and many of them only assume that the elevation profile is already known (M. Ahmed & Svaricek, 2013; Akbari & Lohmann, 2008, 2010; Elmadany et al., 2011; Hać, 1992, 1994; Hać & Youn, 1992; Martinus et al., 1996; Marzbanrad et al., 2004; Prokop & Sharp, 1995; Theunissen et al., 2020; Thompson & Pearce, 1998; Tomizuka, 1976). Ahmed and Svaricek (2014) as well as Donahue and Hedrick (2001) provide the geometric formulations for compensating the effect of the vehicle chassis motion disturbance starting from the direct road profile information measured by a Lidar sensor, while Schindler (2009) and Streiter (2008) describe recursive scan-matching and tyre contact regression algorithms for road profile derivation from sensor measurements. Further methods are developed by Göhrle et al. (2015) to accumulate redundant measurements from the sensor, and apply filtering techniques. More recently, D. Zhao et al., and Du (2018) proposes an approach integrating a 3D vision-based sensor, an inertial measurement unit (IMU), a global positioning system (GPS), and cloud-sourced

Table 3
Statistics on the main considered preview-augmented suspension control structures from the literature.

Control strategy		# controllers	Model type (# controllers using)			Application type (# controllers)		Validation (# controllers including)	
			Quarter car	Half car	Full car	Semi-active	Active	Sim.	Exp.
Non-optimal	FB + FF compensation	14	3	5	6	3	11	10	4
Optimal	LQ	42	22	13	7	7	35	38	4
	H_∞ and H_2	11	4	7	0	4	7	9	2
	MPC	16	7	2	7	7	9	10	6

information, and involving a Kalman filter. Similar sensor fusion approaches, based on 3D laser scanners, IMU, and GPS, are also described in Ni et al., and Kong (2020) and L. Wang et al., and Liu (2020).

- The evaluation of more advanced methods for accounting for the expected road profile ahead. In the context of preview suspension control, Göhrle et al. (2015) mentions the impact of road information filtering on the performance of a feedforward preview contribution coupled with a skyhook suspension controller. However, significantly deeper analyses could be carried out on the topic. In fact, advanced simulation studies on ride comfort adopt enveloping models to correctly emulate the tyre-road interaction and the longitudinal vehicle acceleration oscillations induced by irregular road profiles, e.g., see Zhu et al. (2012) and Guo et al., and Yuan (2020). As discussed in this paper, the literature on preview-based suspension control does not seem to include any form of tyre enveloping model, such as the one in Schmitz (2004), in the definition of the road preview profile that is input to the controller. However, the actual tyre geometry and structural stiffness properties can have an important effect on the equivalent road profile for preview suspension control, e.g., it is intuitive to appreciate that in case of a step in the road profile the actual vertical displacement profile of the tyre contact patch will be characterised by a much smoother behaviour. Further research could cover the analysis of the effect of the introduction of tyre enveloping models at different levels of complexity within preview-augmented suspension controllers.
- The integration of preview-augmented suspension control with other suspension control functions. Most of the considered studies on preview-augmented suspension control only target the ride comfort enhancement function, and are not integrated with other typical suspension control functions, e.g., body control to compensate for the effect of the longitudinal and lateral accelerations in traction/braking and cornering. As highlighted in Göhrle et al. (2015), the integration of preview-based control with other suspension control functions is typically easier for non-optimal controllers, which are characterised by a high level of modularity, as for these controllers the reference values output by the different control modules can be simply summed, to obtain the resulting actuator command. Further research should cover the development of integrated optimal controllers, and especially MPC implementations, incorporating the whole range of industrially relevant active and semi-active suspension control functions.
- Model predictive control structures integrating several functions in the context of automated vehicles with multiple actuators. This research line could further develop the idea in Wu et al. (2020), which only preliminarily discusses some form of synergy between vehicle speed control and preview suspension control. In fact, as outlined in Ricciardi et al. (2019), in-wheel powertrains could facilitate the pitch control function of active suspension systems, in the context of extended anti-jerk control functionalities, see Scamarcio et al., and Sorniotti (2020) for an extensive discussion on the state-of-the-art of anti-jerk control. Moreover, thanks to their relatively high bandwidth, in-wheel (and possibly on-board as well) electric powertrains could also be evaluated for the preview-based compensation of the longitudinal acceleration oscillations induced by road irregularities, see the preliminary studies in Fukudome (2016), Yamada et al., and Katsuyama (2017) and Beauduin et al., and Katsuyama (2017), within complex control structures using the active/semi-active suspension contribution for the enhancement of the vertical dynamics. This is a completely new area of exploration, which would require the development of appropriate prediction models for the implementation of the longitudinal control functions, and insight into the most effective parametrisation of the MPC algorithms, e.g., in terms of prediction horizon and preview time.
- The extension of preview-augmented suspension control to the vehicle dynamics domain. This survey focused on preview-augmented ride comfort control through active and semi-active suspension systems. However, the significant improvement of vehicle localisation techniques, together with the detailed mapping of the road scenarios, which is already available in navigation systems and will further improve in the context of automated driving, is going to facilitate the implementation of preview-augmented suspension control functions for the enhancement of vehicle dynamics as well. In fact, a significant body of literature, e.g., see Ricco, Percolla, et al., (2020); Ricco, Zanchetta, et al., (2020); Sorniotti and D'Alfio (2007), Williams and Haddad (1995), shows – through simulations and experiments – the potential of enhancing the steady-state and transient cornering response by varying the vertical tyre load distribution among the vehicle corners. In particular, an increase of the lateral load transfer on the front axle, or equivalently a lateral load transfer decrease on the rear axle, tends to increase understeer, and, vice versa, lateral load transfers reductions on the front axle and increments on the rear axle reduce understeer. Although the frequencies associated with vehicle dynamics are significantly lower than those of ride comfort control, the knowledge of the expected trajectory ahead could facilitate the computation of the most appropriate suspension actuator control action, e.g., the suspension controller could behave differently if the vehicle is going to start cornering rather than remaining on its current straight trajectory. This functionality is likely to be able to bring benefits in situations implying quickly variable steering wheel inputs and load transfers. Similarly, preview augmentation could be applied to the vehicle body control algorithms based on suspension control for compensating the roll and pitch effects of longitudinal and lateral accelerations.
- The implementation of advanced vehicle connectivity functions for enhanced suspension control. The trend towards connected and automated driving is likely to bring new vehicle chassis control options. For example, connected vehicles could be used as sensors to progressively update the road profile characteristics, to be systematically mapped in a database set on the cloud, and made available to all relevant connected vehicles (Z. Li et al., 2015). In theory, options based on lead vehicles would enable preview-augmented suspension control also for vehicles not equipped with specific preview sensors and/or estimators. Although preliminary studies, e.g., see the already mentioned Asl and Rideout (2010), Rahman and Rideout (2012), and Song and Wang (2020), present these ideas and possible implementation options, in the opinion of the authors of this survey further work is needed in this area to actually test these algorithms in typical complex real world scenarios, with passenger car prototypes.
- The detailed analysis of the influence of vehicle model fidelity on the performance of the model-based preview-augmented controllers, and especially model predictive controllers. The design of most of the considered controllers relies on the accuracy of the model adopted to predict the vehicle heave, roll, and pitch dynamics. The model fidelity depends on the number of degrees of freedom used to approximate the vehicle dynamics, the details of the formulations (e.g., on whether the roll and pitch moments and heave force induced by the longitudinal and lateral accelerations are included), and on the accuracy of the set of measured or estimated model parameters. The effect of model parameters uncertainties on the controller performance can be in part mitigated with H_∞ design routines (Akbari & Lohmann, 2010) or robust MPC formulations (Yu et al., 2020). However, to the best of our knowledge, a sensitivity analysis of the effect of vehicle model accuracy on the resulting controller performance has not been carried out for preview-augmented suspension control yet, with the limited exception of Louam et al. (1992), where the impact of the quarter car and half car models on the cost function of the LQ strategy is assessed for pulse, step and random road profiles.

Based on the previous points, the authors of this survey are confident

that the science of preview-augmented automotive suspension control is going to remain the object of significant research interest, developments and experimental demonstrations in the years to come.

7. Conclusions

This paper provided an overview of the extensive literature on preview-augmented suspension control, including a critical analysis of the most relevant aspects, with the following main conclusions:

- Any suspension control structure with preview of the road profile elevation can significantly outperform the respective equivalent controller without preview. Such performance benefit can be provided only if a sufficiently long preview time is used. The available analyses also highlight that there exists a preview time threshold beyond which performance does not further improve, while complexity and computational effort increase. As a consequence, preview-augmented controllers should be calibrated according to this preview time threshold, typically of the order of magnitude of a few tenths of second, which can vary with the driving conditions and actuation dynamics. According to one of the considered studies, the ride comfort performance can be improved by preview-based suspension control even in case of low-bandwidth actuators. On the contrary, the vehicle handling benefit of preview-based control, expressed in terms of dynamic tyre loads, is negligible if the available suspension actuators have <4 Hz bandwidth, whatever is the selected preview time, while actuators with >6 Hz bandwidth can provide significant handling enhancements.
- 16% of the considered preview-augmented suspension control structures use formulations that are not based on the optimal control theory. Feedback control augmented with feedforward disturbance compensation is the most frequent control structure typology of this category, which, according to the references, seems to have been implemented on production vehicles. The feedback contribution is a typical non-preview strategy, e.g., it can use skyhook, extended skyhook, state feedback, and output feedback. Also, the overall algorithm can include the compensation of the vehicle body pitch and roll motions caused by the longitudinal and lateral accelerations. The preview-augmented feedforward contribution usually consists of model-based compensators of the effect of the road disturbance on the expected total vertical force and pitch moment applied to the vehicle body, and/or the vertical force variation on each unsprung mass. The controllers of this category tend to be characterised by excellent modularity, as the different control effort contributions can be simply summed together, to generate the total reference control action.
- 84% of the considered control structures are based on optimal control, and more than half of these adopt LQ control. Quadratic cost function formulations are used for LQ and MPC implementations, mostly penalising vehicle body acceleration, suspension displacement, tyre deflection and control effort, and in some cases also sprung mass displacement and displacement rate. H_∞ and H_2/H_∞ controllers require iterative routines, which are based on the robust stability and/or performance criteria of the specific control formulation, but are less intuitively related to the performance of the resulting system, i.e., their design requires a rather deep understanding of the underlying theory, which could represent a limiting factor in the context of the automotive industry. The model formulations are linear in all LQ and H_∞ controllers, and in nearly all MPC cases, and include quarter car, half car and full car models, in decreasing order in terms of number of implementations. For semi-active suspensions, specific actuator constraints have to be included outside the feedback controller in LQ and H_∞ control structures, and within the feedback controller formulation in case of MPC. Most of the preview-augmented MPCs are based on the implicit, i.e., online, solution of the optimal control problem, and thus require relatively high computational effort, which nowadays should not represent a major issue anymore, and low memory utilisation.
- The performance comparisons of preview-augmented suspension controllers are limited to a low number of papers, i.e., less than 15% of the considered ones (see Table 2), which highlights an important gap in the literature, also considering – in many cases – the lack of detailed explanations on objective calibration criteria. From a general viewpoint, non-optimal formulations based on the combination of feedback control and feedforward disturbance compensators, as well as LQ implementations, cannot formally account for system constraints, which, instead, are considered in H_2/H_∞ formulations and – more explicitly – in MPCs. The available comparisons tend to highlight a rather modest performance of LQ implementations with respect to all other preview-augmented controllers (see Table 2), while, on the other side of the spectrum, MPC emerges – by limited margin – as the best performing control structure. Given the current popularity of MPC in the area of vehicle chassis and path tracking control, facilitated by the introduction of computationally powerful automotive control hardware and efficient real-time solvers, MPC can be considered the natural control structure choice for future preview-augmented suspension control, even if it can be less easily integrated with other suspension control functions than non-optimal controllers.
- The ongoing trend towards driving automation and the implementation of novel automated vehicle concepts, enabling the passengers to carry out other activities while the vehicle is autonomously driven, requires the enhancement of the comfort level of passenger cars, which is likely to stimulate further research on preview-augmented suspension control. According to the authors of this survey, potential future developments include: a) the improvement of the sensing technologies for the detection of the road profile ahead, with special focus on sensor fusion; b) the evaluation of more advanced methods, e.g. based on tyre enveloping models, for considering the effect of the expected road profile ahead within the controller; c) the integration of the optimal preview-augmented suspension controllers for ride comfort enhancement, and especially of MPC structures, with other suspension control functions, e.g., body control to compensate for the effect of the longitudinal and lateral accelerations in traction/braking and cornering; d) MPC structures integrating several functions in the context of automated vehicles with multiple actuators, e.g., including synergies between powertrain/s and suspension actuators for the concurrent enhancement of pitch control and longitudinal dynamics; e) the extension of preview-augmented suspension control to the vehicle dynamics domain, e.g., to vary the vertical tyre load distribution depending on the current position and state of the vehicle, and the expected trajectory ahead; f) more extensive experimental implementations of advanced vehicle connectivity functions for enhanced suspension control; and g) the analysis of the influence of vehicle model fidelity on the performance of model-based controllers, with particular attention to model predictive controllers.

Declaration of Competing Interest

The authors declare that they have no known competing financial interests or personal relationships that could have appeared to influence the work reported in this paper.

Acknowledgement

This work was supported in part by the Horizon 2020 Programme of the European Commission under grant agreements no. 734832 (CLOVER project) and 872907 (OWHEEL project).

References

Ahmed, M. M., & Svaricek, F. (2014). Preview optimal control of vehicle semi-active suspension based on partitioning of chassis acceleration and tire load spectra. In *2014 European control conference, ECC 2014* (pp. 1669–1674). https://doi.org/10.1109/ECC.2014.6862615. https://doi.org/.

Ahmed, M., & Svaricek, F. (2013). Preview control of semi-active suspension based on a half-car model using Fast Fourier Transform. In *2013 10th international multi-conference on systems, signals and devices, SSD 2013* (pp. 1–6). https://doi.org/10.1109/SSD.2013.6564120. https://doi.org/.

Akbari, A., Koch, G., Pellegrini, E., Spirk, S., & Lohmann, B. (2010). Multi-objective preview control of active vehicle suspensions: Experimental results. *2010 2nd International Conference on Advanced Computer Control, 3*, 497–502.

Akbari, A., & Lohmann, B. (2008). Multi-objective preview control of active vehicle suspensions. *IFAC Proceedings Volumes (IFAC-PapersOnline), 41*(Issue 2), 3398–3403. https://doi.org/10.3182/20080706-5-KR-1001.00577. https://doi.org/.

Akbari, A., & Lohmann, B. (2010). Output feedback H∞/GH2 preview control of active vehicle suspensions: A comparison study of LQG preview. *Vehicle System Dynamics, 48*(12), 1475–1494. https://doi.org/10.1080/00423110903509327. https://doi.org/.

Asl, H. A., & Rideout, G. (2010). Using lead vehicle response to generate preview functions for active suspension of convoy vehicles. In *Proceedings of the 2010 American Control Conference, ACC 2010* (pp. 4594–4600). https://doi.org/10.1109/acc.2010.5530881. https://doi.org/.

Badiru, I., & Cwycyshyn, W. B. (2013). Customer focus in ride development. *SAE technical papers 2013-01-1355*. https://doi.org/10.4271/2013-01-1355. https://doi.org/.

Beauduin, T., Yamada, S., Fujimoto, H., Kanou, T., & Katsuyama, E. (2017). Control-oriented modelling and experimental modal analysis of electric vehicles with geared in-wheel motors. In *IEEE/ASME international conference on advanced intelligent mechatronics* (pp. 541–546). AIM. https://doi.org/10.1109/AIM.2017.8014073. https://doi.org/.

Bemporad, A., Borrelli, F., & Morari, M. (2000a). The explicit solution of constrained LP-based receding horizon control. *Proceedings of the 39th IEEE Conference on Decision and Control, 1*, 632–637. https://doi.org/10.1109/cdc.2000.912837. https://doi.org/.

Bemporad, A., Borrelli, F., & Morari, M. (2002b). Model predictive control based on linear programming~ the explicit solution. *IEEE Transactions on Automatic Control, 47*(12), 1974–1985.

Bemporad, A., Borrelli, F., & Morari, M. (2000c). Optimal controllers for hybrid systems: stability and piecewise linear explicit form. *Proceedings of the 39th IEEE Conference on Decision and Control (Cat. No. 00CH37187), 2*, 1810–1815. https://doi.org/10.1109/CDC.2000.912125. https://doi.org/.

Bemporad, A., Morari, M., Dua, V., & Pistikopoulos, E. N. (2000). The explicit solution of model predictive control via multiparametric quadratic programming. *Proceedings of the 2000 American Control Conference. ACC (IEEE Cat. No. 00CH36334), 2*, 872–876. https://doi.org/10.1109/ACC.2000.876624. https://doi.org/.

Bender, E. K. (1968). Optimum linear preview control with application to vehicle suspension. *Journal of Basic Engineering, 90*(2), 213–221. https://doi.org/10.1115/1.3605082. https://doi.org/.

Brown, R. K., Pusey, J., Murugan, M., & Le, D. (2011). Comparison of performance effectiveness of generalized predictive control algorithms developed for a simplified ground vehicle suspension system. *SAE Technical Papers 2011-01-2162*. https://doi.org/10.4271/2011-01-2162. https://doi.org/.

6841, 19876841, B. S. (1987). *Measurement and evaluation of human exposure to whole-body mechanical vibration and repeated shock*. BSI.

Burkhard, G., Vos, S., Munzinger, N., Enders, E., & Schramm, D. (2018). Requirements on driving dynamics in autonomous driving with regard to motion and comfort. *Internationales Stuttgarter Symposium, 18*, 683–697. https://doi.org/10.1007/978-3-658-21194-3_53. https://doi.org/.

Campolo, C., Molinaro, A., Iera, A., & Menichella, F. (2017). *Emerging technology for 5g enabled vehicular networks 5g network slicing for vehicle-to-everything services* (pp. 38–45). IEEE Wireless Communications. *December*.

Canale, M., Milanese, M., & Novara, C. (2006). Semi-active suspension control using "fast" model-predictive techniques. *IEEE Transactions on Control Systems Technology, 14*(6), 1034–1046. https://doi.org/10.1109/TCST.2006.880196. https://doi.org/.

Cao, D., Song, X., & Ahmadian, M. (2011). Editors' perspectives: Road vehicle suspension design, dynamics, and control. *Vehicle System Dynamics, 49*(1–2), 3–28. https://doi.org/10.1080/00423114.2010.532223. https://doi.org/.

Chen, S., He, R., Liu, H., & Yao, M. (2012). Probe into necessity of active suspension based on LQG Control. *Physics Procedia, 25*, 932–938. https://doi.org/10.1016/j.phpro.2012.03.180. https://doi.org/.

Cormen, T. H., Leiserson, C. E., Rivest, R. L., & Stein, C. (2010). *Introduction to algorithms* (3th Ed.). MIT Press https://mitpress.mit.edu/books/introduction-algorithms-third-edition.

Cseko, L. H., Kvasnica, M., & Lantos, B. (2010). Analysis of the explicit model predictive control for semi-active suspension. *Periodica Polytechnica Electrical Engineering, 54*(1–2), 41–58. https://doi.org/10.3311/pp.ee.2010-1-2.05. https://doi.org/.

Cseko, L. H., Kvasnica, M., & Lantos, B. (2015). Explicit MPC-Based RBF neural network controller design with discrete-time actual kalman filter for semiactive suspension. *IEEE Transactions on Control Systems Technology, 23*(5), 1736–1753. https://doi.org/10.1109/TCST.2014.2382571. https://doi.org/.

Cvok, I., Deur, J., Eric Tseng, H., & Hrovat, D. (2020). Comparative performance analysis of active and semi-active suspensions with road preview control. *Lecture Notes in Mechanical Engineering, 1*, 1808–1818. https://doi.org/10.1007/978-3-030-38077-9_206. https://doi.org/.

De Bruyne, S., Van Der Auweraer, H., Anthonis, J., Desmet, W., & Swevers, J. (2012). Preview control of a constrained hydraulic active suspension system. In *Proceedings of the IEEE conference on decision and control* (pp. 4400–4405). https://doi.org/10.1109/CDC.2012.6425847. https://doi.org/.

Desikan, A., & Kalaichelvi, V. (2015). Design for a preview control of semi-active suspension system using fuzzy-logic and image processing techniques. In *IEEE international conference on electro information technology* (pp. 224–229). https://doi.org/10.1109/EIT.2015.7293426. *2015-June*https://doi.org/.

Dessort, R., & Chucholowski, C. (2017). Explicit model predictive control of semi-active suspension systems using Artificial Neural Networks (ANN). In *8th international munich chassis symposium 2017* (pp. 207–228). https://doi.org/10.1007/978-3-658-18459-9_15. https://doi.org/.

Dhiman, A., Chien, H. J., & Klette, R. (2017). Road surface distress detection in disparity space. In *International conference image and vision computing New Zealand, 2017-Decem* (pp. 1–6). https://doi.org/10.1109/IVCNZ.2017.8402459. https://doi.org/.

Diels, C., & Bos, J. E. (2015). User interface considerations to prevent self-driving carsickness. In *Adjunct proceedings of the 7th international conference on automotive user interfaces and interactive vehicularapplications* (pp. 14–19). https://doi.org/10.1145/2809730.2809754. *AutomotiveUI 2015*https://doi.org/.

Diels, C., & Bos, J. E. (2015). Self-driving carsickness. *Applied Ergonomics, 53*(Part B), 374–382. https://doi.org/10.1016/j.apergo.2015.09.009. https://doi.org/.

Diels, C., Erol, T., Kukova, M., Wasser, J., Cieslak, M., Miglani, A., Mansfield, N., Hodder, S., & Bos, J. (2017). *Designing for comfort in shared and automated vehicles (SAV): A conceptual framework* (pp. 1–8). Loughborough University Institutional Repository. *June*.

Donahue, M. D., & Hedrick, J. K. (2001). *Implementation of an active suspension, preview controller for improved ride comfort. Th.* The University at Berkeley.

Drgoňa, J., Klaučo, M., Janeček, F., & Kvasnica, M. (2017). Optimal control of a laboratory binary distillation column via regionless explicit MPC. *Computers and Chemical Engineering, 96*, 139–148. https://doi.org/10.1016/j.compchemeng.2016.10.003. https://doi.org/.

Elbanhawi, M., Simic, M., & Jazar, R. (2015). In the passenger seat: investigating ride comfort measures in autonomous cars. *IEEE Intelligent Transportation Systems Magazine, 7*(3), 4–17. https://doi.org/10.1109/MITS.2015.2405571. https://doi.org/.

Elmadany, M. M., Al Bassam, B. A., & Fayed, A. A. (2011). Preview control of slow-active suspension systems. *JVC/Journal of Vibration and Control, 17*(2), 245–258. https://doi.org/10.1177/1077546310362451. https://doi.org/.

Elmadany, M. M., & Abduljabbar, Z. S. (1999). Linear quadratic Gaussian control of a quarter-car suspension. *Vehicle System Dynamics, 32*(6), 479–497. https://doi.org/10.1076/vesd.32.6.479.4224. https://doi.org/.

Falcone, P., Borrelli, F., Asgari, J., Tseng, H. E., & Hrovat, D. (2007). Predictive active steering control for autonomous vehicle systems. *IEEE Transactions on Control Systems Technology, 15*(3), 566–580. https://doi.org/10.1109/TCST.2007.894653. https://doi.org/.

Faraj, R., Graczykowski, C., & Holnicki-Szulc, J. (2019). Adaptable pneumatic shock absorber. *JVC/Journal of Vibration and Control, 25*(3), 711–721. https://doi.org/10.1177/1077546318795532. https://doi.org/.

Feng, J. P., Bei, S. Y., Yuan, C. Y., & Zhang, L. C. (2009). Research on wheelbase preview control for vehicle semi-active suspension based on neural networks. In *3rd international symposium on intelligent information technology application* (pp. 290–293). IITA. https://doi.org/10.1109/IITA.2009.351. *2009, 3*https://doi.org/.

Förstberg, J. (2000). Ride comfort and motion sickness in tilting trains. *Th. Institutionen för farkostteknik*. http://www.diva-portal.org/smash/record.jsf?pid=diva2%3A8728&dswid=-575.

Fukuda, T., Zhang, X., Hasegawa, Y., Matsuno, T., & Hoshino, H. (2004). Preview posture control and impact load control of rough terrain vehicle with interconnected suspension. *2004 IEEE/RSJ International Conference on Intelligent Robots and Systems (IROS)(IEEE Cat. No. 04CH37566), 1*, 761–766. https://doi.org/10.1109/IROS.2004.1389444. https://doi.org/.

Fukudome, H. (2016). Reduction of longitudinal vehicle vibration using in-wheel motors. *SAE technical papers 2016-01-1668*. https://doi.org/10.4271/2016-01-1668. https://doi.org/.

Gallep, J., & Müller, S. (2018). Vehicle Guidance Control for Automated Driving Considering Motion Sickness. In *14th International Symposium on Advanced Vehicle Control*. AVEC18.

Gangadharan, K. V., Sujatha, C., & Ramamurti, V. (2004). Experimental and analytical ride comfort evaluation of a railway coach. In *Proceedings of the A conference & exposition on structural dynamics (SEM ORG IMAC XXII* (pp. 1–15).

Gavin, H. P., Hanson, R. D., & Filisko, F. E. (1996). Electrorheological dampers, part i: analysis and design. *Journal of Applied Mechanics, Transactions ASME, 63*(3), 669–675. https://doi.org/10.1115/1.2823348. https://doi.org/.

Genta, G., & Morello, L. (2019). *The automotive chassis: Volume 2: System design* (2nd Ed.). Springer Nature.

Genta, G., & Morello, L. (2009). *The automotive chassis: Volume 1: Components dessign* (1st Ed.). Springer Nature.

Giorgetti, N., Bemporad, A., Tseng, H. E., & Hrovat, D. (2006). Hybrid model predictive control application towards optimal semi-active suspension. *International Journal of Control, 79*(5), 521–533. https://doi.org/10.1080/00207170600593901. https://doi.org/.

Göhrle, C., Schindler, A., Wagner, A., & Sawodny, O. (2013). Model Predictive Control of semi-active and active suspension systems with available road preview. In *2013 European control conference, ECC 2013* (pp. 1499–1504). https://doi.org/10.23919/ecc.2013.6669185. https://doi.org/.

Göhrle, C., Schindler, A., Wagner, A., & Sawodny, O. (2014). Design and vehicle implementation of preview active suspension controllers. *IEEE Transactions on*

Control Systems Technology, 22(3), 1135–1142. https://doi.org/10.1109/TCST.2013.2272342. https://doi.org/.

Göhrle, C., Schindler, A., Wagner, A., & Sawodny, O. (2015). Road profile estimation and preview control for low-bandwidth active suspension systems. *IEEE/ASME Transactions on Mechatronics, 20*(5), 2299–2310. https://doi.org/10.1109/TMECH.2014.2375336. https://doi.org/.

Göhrle, C., Wagner, A., Schindler, A., & Sawodny, O. (2012). Active suspension controller using MPC based on a full-car model with preview information. In *Proceedings of the American control conference* (pp. 497–502). https://doi.org/10.1109/acc.2012.6314680. https://doi.org/.

Gopala Rao, L. V. V., & Narayanan, S. (2008). Preview control of random response of a half-car vehicle model traversing rough road. *Journal of Sound and Vibration, 310* (1–2), 352–365. https://doi.org/10.1016/j.jsv.2007.08.004. https://doi.org/.

Gordon, T. J., & Sharp, R. S. (1998). On improving the performance of automotive semi-active suspension systems through road preview. *Journal of Sound and Vibration, 217* (1), 163–182. https://doi.org/10.1006/jsvi.1998.1766. https://doi.org/.

Guo, Z., Wu, W., & Yuan, S. (2020). Longitudinal-vertical dynamics of wheeled vehicle under off-road conditions. *Vehicle System Dynamics*, 1–22. https://doi.org/10.1080/00423114.2020.1823003. https://doi.org/.

Gysen, B. L. J., Paulides, J. J. H., Janssen, J. L. G., & Lomonova, E. A. (2010). Active electromagnetic suspension system for improved vehicle dynamics. *IEEE Transactions on Vehicular Technology, 59*(3), 1156–1163. https://doi.org/10.1109/TVT.2009.2038706. https://doi.org/.

Hać, A., & Youn, I. (1992). Optimal semi-active suspension with preview based on a quarter car model. *Journal of Vibration and Acoustics, Transactions of the ASME, 114* (1), 84–92. https://doi.org/10.1115/1.2930239. https://doi.org/.

Hać, Aleksander. (1992). Optimal linear preview control of active vehicle suspension. *Vehicle System Dynamics, 21*(1), 167–195. https://doi.org/10.1080/00423119208969008. https://doi.org/.

Hać, Aleksander. (1994). Decentralized control of active vehicle suspensions with preview. In *Proceedings of the American Control Conference* (pp. 1952–1956). https://doi.org/10.1109/acc.1994.752416. https://doi.org/.

Heißing, B., & Ersoy, M. (2011). *Chassis handbook*. Wiesbaden. https://doi.org/10.1007/978-3-8348-9789-3 (Chapter 5)https://doi.org/.

Hoberock, L. L. (1977). A survey of longitudinal acceleration comfort studies in ground transportation vehicles. *Journal of Dynamic Systems, Measurement and Control, Transactions of the ASME, 99*(2), 76–84. https://doi.org/10.1115/1.3427093. https://doi.org/.

Houzhong, Z., Jiasheng, L., Chaochun, Y., Xiaoqiang, S., & Yingfeng, C. (2019). Application of explicit model predictive control to a vehicle semi-active suspension system. *Journal of Low Frequency Noise Vibration and Active Control, 39*(3), 772–786. https://doi.org/10.1177/1461348418822170. https://doi.org/.

Hrovat, D. (1993). Applications of optimal control to advanced automotive suspension design. *Journal of Dynamic Systems, Measurement and Control, Transactions of the ASME, 115*(2B), 328–342. https://doi.org/10.1115/1.2899073. https://doi.org/.

SAE standard J3016 (2016). *Taxonomy and definitions for terms related to driving automation systems for on-road motor vehicles*.

ISO 2631-1. (1997). *2631-1: Mechanical vibration and shock-evaluation of human exposure to whole-body vibration-Part 1: General requirements*.

ISO 8608. (1995). *ISO 8608 : Mechanical vibration, road surface profiles, reporting of measured data: International standard. 2016*. https://books.google.com/books?id=1kyioAEACAAJ.

Iwata, Y., & Nakano, M. (1976). Optimum preview control of vehicle air suspensions. *Bulletin of JSME, 19*(138), 1485–1489. https://doi.org/10.1299/jsme1958.19.1485. https://doi.org/.

Kaldas, M., Caliskan, K., Henze, R., & Küçükay, F. (2014). Preview enhanced rule-optimized fuzzy logic damper controller. *SAE International Journal of Passenger Cars - Mechanical Systems, 7*(2), 804–815. https://doi.org/10.4271/2014-01-0868. https://doi.org/.

Kaldas, M. M. S., & Soliman, A. M. A. (2014). Influence of active suspension preview control on vehicle ride and braking performance. *SAE International Journal of Passenger Cars - Mechanical Systems, 7*(2), 793–803. https://doi.org/10.4271/2014-01-0862. https://doi.org/.

Karlsson, N., Dahleh, M., & Hrovat, D. (2001). Nonlinear active suspension with preview. *Proceedings of the American Control Conference, 4*(3), 2640–2645. https://doi.org/10.1109/ACC.2001.946273. https://doi.org/.

Kawamoto, Y., Suda, Y., Inoue, H., & Kondo, T. (2008). Electro-mechanical suspension system considering energy consumption and vehicle manoeuvre. *Vehicle System Dynamics, 46*(supp.1), 1053–1063. https://doi.org/10.1080/00423110802056263. https://doi.org/.

Kim, H. J., Seok Yang, H., & Park, Y. P. (2002). Improving the vehicle performance with active suspension using road-sensing algorithm. *Computers and Structures, 80*(18–19), 1569–1577. https://doi.org/10.1016/S0045-7949(02)00110-4. https://doi.org/.

Kiran, B. R., Roldão, L., Irastorza, B., Verastegui, R., Süss, S., Yogamani, S., Talpaert, V., Lepoutre, A., & Trehard, G. (2019). Real-time dynamic object detection for autonomous driving using prior 3D-maps. In *Lecture Notes in Computer Science (Including Subseries Lecture Notes in Artificial Intelligence and Lecture Notes in Bioinformatics), 11133 LNCS* (pp. 567–582). https://doi.org/10.1007/978-3-030-11021-5_35. https://doi.org/.

Kwon, B. S., Kang, D., & Yi, K. (2020). Wheelbase preview control of an active suspension with a disturbance-decoupled observer to improve vehicle ride comfort. *Proceedings of the Institution of Mechanical Engineers, Part D: Journal of Automobile Engineering, 234* (6), 1725–1745. https://doi.org/10.1177/0954407019886499. https://doi.org/.

Langlois, R. G., & Anderson, R. J. (1995). Preview control algorithms for the active suspension of an off-road vehicle. *In Vehicle System Dynamics, 24*(1). https://doi.org/10.1080/00423119508969082 (Vol., Issue). https://doi.org/.

Langlois, R. G., Hanna, D. M., & Anderson, R. J. (1992). Implementing preview control on an off-road vehicle with active suspension. *Vehicle System Dynamics, 20*(sup1), 340–353. https://doi.org/10.1080/00423119208969408. https://doi.org/.

Leatherwood, J. D., & Barker, L. M. (1984). A user-oriented and computerized model for estimating vehicle ride quality. *NASA Technical Papers* (p. 2299).

Li, P., Lam, J., & Cheung, K. C. (2014). Multi-objective control for active vehicle suspension with wheelbase preview. *Journal of Sound and Vibration, 333*(21), 5269–5282. https://doi.org/10.1016/j.jsv.2014.06.017. https://doi.org/.

Li, P., Lam, J., & Cheung, K. C. (2014b). Velocity-dependent multi-objective control of vehicle suspension with preview measurements. *Mechatronics, 24*(5), 464–475. https://doi.org/10.1016/j.mechatronics.2014.04.008. https://doi.org/.

Li, Z., Kolmanovsky, I., Atkins, E., Lu, J., & Filev, D. (2015). H∞ filtering for cloud-aided semi-active suspension with delayed road information. *IFAC-PapersOnLine, 48*(12), 275–280. https://doi.org/10.1016/j.ifacol.2015.09.390. https://doi.org/.

Little, E., Handrickx, P., Grote, P., Mergay, M., & Deel, J. (1999). Ride comfort analysis: Practice and procedures. *SAE Technical Papers 990053*. https://doi.org/ 10.4271/990053.

Louam, N., Wilson, D. A., & Sharp, R. S. (1992). Optimization and performance enhancement of active suspensions for automobiles under preview of the road. *Vehicle System Dynamics, 21*(1), 39–63. https://doi.org/10.1080/00423119208969001. https://doi.org/.

Lozia, Z. (1992). An analysis of vehicle behaviour during lane-change manoeuvre on an uneven ROAD surface. *Vehicle System Dynamics, 20*(sup1), 417–431. https://doi.org/10.1080/00423119208969413. https://doi.org/.

Ma, L., Li, Y., Li, J., Wang, C., Wang, R., & Chapman, M. A. (2018). Mobile laser scanned point-clouds for road object detection and extraction: A review. *Remote Sensing, 10* (10), 1–33. https://doi.org/10.3390/rs10101531. https://doi.org/.

Maciejewski, I., Kiczkowiak, T., & Krzyzynski, T. (2011). Application of the Pareto-optimal approach for selecting dynamic characteristics of seat suspension systems. *Vehicle System Dynamics, 49*(12), 1929–1950. https://doi.org/10.1080/00423114.2011.560270. https://doi.org/.

Maciejowski, J. M., Goulart, P. J., & Kerrigan, E. C. (2007). Constrained control using model predictive control. *Advanced Strategies in Control Systems with Input and Output Constraints. Lecture Notes in Control and Information Sciences, 346*, 273–291. https://doi.org/10.1007/978-3-540-37010-9_9. https://doi.org/.

Mai, V. N., Yoon, D. S., Choi, S. B., & Kim, G. W. (2020). Explicit model predictive control of semi-active suspension systems with magneto-rheological dampers subject to input constraints. *Journal of Intelligent Material Systems and Structures, 31*(9), 1157–1170. https://doi.org/10.1177/1045389X20914404. https://doi.org/.

Martins, I., Esteves, J., Marques, G. D., & Pina da Silva, F. (2006). Permanent-magnets linear actuators applicability in automobile active suspensions. *IEEE Transactions on Vehicular Technology, 55*(1), 86–94. https://doi.org/10.1109/TVT.2005.861167. https://doi.org/.

Martinus, D., Soenarko, B., & Nazaruddin, Y. Y. (1996). Optimal control design with preview for semi-active suspension on a half-vehicle model. In *Proceedings of the IEEE conference on decision and control* (pp. 2355–3592). https://doi.org/10.1109/cdc.1996.573539. https://doi.org/.

Marzbanrad, J., Ahmadi, G., Zohoor, H., & Hojjat, Y. (2004). Stochastic optimal preview control of a vehicle suspension. *Journal of Sound and Vibration, 275*(3–5), 973–990. https://doi.org/10.1016/S0022-460X(03)00812-5. https://doi.org/.

Mashadi, B., & Crolla, D. A. (2005). Influence of ride motions on the handling behaviour of a passenger vehicle. *Proceedings of the Institution of Mechanical Engineers, Part D: Journal of Automobile Engineering, 219*(9), 1047–1058. https://doi.org/10.1243/095440705X34702. https://doi.org/.

Mastinu, G., Pennati, M., Gobbi, M., Previati, G., & Ballo, F. (2017). Evolution of the ride comfort of Alfa Romeo cars since 1955 until 2005. *SAE technical papers 2017-01-1484*. https://doi.org/10.4271/2017-01-1484. https://doi.org/.

Mehra, R. K., Amin, J. N., Hedrick, K. J., Osorio, C., & Gopalasamy, S. (1997). Active suspension using preview information and model predictive control. *IEEE Conference on Control Applications - Proceedings*, 860–865. https://doi.org/10.1109/cca.1997.627769. https://doi.org/.

Metzler, M., Tavernini, D., Gruber, P., & Sorniotti, A. (2020). On prediction model fidelity in explicit nonlinear model predictive vehicle stability control. *IEEE Transactions on Control Systems Technology*, 1–17. https://doi.org/10.1109/tcst.2020.3012683. https://doi.org/.

Milliken, W. F., & Milliken, D. L. (1995). Race car vehicle dynamics. *In Society of Automotive Engineers, 400*(16).

Milz, S., Arbeiter, G., Witt, C., Abdallah, B., & Yogamani, S. (2018). Visual SLAM for automated driving: Exploring the applications of deep learning. In *IEEE computer society conference on computer vision and pattern recognition workshops* (pp. 360–370). https://doi.org/10.1109/CVPRW.2018.00062. https://doi.org/.

Montanez, G., Patino, D., & Mendez, D. (2015). Comparison of model predictive control techniques for active suspension. In *International conference on applied electronics* (pp. 157–160).

Morato, M. M., Nguyen, M. Q., Sename, O., & Dugard, L. (2019). Design of a fast real-time LPV model predictive control system for semi-active suspension control of a full vehicle. *Journal of the Franklin Institute, 356*(3), 1196–1224. https://doi.org/10.1016/j.jfranklin.2018.11.016. https://doi.org/.

Nastac, S., & Picu, M. (2010). Evaluating methods of whole-body-vibration exposure in trains. *Ann."Dunarea De Jos" Univ. Galati, Fasc. XIV Mech. Eng, 2*, 55–60.

Nguyen, T., Xie, M., Liu, X., Arunachalam, N., Rau, A., Lechner, B., Busch, F., & Wong, Y. D. (2019). Platooning of autonomous public transport vehicles: The influence of ride comfort on travel delay. *Sustainability (Switzerland)*, (19), 11. https://doi.org/10.3390/su11195237. https://doi.org/.

Ni, T., Li, W., Zhao, D., & Kong, Z. (2020). Road profile estimation using a 3D sensor and intelligent vehicle. *Sensors (Switzerland), 20*(13), 1–17. https://doi.org/10.3390/s20133676. https://doi.org/.

Oraby, W. A. H., Aly, M. A., El-Demerdash, S. M., & Selim, A. M. (2007). Influence of active suspension preview control on the vehicle lateral dynamics. *SAE technical papers 2007-01-2347*. https://doi.org/10.4271/2007-01-2347. https://doi.org/.

Paddan, G. S., & Griffin, M. J. (2002). Evaluation of whole-body vibration in vehicles. *Journal of Sound and Vibration, 253*(1), 195–213. https://doi.org/10.1006/jsvi.2001.4256. https://doi.org/.

Pang, H., Wang, Y., Zhang, X., & Xu, Z. (2019). Robust state-feedback control design for active suspension system with time-varying input delay and wheelbase preview information. *Journal of the Franklin Institute, 356*(4), 1899–1923. https://doi.org/10.1016/j.jfranklin.2019.01.011. https://doi.org/.

Pazooki, A., Cao, D., Rakheja, S., & Boileau, P.É. (2011). Ride dynamic evaluations and design optimisation of a torsio-elastic off-road vehicle suspension. *Vehicle System Dynamics, 49*(9), 1455–1476. https://doi.org/10.1080/00423114.2010.516833. https://doi.org/.

Pearce, C. E. M., & Thompson, A. G. (2004). Spectral decomposition methods for the computation of RMS values in an active suspension. *Vehicle System Dynamics, 42*(6), 395–411. https://doi.org/10.1080/0042311042000266801. https://doi.org/.

Poussot-Vassal, C., Spelta, C., Sename, O., Savaresi, S. M., & Dugard, L. (2012). Survey and performance evaluation on some automotive semi-active suspension control methods: A comparative study on a single-corner model. *Annual Reviews in Control, 36*(1), 148–160. https://doi.org/10.1016/j.arcontrol.2012.03.011. https://doi.org/.

Prabakar, R. S., Sujatha, C., & Narayanan, S. (2009). Optimal semi-active preview control response of a half car vehicle model with magnetorheological damper. *Journal of Sound and Vibration, 326*(3–5), 400–420. https://doi.org/10.1016/j.jsv.2009.05.032. https://doi.org/.

Prokop, G., & Sharp, R. S. (1995). Performance enhancement of limited-bandwidth active automotive suspensions by road preview. *IEE Proceedings: Control Theory and Applications, 142*(2), 140–148. https://doi.org/10.1049/ip-cta:19951772. https://doi.org/.

Rahman, M., & Rideout, G. (2012). Using the lead vehicle as preview sensor in convoy vehicle active suspension control. *Vehicle System Dynamics, 50*(12), 1923–1948. https://doi.org/10.1080/00423114.2012.707801. https://doi.org/.

Reimpell, J., Stoll, H., & Betzler, J. (2001). *The automotive chassis: Engineering principles* (2nd Ed.).

Reybrouck, K., Vandersmissen, B., & Six, K. (2012). ACOCAR ultimate comfort and safety through the energy-efficient active damping system of Tenneco. In *21st Aachen colloquium automobile and engine technology* (pp. 1–15).

Ricciardi, V., Ivanov, V., Dhaens, M., Vandersmissen, B., Geraerts, M., Savitski, D., & Augsburg, K. (2019). Ride blending control for electric vehicles. *World Electric Vehicle Journal, 10*(2). https://doi.org/10.3390/wevj10020036. https://doi.org/.

Ricco, M., Percolla, A., Rizzo, G. C., Zanchetta, M., Tavernini, D., Dhaens, M., Geraerts, M., Vigliani, A., Tota, A., & Sorniotti, A. (2020). On the model-based design of front-to-total anti-roll moment distribution controllers for yaw rate tracking. *Vehicle System Dynamics*. https://doi.org/10.1080/00423114.2020.1825753. https://doi.org/.

Ricco, M., Zanchetta, M., Rizzo, G. C., Tavernini, D., Sorniotti, A., Chatzikomis, C., Velardocchia, M., Geraerts, M., & Dhaens, M. (2020). On the design of yaw rate control via variable front-to-total anti-roll moment distribution. *IEEE Transactions on Vehicular Technology, 69*(2), 1388–1403. https://doi.org/10.1109/TVT.2019.2955902. https://doi.org/.

Roh, H. S., & Park, Y. (1998). Preview control of active vehicle suspensions based on a state and input estimator. *SAE Technical Papers 981121*. https://doi.org/10.4271/981121. https://doi.org/.

Ryu, S., Kim, Y., & Park, Y. (2008). Robust H∞ preview control of an active suspension system with norm-bounded uncertainties. *International Journal of Automotive Technology, 9*(5), 585–592. https://doi.org/10.1007/s12239-008-0069-7. https://doi.org/.

Ryu, S., Park, Y., & Suh, M. (2011). Ride quality analysis of a tracked vehicle suspension with a preview control. *Journal of Terramechanics, 48*(6), 409–417. https://doi.org/10.1016/j.jterra.2011.09.002. https://doi.org/.

Sakami, M., Kamiya, J., & Shimogo, T. (1976). Optimal preview control of vehicle suspension. *Bulletin of JSME, 19*(129), 265–273. https://doi.org/10.1299/jsme1958.19.265. https://doi.org/.

Sam, Y. M., & Hudha, K. (2006). Modelling and force tracking control of hydraulic actuator for an active suspension system. In *2006 1st IEEE conference on industrial electronics and applications* (pp. 2–7). https://doi.org/10.1109/ICIEA.2006.257242. https://doi.org/.

Saruchi, S. A., Ariff, M. H. M., Zamzuri, H., Amer, N. H., Wahid, N., Hassan, N., & Kassim, K. A. A. (2020). Novel motion sickness minimization control via fuzzy-PID controller for autonomous vehicle. *Applied Sciences (Switzerland), 10*(14). https://doi.org/10.3390/app10144769. https://doi.org/.

Savaresi, S. M., Poussot-Vassal, C., Spelta, C., Sename, O., & Dugard, L. (2010). *Semi-active suspension control design for vehicles*. Elsevier.

Savaresi, S. M., & Silani, E. (2004). On the optimal predictive control algorithm for comfort-oriented semi-active suspensions. *SAE Technical Papers 2004-01-2088*. https://doi.org/10.4271/2004-01-2088. https://doi.org/.

Scamarcio, A., Gruber, P., De Pinto, S., & Sorniotti, A. (2020). Anti-jerk controllers for automotive applications: A review. *Annual Reviews in Control, 50*, 174–189. https://doi.org/10.1016/j.arcontrol.2020.04.013. https://doi.org/.

Scamarcio, A., Metzler, M., Gruber, P., De Pinto, S., & Sorniotti, A. (2020). Comparison of anti-jerk controllers for electric vehicles with on-board motors. *IEEE Transactions on Vehicular Technology, 69*(10), 10681–10699. https://doi.org/10.1109/TVT.2020.2997815. https://doi.org/.

Schindler, A. (2009). *Neue Konzeption und erstmalige realisierung eines aktiven Fahrwerks mit preview-strategie (Vol. 31)*. KIT Scientific Publishing.

Schmitz, A. J. (2004). *A semi-empirical three-dimensional model of the pneumatic tyre rolling over arbitrarily uneven road surfaces. Th.* Technische Universiteit Delft.

Sezgin, A., & Yagiz, N. (2012). Analysis of passenger ride comfort. *MATEC Web of Conferences, 1*, 10–13. https://doi.org/10.1051/matecconf/20120103003. https://doi.org/.

Sharkawy, A. B. (2005). Fuzzy and adaptive fuzzy control for the automobiles' active suspension system. *Vehicle System Dynamics, 43*(11), 795–806. https://doi.org/10.1080/00423110500097783. https://doi.org/.

Sharp, R. S., & Peng, H. (2011). Vehicle dynamics applications of optimal control theory. *Vehicle System Dynamics, 49*(7), 1073–1111. https://doi.org/10.1080/00423114.2011.586707. https://doi.org/.

Siegel, J. E., Erb, D. C., & Sarma, S. E. (2018). A survey of the connected vehicle Landscape - Architectures, enabling technologies, applications, and development areas. *IEEE Transactions on Intelligent Transportation Systems, 19*(8), 2391–2406. https://doi.org/10.1109/TITS.2017.2749459. https://doi.org/.

Skogestad, S., & Postlethwaite, I. (2007). *Multivariable feedback control: Analysis and design*.

Soliman, A. M. A., & Crolla, D. A. (2001). Limited bandwidth active suspension employing wheel base preview. *SAE Technical Papers 2001-01-1063*. https://doi.org/10.4271/2001-01-1063. https://doi.org/.

Soliman, A. M. A., & Kaldas, M. M. S. (2019). Semi-active suspension systems from research to mass-market – a review. *Journal of Low Frequency Noise, Vibration and Active Control*, 1–19. https://doi.org/10.1177/1461348419876392. https://doi.org/.

Song, S., & Wang, J. (2020). Incremental model predictive control of active suspensions with estimated road preview information from a lead vehicle. *Journal of Dynamic Systems, Measurement, and Control*, (12), 142. https://doi.org/10.1115/1.4047962. https://doi.org/.

Sorniotti, A., & D'Alfio, N. (2007). Vehicle dynamics simulation to develop an active roll control system. *SAE Technical Papers 2007-01-0828*. https://doi.org/10.4271/2007-01-0828. https://doi.org/.

Spencer, B. F., Dyke, S. J., Sain, M. K., & Carlson, J. D. (1997). Phenomenological model for magnetorheological dampers. *Journal of Engineering Mechanics, 123*(3), 230–238. https://doi.org/10.1061/(asce)0733-9399(1997)123:3(230). https://doi.org/.

Streiter, R. (2008). Active preview suspension system. *ATZ Worldwide, 110*(5), 4–11. https://doi.org/10.1007/BF03225003. https://doi.org/.

Sugasawa, F., Kobayashi, H., Kakimoto, T., Shiraishi, Y., & Tateishi, Y. (1985). Electronically controlled shock absorber system used as a road sensor which utilizes super sonic waves. *SAE Technical Papers 851652*. https://doi.org/10.4271/851652. https://doi.org/.

Theunissen, J. (2019). *Explicit model predictive control for active suspension systems with preview. Th.* University of Surrey.

Theunissen, J., Sorniotti, A., Gruber, P., Fallah, S., Dhaens, M., Reybrouck, K., Lauwerys, C., Vandersmissen, B., Al Sakka, M., & Motte, K. (2019). Explicit model predictive control of an active suspension system. In *9th international munich chassis symposium 2018* (pp. 201–214). https://doi.org/10.1007/978-3-658-22050-1_17. https://doi.org/.

Theunissen, J., Sorniotti, A., Gruber, P., Fallah, S., Ricco, M., Kvasnica, M., & Dhaens, M. (2020). Regionless explicit model predictive control of active suspension systems with preview. *IEEE Transactions on Industrial Electronics, 67*(6), 4877–4888. https://doi.org/10.1109/TIE.2019.2926056. https://doi.org/.

Thompson, A. G., & Davis, B. R. (2000). RMS values for control force, suspension stroke and tyre deflection in an active suspension. *Vehicle System Dynamics, 34*(2), 143–150. https://doi.org/10.1076/0042-3114(200008)34:2;1-G;FT143. https://doi.org/.

Thompson, A. G., & Davis, B. R. (2003). RMS values of force, stroke and tyre deflection in a half-car model with preview controlled active suspension. *Vehicle System Dynamics, 39*(3), 245–253. https://doi.org/10.1076/vesd.39.3.245.14153. https://doi.org/.

Thompson, A. G., & Davis, B. R. (2005). Computation of the rms state variables and control forces in a half-car model with preview active suspension using spectral decomposition methods. *Journal of Sound and Vibration, 285*(3), 571–583. https://doi.org/10.1016/j.jsv.2004.08.017. https://doi.org/.

Thompson, A. G., Davis, B. R., & Pearce, C. E. M. (1980). An optimal linear active suspension with finite road preview. *SAE Transactions, 89*(2), 2009–2020. https://www.jstor.org/stable/44633818.

Thompson, A. G., & Pearce, C. E. M. (1998). Physically realisable feedback controls for a fully active preview suspension applied to a half-car model. *Vehicle System Dynamics, 30*(1), 17–35. https://doi.org/10.1080/00423119808969433. https://doi.org/.

Thompson, A. G., & Pearce, C. E. M. (2001a). Direct computation of the performance index for an optimally controlled active suspension with preview applied to a half-car model. *Vehicle System Dynamics, 35*(2), 121–137. https://doi.org/10.1076/vesd.35.2.121.2035. https://doi.org/.

Thompson, A. G., & Pearce, C. E. M. (2001b). Performance index for a preview active suspension applied to a quarter-car model. *Vehicle System Dynamics, 35*(1), 55–66. https://doi.org/10.1076/vesd.35.1.55.5616. https://doi.org/.

Thompson, A. G., & Pearce, C. E. M. (2003). RMS values for force, stroke and deflection in a quarter-car model active suspension with preview. *Vehicle System Dynamics, 39*(1), 57–75. https://doi.org/10.1076/vesd.39.1.57.8242. https://doi.org/.

Tomizuka, M. (1975). Optimal continuous finite preview problem. *IEEE Transactions on Automatic Control, 20*(3), 362–365. https://doi.org/10.1109/TAC.1975.1100962. https://doi.org/.

Tomizuka, M. (1976). Optimum linear preview control with application to vehicle suspension"—revisited. *Journal of Dynamic Systems, Measurement and Control, Transactions of the ASME, 98*(3), 309–315. https://doi.org/10.1115/1.3427040. https://doi.org/.

Tota, A., Velardocchia, M., & Güvenç, L. (2018). Path tracking control for autonomous driving applications. *Advances in Service and Industrial Robotics. RAAD 2017. Mechanisms and Machine Science, 49*, 456–467. https://doi.org/10.1007/978-3-319-61276-8_49. https://doi.org/.

Tseng, H. E., & Hrovat, D. (2015). State of the art survey: active and semi-active suspension control. *Vehicle System Dynamics, 53*(7), 1034–1062. https://doi.org/10.1080/00423114.2015.1037313. https://doi.org/.

Ueno, K., Fujibayashi, T., Sasaki, M., Konishi, M., & Takahashi, T. (2018). Vehicle control techniques for safety, environmental performance, and ride comfort. *Hitachi Review, 67*(1), 064–071.

Ulsoy, A. G., Peng, H., & Çakmakci, M. (2012). *Automotive control systems*. Cambridge University Press.

Ursu, I., Ursu, F., & Vladimirescu, M. (1997). The synthesis of two suboptimal electrohydraulic suspensions, active and semiactive, employing the receding horizon method. *Nonlinear Analysis, Theory, Methods and Applications, 30*(4). https://doi.org/10.1016/S0362-546X(97)00283-6, 1977–1984https://doi.org/.

Vahidi, A., & Eskandarian, A. (2002). Influence of preview uncertainties in the preview control of vehicle suspensions. *Proceedings of the Institution of Mechanical Engineers, Part K: Journal of Multi-Body Dynamics, 216*(4), 295–301. https://doi.org/10.1243/146441902320992383. https://doi.org/.

Van Der Aa, M. A. H., Muijderman, J. H. E. A., & Veldpaus, F. E. (1997). Constrained optimal control of semi-active suspension systems with preview. *Vehicle System Dynamics, 28*(4–5), 307–323. https://doi.org/10.1080/00423119708969359. https://doi.org/.

Vella, A. D., Vigliani, A., Tota, A., & Lisitano, D. (2020). Experimental ride comfort analysis of an electric light vehicle in urban scenario. *SAE technical papers 2020-01-1086*. https://doi.org/10.4271/2020-01-1086. https://doi.org/.

Wang, H., Tota, A., Aksun-Guvenc, B., & Guvenc, L. (2018). Real time implementation of socially acceptable collision avoidance of a low speed autonomous shuttle using the elastic band method. *Mechatronics, 50*, 341–355. https://doi.org/10.1016/j.mechatronics.2017.11.009. https://doi.org/.

Wang, L., Zhao, D., Ni, T., & Liu, S. (2020). Extraction of preview elevation information based on terrain mapping and trajectory prediction in real-time. *IEEE Access, 8*, 76618–76631. https://doi.org/10.1109/ACCESS.2020.2984034. https://doi.org/.

Williams, D. E., & Haddad, W. M. (1995). Nonlinear control of roll moment distribution to influence vehicle yaw characteristics. *IEEE Transactions on Control Systems Technology, 3*(1), 110–116. https://doi.org/10.1109/87.370716. https://doi.org/.

Wu, J., Zhou, H., Liu, Z., & Gu, M. (2020). Ride comfort optimization via speed planning and preview semi-active suspension control for autonomous vehicles on uneven roads. *IEEE Transactions on Vehicular Technology, 69*(8), 8343–8355. https://doi.org/10.1109/tvt.2020.2996681. https://doi.org/.

Yamada, S., Beauduin, T., Fujimoto, H., Kanou, T., & Katsuyama, E. (2017). Model-based longitudinal vibration suppression control for electric vehicles with geared in-wheel motors. In *IEEE/ASME international conference on advanced intelligent mechatronics, AIM* (pp. 517–522). https://doi.org/10.1109/AIM.2017.8014069. https://doi.org/.

Yamamoto, A., Sugai, H., Kanda, R., & Buma, S. (2014). Preview ride comfort control for electric active suspension (eActive3). *SAE technical paper*. https://doi.org/10.4271/2014-01-0057. https://doi.org/.

Yeh, E. C., & Tsao, Y. J. (1994). A fuzzy preview control scheme of active suspension for rough road. *International Journal of Vehicle Design, 15*(1–2), 166–180. https://doi.org/10.1504/IJVD.1994.061914. https://doi.org/.

Yoshimura, T., Edokoro, K., & Ananthanarayana, N. (1993). An active suspension model for rail/vehicle systems with preview and stochastic optimal control. *Journal of Sound and Vibration, 166*(3), 507–519. https://doi.org/10.1006/jsvi.1993.1309. https://doi.org/.

Youn, I., Tchamna, R., Lee, S. H., Uddin, N., Lyu, S. K., & Tomizuka, M. (2014). Preview suspension control for a full tracked vehicle. *International Journal of Automotive Technology, 15*(3), 399–410. https://doi.org/10.1007/s12239-014-0042-6. https://doi.org/.

Yu, J., Pei, X., Guo, X., Lin, J. G., & Zhu, M. (2020). Path tracking framework synthesizing robust model predictive control and stability control for autonomous vehicle. *Proceedings of the Institution of Mechanical Engineers, Part D: Journal of Automobile Engineering, 234*(9), 2330–2341. https://doi.org/10.1177/0954407020914666. https://doi.org/.

Zhao, D., Wang, L., Li, Y., & Du, M. (2018). Extraction of preview elevation of road based on 3D sensor. *Measurement: Journal of the International Measurement Confederation, 127*, 104–114. https://doi.org/10.1016/j.measurement.2018.05.062. https://doi.org/.

Zhao, J., Hua, X., Cao, Y., Fan, L., Mei, X., & Xie, Z. (2019). Design of an integrated controller for active suspension systems based on wheelbase preview and wavelet noise filter. *Journal of Intelligent and Fuzzy Systems, 36*(4), 3911–3921. https://doi.org/10.3233/JIFS-181117. https://doi.org/.

Zhao, X., Kremb, M., & Schindler, C. (2013). Assessment of wheel loader vibration on the riding comfort according to ISO standards. *Vehicle System Dynamics, 51*(10), 1548–1567. https://doi.org/10.1080/00423114.2013.814798. https://doi.org/.

Zhu, J. J., Khajepour, A., Esmailzadeh, E., & Kasaiezadeh, A. (2012). Ride quality evaluation of a vehicle with a planar suspension system. *Vehicle System Dynamics, 50*(3), 395–413. https://doi.org/10.1080/00423114.2011.592591. https://doi.org/.

Johan Theunissen received the M.Sc. degree in electromechanical engineering from the K.U. Leuven, Leuven, Belgium, in 2008, and the Ph.D. degree in automotive engineering from the University of Surrey, Guildford, U.K., in 2019. He has recently founded Simmanco, an engineering company focusing on mechatronics and automotive. Earlier in his career, he worked for Ford Motor Company, Flanders' DRIVE and Tenneco Automotive Europe, as a Project Engineer and a Project Manager.

Antonio Tota received the M.Sc. degree in mechanical engineering and the Ph.D. degree in mechanical engineering from the Politecnico di Torino, Turin, Italy, in 2013 and 2017, respectively. He is a Research Fellow in Vehicle Dynamics and Control with the Politecnico di Torino, Italy. His research interests include vehicle dynamics control and off-road autonomous driving. He also worked as a Research Fellow in Advance Vehicle Engineering with the University of Surrey, Guildford, U.K.

Patrick Gruber received the M.Sc. degree in motorsport engineering and management from Cranfield University, Cranfield, U.K., in 2005, and the Ph.D. degree in mechanical engineering from the University of Surrey, Guildford, U.K., in 2009. He is a Professor in Advanced Vehicle Systems Engineering with the University of Surrey. His research interests include vehicle dynamics and tyre dynamics with special focus on friction behaviour.

Miguel Dhaens received the M.Sc. degree in electromechanical engineering from KIH, Ostend, Belgium. He is Engineering Manager of the Global Research Ride Performance Team of Tenneco, and responsible for defining the research road map and coordinating the global research activities of Tenneco's Ride Performance business, which includes vehicle dynamics, damping solutions, mechatronics, material science, manufacturing technologies and predictive tools. Before joining Tenneco, he worked with the Formula One team of Toyota Motorsport GmbH, Germany, as Manager of the engine, testing and advanced strategies teams, and with Flanders' DRIVE as R&D Manager.

Aldo Sorniotti received the M.Sc. degree in mechanical engineering and the Ph.D. degree in applied mechanics from the Politecnico di Torino, Turin, Italy, in 2001 and 2005, respectively. He is a Professor in Advanced Vehicle Engineering with the University of Surrey, Guildford, U.K., where he coordinates the Centre for Automotive Engineering. His research interests include vehicle dynamics control and transmission systems for electric and hybrid electric vehicles.